ESC-TR-85-213

Technical Report
698 (Rev. 1)

Emitter Location with LES-8/9 Using Differential Time-of-Arrival and Differential Doppler Shift

J.E. Kaufmann
W.K. Hutchinson

21 August 1985
Reissued 31 March 2000

Lincoln Laboratory
MASSACHUSETTS INSTITUTE OF TECHNOLOGY
LEXINGTON, MASSACHUSETTS

Prepared for the Department of the Air Force
under Contract F19628-85-C-0002.

The work reported in this document was performed at Lincoln Laboratory, a center for research operated by Massachusetts Institute of Technology. The work was sponsored by the Department of the Air Force under Contract F19628-85-C-0002.

This technical report has been reviewed and is approved for publication.

FOR THE COMMANDER

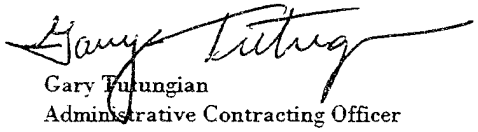

Gary Tutungian
Administrative Contracting Officer
Plans and Program Directorate
Contracted Support Management

MASSACHUSETTS INSTITUTE OF TECHNOLOGY
LINCOLN LABORATORY

EMITTER LOCATION WITH LES-8/9 USING DIFFERENTIAL TIME-OF-ARRIVAL AND DIFFERENTIAL DOPPLER SHIFT

J.E. KAUFMANN
W.K. HUTCHINSON
Group 68

TECHNICAL REPORT 698 (Rev. 1)

21 August 1985
Reissued 31 March 2000

LEXINGTON MASSACHUSETTS

ABSTRACT

Development of an emitter-location capability using differential time-of-arrival (DTOA) and different Doppler shift (DD) with the Lincoln Experimental Satellites 8 and 9 (LES-8/9) is described. Location of UHF sources over a large part of the earth can be estimated from observations as short as a few seconds by the two satellites. The principles of this emitter-location method, DTOA and DD estimation procedures, and limitations on location-estimation accuracy are discussed. Results of tests using transmissions from Lincoln Laboratory, Lexington, Massachusetts, and from a USAF transmitter at Hall Beach, Canada, demonstrate the level of accuracy achievable in practice with LES-8/9.

This report was originally Classified. It is being reissued with corrections of a few minor errors and misprints.

ACKNOWLEDGMENTS

The authors gratefully acknowledge the valuable contributions of a number of individuals in this project. Ellen Swenson and Stephen Kolek were responsible for the software development and for data-processing support in the operational phases of this effort. The LESOC crew—Harold Hoover, Ted Sarantos, and Albert Richard—provided the support services which made possible the use of LES-8/9, sometimes at odd hours of the day or night. James Will provided assistance in collection and post-processing of data from the satellites. Malcolm Coley, Susan Salvia, and Nancy Helfrich handled the orbit-fitting calculations for LES-8/9. The Cessna aircraft and pilot used in the airborne-emitter experiment were made available by Lincoln Laboratory's Division 4. This work also benefited from technical discussions with Frank Floyd. Finally, William Ward provided advice and encouragement, and this document was improved by his editorial assistance.

TABLE OF CONTENTS

LIST OF ILLUSTRATIONS

LIST OF TABLES

1. INTRODUCTION

The emitter-location capability of the Lincoln Experimental Satellites 8 and 9 (LES-8/9) is a fortuitous development resulting from the satellites' unique operational characteristics. LES-8 and LES-9 are essentially identical communications satellites designed to demonstrate advanced technologies for UHF and K-band communications for a variety of mobile and fixed ground terminals. A summary of their capabilities and features is given in Table 1-1. No specific consideration was given to performing emitter-location work in the design of LES-8/9. This capability was recognized and developed only after launch.

TABLE 1-1

LES-8/9 Spacecraft

- ≈1000 lb (mass) each
- 3-axis-stabilized to Earth
- Circular, synchronous, near-ecliptic coplanar orbits
- RTG power supplies
- K-band/UHF communications
- Spacecraft-to-spacecraft cross-linking (K-band)
- Flexible on-board signal-processing
- Spread spectrum (frequency-hopping) for anti-jam
- Autonomous attitude control and stationkeeping
- Cold-gas (ammonia) on-board propulsion
- Comprehensive telemetry and command

The satellites operate in synchronous, circular orbits with an approximately 25-degree inclination with respect to the equator. The resultant ground tracks appear as figure-eight patterns (see Figure 1). The uplink receivers in the two satellites use on-board frequency synthesizers that can be commanded to tune the range of 297.2 to 399.6 MHz in steps of approximately 195 Hz. The receiver master oscillators are highly stable: short-term stability is better than 6 parts in 10^9 per 100 μs and long-term drift is less than one part in 10^{11} per day. The oscillators can be checked and trimmed from the ground. Antennas for UHF consist of greater-than-earth-coverage crossed-dipole arrays. The satellites possess a substantial amount of flexible on-board signal-processing capability, and crosslinks between LES-8 and LES-9 are provided at 36/38 GHz for intersatellite data relay. Accurate satellite ephemerides are obtained from Lincoln

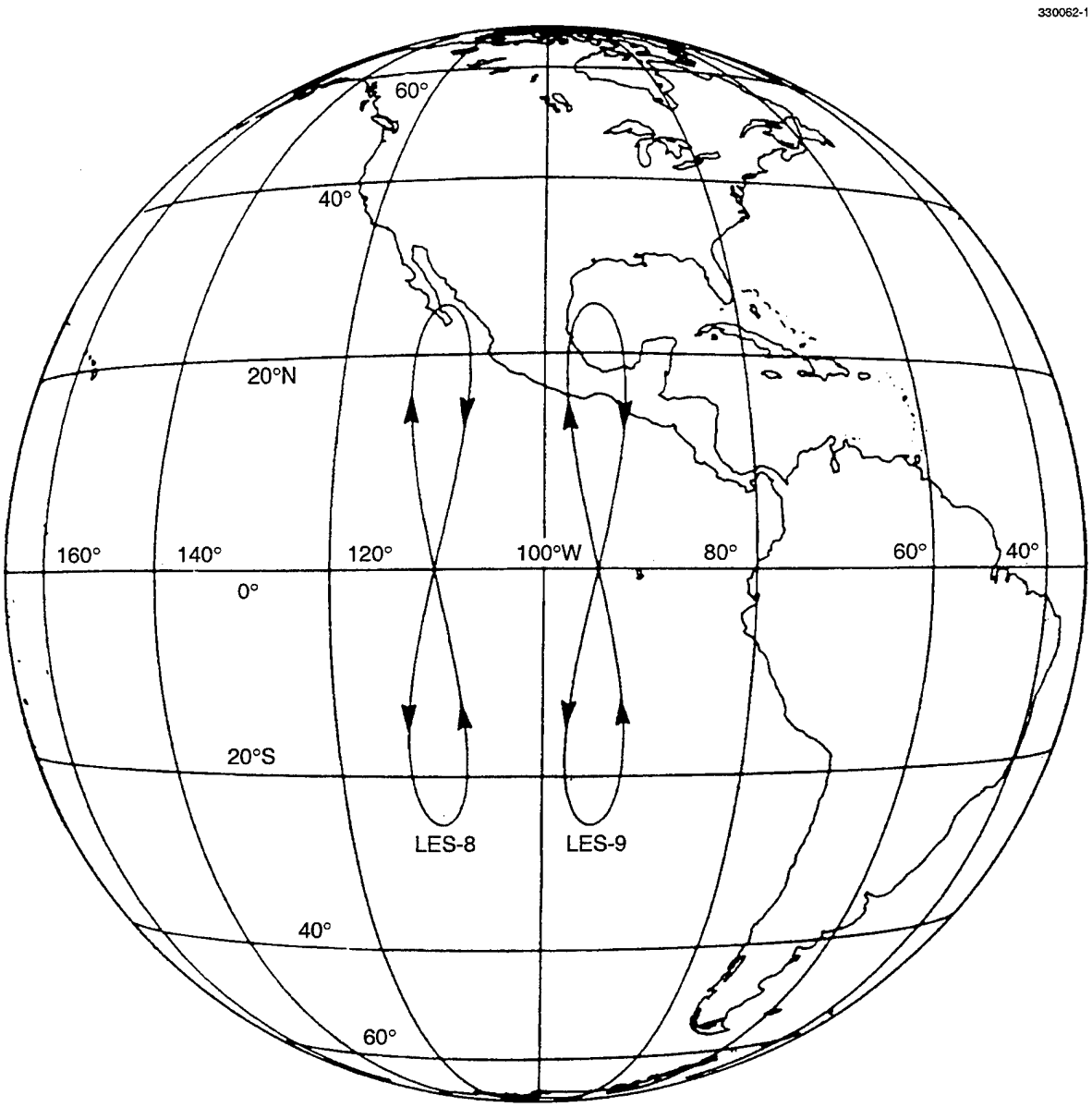

Figure 1. Ground tracks of orbits of LES-8 and LES-9.

Laboratory's in-house orbit-fitting Planetary Ephemeris Program[1]. The spacecraft have been operating successfully since their launch on March 15, 1976. Complete documentation on the operational aspects of the satellites can be found in Reference 2.

In October of 1977, after completion of more than one year of extensive testing, the satellites were handed over to the military as operational resources. Shortly beforehand, RFI of unknown origin was observed in LES-9's broadband UHF-to-UHF transponder. Investigations into the source of interference eventually led to the development of several satellite-based techniques for emitter location using LES-8/9. The early source-location efforts exploited the motion of the satellites relative to earth and employed the single-satellite techniques of terminator motion and Doppler trace-matching.

Although these techniques were used successfully to locate sources of RFI on occasion, certain inherent drawbacks limit their usefulness. In particular, the terminator-motion approach requires a monitoring period of at least one or two days to establish times of "rise" and "set" of the source as seen by one satellite in order to compute a location estimate. The technique is suitable, therefore, only for sources which operate on a more or less continuous basis and are located outside the area of all-day satellite visibility. Doppler trace-matching, on the other hand, typically requires several hours of observation before a reliable location estimate can be produced. However, transmitters with frequency instabilities or suppressed-carrier modulations can confuse the Doppler estimates and severely degrade location accuracy.

Eventually it was recognized that LES-8 and LES-9 possess the capability of being used *simultaneously* to monitor an RFI source and to relay received-signal data from both satellites back to a ground station by virtue of the crosslinks and their on-board signal-processing capabilities. In 1981 a two-satellite emitter-location technique exploiting differential time-of-arrival (DTOA) and differential Doppler shift (DD) of a signal as received in two satellites was implemented. The use of this technique eliminates many of the disadvantages of the single-satellite techniques. A single observation as short as a few seconds in duration, taken by both satellites at the same time, can suffice to give a location estimate, and the DD measurement is insensitive to transmitter frequency fluctuations. Furthermore, it is applicable to emitters over a wide range of the visible earth as both LES-8 and LES-9 have a large coverage area in common.

At the ground receiving terminal, both DTOA and DD are estimated jointly by cross-correlating the received-signal information from the two satellites. With knowledge of the satellite positions and velocities, the estimates of DTOA and DD are each used to compute a locus of possible transmitter locations on earth. The intersection of a pair of loci from the DTOA/DD data from one observation gives the emitter-location estimate, as illustrated in Figure 2.

This LES-8/9 emitter-location system has strong parallels to a DTOA/DD system conceived for tactical applications using airborne receiving platforms. This so-called Emitter Location System (ELS) was to be implemented as part of the precision Location Strike System (PLSS) and was studied extensively in the early 1970s by IBM, McDonnell-Douglas, GTE-Sylvania and others.

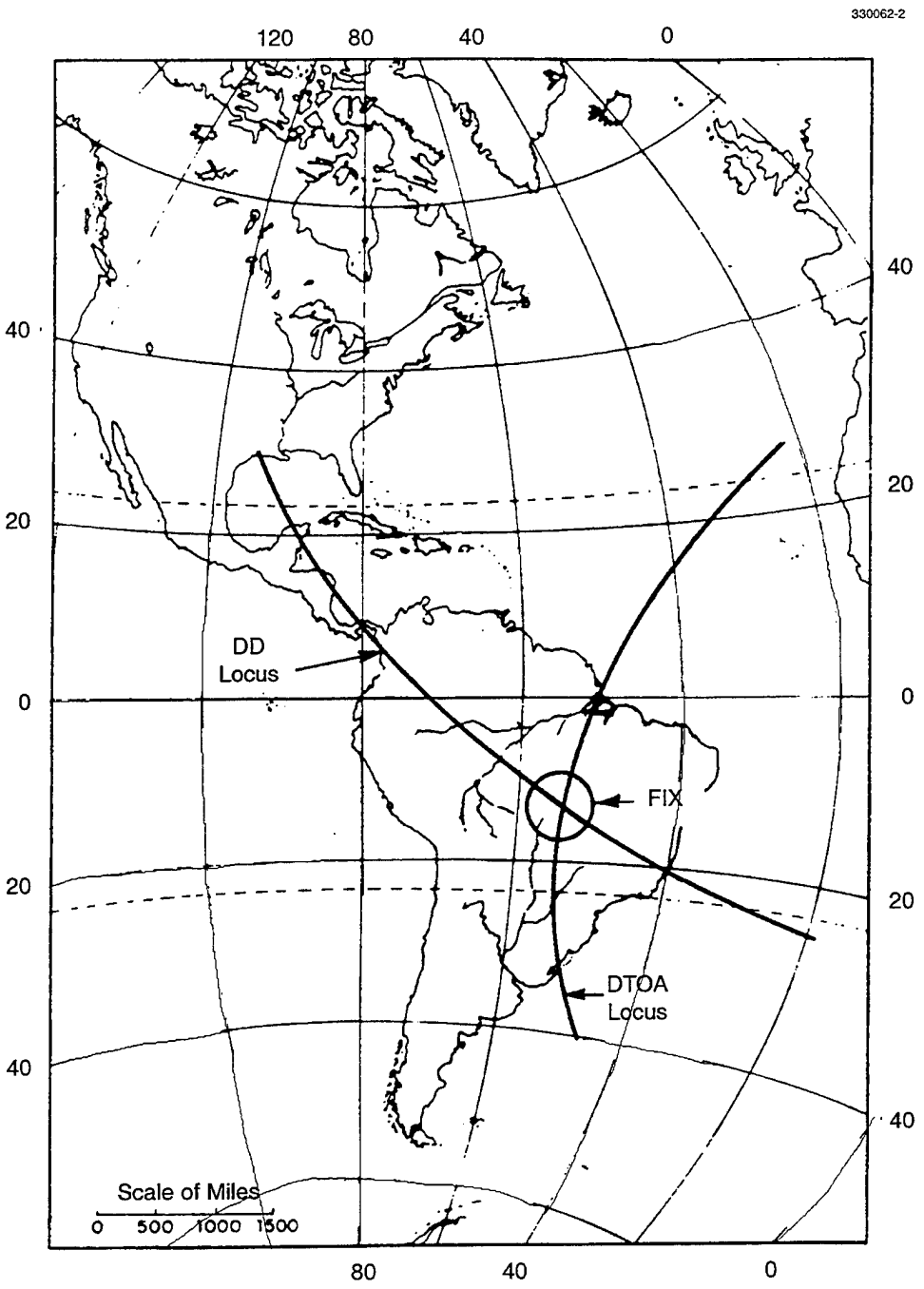

Figure 2. DTOA/DD lines of position.

The objective behind the LES-8/9 work was to invest a moderate effort to develop and demonstrate a satellite-based emitter-location capability using DTOA/DD by exploiting already-existing satellite capabilities. The resulting system provides a resource whereby occasional problems of interference to military UHF satellite communications can be resolved by determining the origins of the interference. The primary mission of LES-8/9, however, continues to be one of providing communications to military users.

The organization of this report is as follows: Section 2 sets forth the principles whereby the position of an RF source on the earth can be determined by the DTOA and DD of its signal as received in the two satellite receivers. The key signal-processing issue is accurate estimation of the DTOA and DD from the received-signal data. Section 3 describes the estimation procedure which is based on cross-correlation methods. Section 4 discusses the limitations on how accurately a source may be located, due to effects of random phenomena, such as received noise, and of unknown system errors, including imperfections in the satellites' receivers, inaccuracies in knowledge of the satellites' ephemerides, and motion of the source itself. To demonstrate the location-estimation accuracy attainable from LES-8/9, a series of tests using UHF transmissions from Lincoln Laboratory, Lexington, a USAF transmitter in Hall Beach, Canada, and from an airborne transmitter was carried out. The results of those tests are given in Section 5.

2. PRINCIPLES OF EMITTER LOCATION USING DTOA/DD

With two satellites, emitter location can be performed using DTOA only, DD only, or both DTOA and DD together. The principles of these approaches are discussed here. The combined DTOA/DD method is usually preferred because it can in principle provide an essentially instantaneous "fix."

2.1 DTOA TECHNIQUE

The DTOA method is explained by referring to the geometry shown in Figure 3. The vectors $\underline{r}_8$ and $\underline{r}_9$ represent the positions of LES-8 and LES-9, respectively, and $\underline{r}_T$, the transmitter position, with the

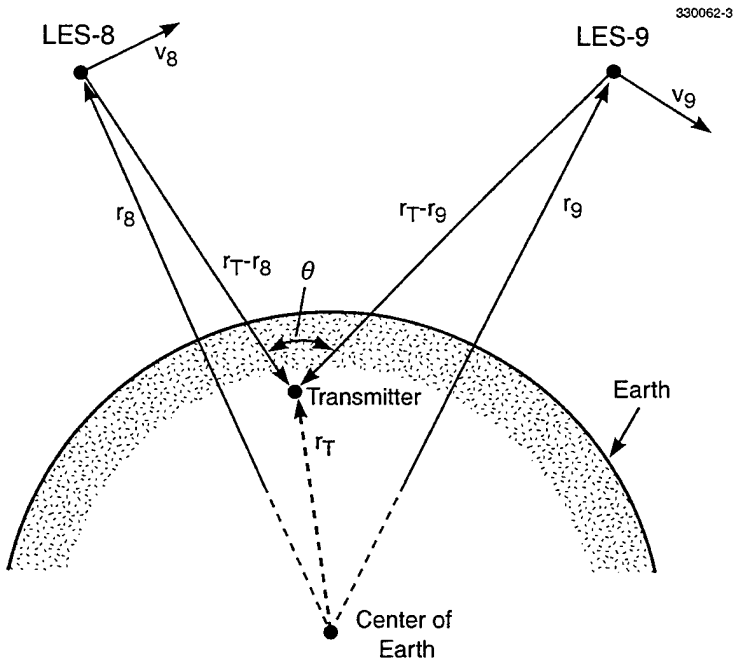

Figure 3. Satellite/emitter geometry.

origin at the center of the earth. The range difference from the transmitter to each satellite produces a difference τ in the time-of-arrival of the signal in each satellite receiver,

$$\tau = \frac{1}{c}\left(|\underline{r}_T - \underline{r}_9| - |\underline{r}_T - \underline{r}_8|\right) \tag{2.1}$$

where c is the propagation velocity (speed of light). For constant τ, the locus of possible transmitter locations $\underline{r}_T$ defined by (2.1) is a hyperboloid. Assuming the transmitter lies on the surface of the earth results in the constraint

$$|\underline{r}_T| = R_E \tag{2.2}$$

where R_E is the radius of the earth. The actual value of R_E will vary slightly with $\underline{r}_T$ since the earth is somewhat non-spherical. The intersection of the surfaces given by (2.1) and (2.2) yield a line-of-position (LOP) of possible transmitter sites on earth.

The intersection of at least two such lines defines the "fix." Since one observation yields only a single LOP, two or more observations, taken at different times with different satellite/emitter orientations, are needed to produce the required intersecting loci. To avoid the situation where the LOPs intersect nearly parallel to one another with resultant poor location-estimation accuracy, a substantial change in satellite positions relative to the emitter is required between observations. With LES-8/9, a wait of one to several hours between periods of data-taking is needed. Note that if the two satellites were geostationary, it would not be possible to carry out this operation.

It is noted that the DTOA method corresponds to an inversion of navigation techniques which use time difference-of-arrival. Examples include LORAN and the NAVSTAR/GPS, systems with which a user can determine his own position by measurement of the arrival times of identical signals transmitted simultaneously from several time-synchronized transmitters in different known locations. The transmitters are land-based in LORAN and deployed in satellites in the case of NAVSTAR/GPS.

It is assumed in (2.1) that the delay τ remains constant over the observation interval. Because of satellite motion, this is not strictly true. However, the first-order effect of the motion is simply to induce a Doppler shift in the frequency of the received signal. In the case of LES-8/9, the rate of change of the delay is small enough that τ can, in fact, be considered constant for the purposes of solving the position equations (2.1) and (2.2), and the Doppler shift appears as an entirely independent phenomenon. Using the Doppler information allows location of an emitter by the DD method discussed in the next section.

2.2 DD TECHNIQUE

Referring again to Figure 3, the satellite velocities $\underline{v}_8$ and $\underline{v}_9$ with respect to the earth have components in the direction of the transmitter, inducing Doppler shifts in the received signals. The DD measurement gives the difference f between the Doppler shifts at the two receivers,

$$f = \left(\underline{v}_9 \cdot \underline{i}_9 - \underline{v}_8 \cdot \underline{i}_8\right)\frac{f_o}{c} \tag{2.3}$$

where

$$\underline{i}_9 = \frac{\underline{r}_T - \underline{r}_9}{|\underline{r}_T - \underline{r}_9|}$$

$$\underline{i}_8 = \frac{\underline{r}_T - \underline{r}_8}{|\underline{r}_T - \underline{r}_8|}$$

are the unit vectors along the lines-of-sight between the emitter and LES-9 and LES-8, respectively, and f_o is the center frequency of the transmitted signal. For constant f, the intersection of the surface described by (2.3) with the earth's surface generates an LOP for possible transmitter sites. As with DTOA, at least two different LOPs, obtained from observations at different times, are needed to obtain a "fix." With LES-8/9, an inter-observation wait of one to several hours is needed to produce LOPs which provide reasonable location-estimation accuracy. The DD measurement exploits the motion of the satellites with respect to the earth and, therefore, cannot be performed with both satellites geostationary.

Several assumptions are made: (1) the Doppler effect is being modeled as a simple frequency translation of the signal spectrum, which requires that the signal bandwidth B in the satellite receivers satisfy $B<<f_o$; (2) relativistic Doppler effects are ignored. However, it is easily shown that for the velocities involved with LES-8/9, the errors in so doing are negligible; (3) the transmitter is not moving. Any motion will impart an additional Doppler shift which is not accounted for by (2.3) and will thus cause errors in the location estimate. This problem is discussed more fully in Sections 4 and 5; and (4) the rate of change of the DD over the observation interval is assumed to be zero. Otherwise estimation of the DD rate-of-change (which itself is another emitter-location observable) might be required too, to avoid impairment of the DTOA/DD estimation.

An advantage of the DD technique over Doppler trace-matching (which was accomplished on previous occasions with LES-8/9 and is discussed in Reference 3) is that the DD estimate is relatively insensitive to transmitter frequency instability. The differential nature of the DD measurement causes any frequency fluctuations from the source to cancel out in the estimate, provided the differential time delay between the two received data segments is compensated for.

2.3 COMBINED DTOA/DD TECHNIQUE

Exploiting *both* DTOA and DD information from the same observation is the preferred approach. Because DTOA depends on the range to the emitter, and DD on the range rate, the two observables can be regarded as being independent, with the result that the loci they generate differ from each other. The intersection of the two loci gives the location estimate, and in practice it is found that they tend to be nearly orthogonal at their intersection for a wide range of locations on earth. Figure 4 shows a family of typical loci. The exact nature of the loci depends on the particular satellite positions and velocities with respect to the emitter.

The key aspect of the combined DTOA/DD technique is that a *single* observation, which for LES-8/9, can be as little as one second in duration in some instances, suffices, in principle, to provide an emitter-location estimate. In practice, averaging over multiple observations taken at different times can be employed for improved location accuracy. An essentially instantaneous "fix" could be obtained if the data were to be processed in real (or near-real) time. In the application of LES-8/9, however, an instant turnaround capability is not required, so that real-time processing is not employed.

One of the major tasks, then, is to obtain accurate DTOA/DD estimates from the received-signal data. The next chapter covers the signal-processing operations which occur both in the satellites and at the ground terminal, ultimately resulting in joint estimates of DTOA and DD from each observation.

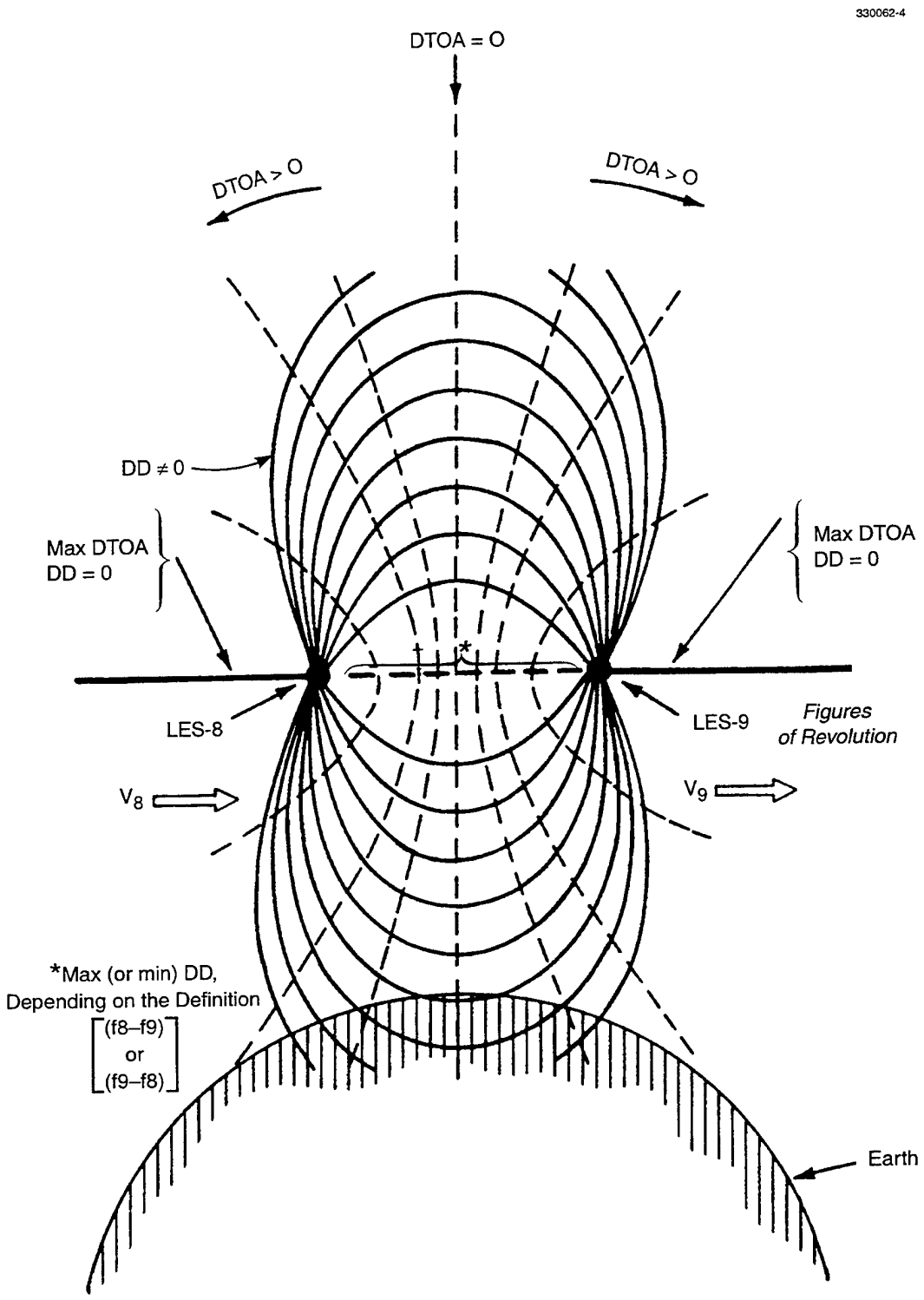

Figure 4. Illustrative DTOA and DD loci.

3. DTOA/DD ESTIMATION

Accurate determination of an emitter's location requires accurate estimation of its DTOA and DD in the presence of received noise and other disturbances. Received-signal information is repeated back to a ground terminal (at Lexington) where the data from the two satellites is cross-correlated to obtain the DTOA/DD estimates. The various signal-processing operations which occur in the satellites and on the ground are described here.

3.1 SATELLITE SIGNAL PROCESSING

Figure 5 shows the overall flow of signal to and from the satellites. Each satellite can be commanded to operate in either a narrowband or wideband mode. The emitter-location function uses the sampled-data channels of LES-8/9, illustrated in block-diagram form in Figure 6. Inphase (I) and quadrature (Q) mixer outputs at baseband are lowpass filtered in either a 3.5 kHz (narrowband) or 35 kHz (wideband) bandwidth. The I and Q waveforms are then hard-limited and each sampled at a 5-kHz (narrowband) or 50-kHz (wideband) rate. The resultant I and Q bit streams are multiplexed together to provide an effective signal data rate of either 10 or 100 kbps. Link management and control information is then multiplexed with the data streams in both satellites. This additional information provides data framing and other functions, and is made available by overwriting the first four of every 50 bits of signal data. Thus eight percent of the signal bits are lost to link overhead.

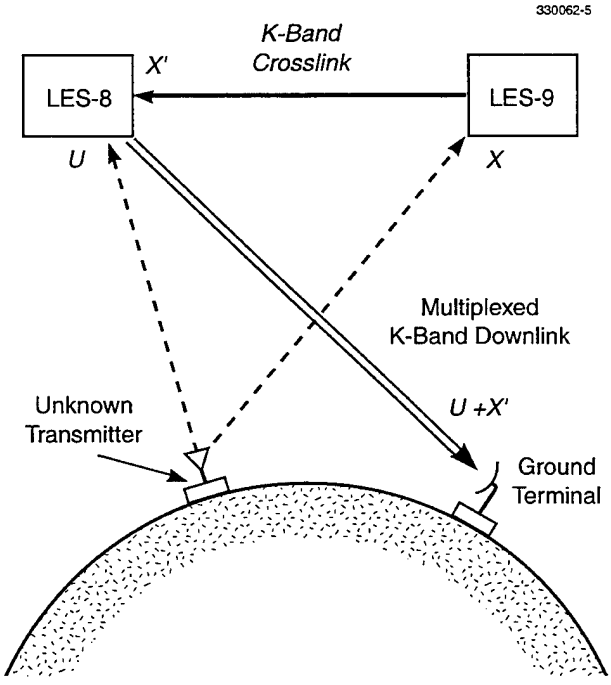

Figure 5. Signal flow through LES-8/9.

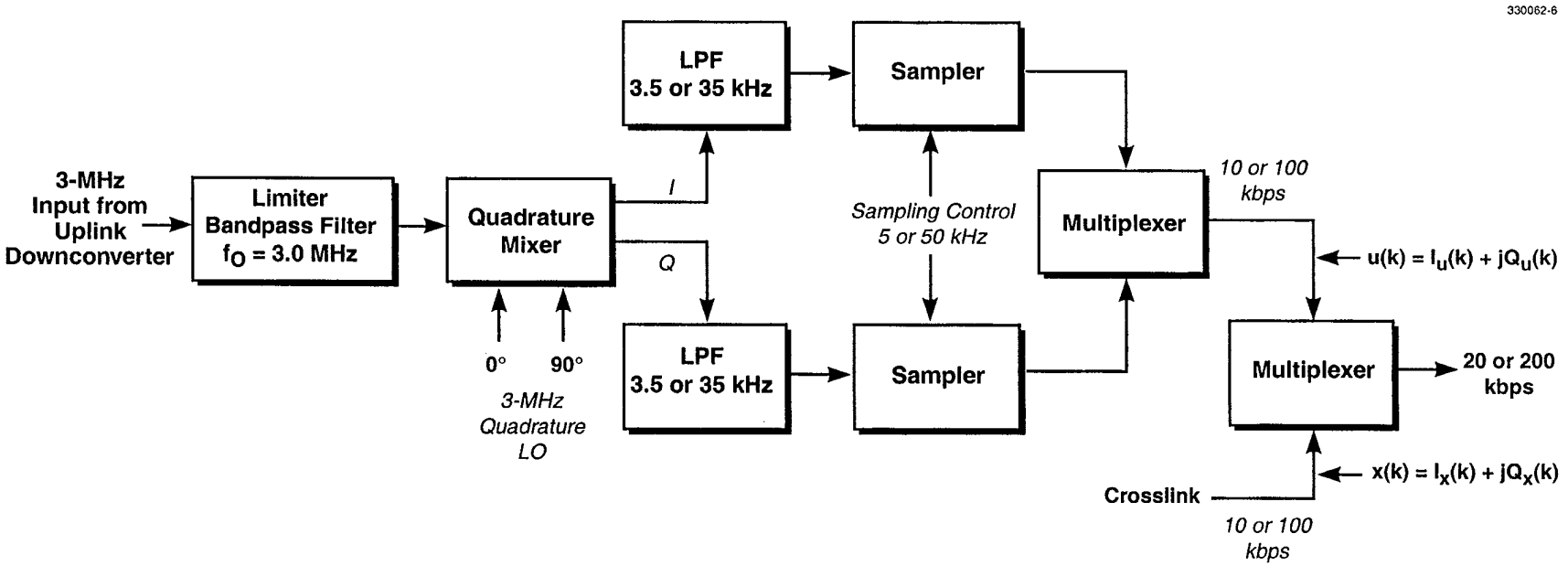

Figure 6. LES-8/9 sampled-data channel.

In LES-8 the data is differentially encoded and modulates a BPSK K-band downlink to the ground station in Lexington. The LES-9 data is relayed via the K-band crosslink to LES-8 where it is multiplexed with the uplink data being received concurrently by LES-8 and both data streams are then transmitted to Lexington. The LES-9 data, as recovered at the ground terminal, is time-delayed with respect to the LES-8 data by the amount of the DTOA *plus* the crosslink propagation delay. The crosslink delay must be calculated from the satellite ephemerides and subtracted out to effectively time-synchronize the two satellite receivers. Because the received-signal information is recovered from the modulation on the K-band signals, no additional Doppler shift is generated in retransmission of the data on the crosslink and downlink.

Although there is no direct synchronization between the satellites, the satellite receiver oscillators and clocks are tied to highly stable frequency standards. Short-term stability is better than 6 parts in 10^9 per 100 μs while long-term drift is less than one part in 10^{11} per day.

3.2 GROUND-TERMINAL DATA COLLECTION

The individual LES-8 and LES-9 data streams are recovered at the ground terminal by demultiplexing. Figure 7 depicts the overall sequence of ground-terminal processing operations. A PDP-11 minicomputer is used as the data-recording instrument. Data-storage capabilities of the PDP-11 allow the accumulation of data in intervals up to a 10 s long in the narrowband mode or 1 s in wideband, the limit being a total of 200,000 data bits per observation. Between intervals, the information is written onto a disk before more data is collected. Thus received-signal information is not actually recorded continuously but rather over a series of disjoint time intervals. The time intervals are short enough that the DD can be treated as being constant over each interval.

The key operation is the cross-correlation of the signal data from LES-8 and LES-9 to obtain the DTOA/DD estimates. The correlation program is not performed in real time since an instantaneous response capability is not required for the LES-8/9 application. Nonetheless a near-real-time system could be implemented with appropriate software and hardware.

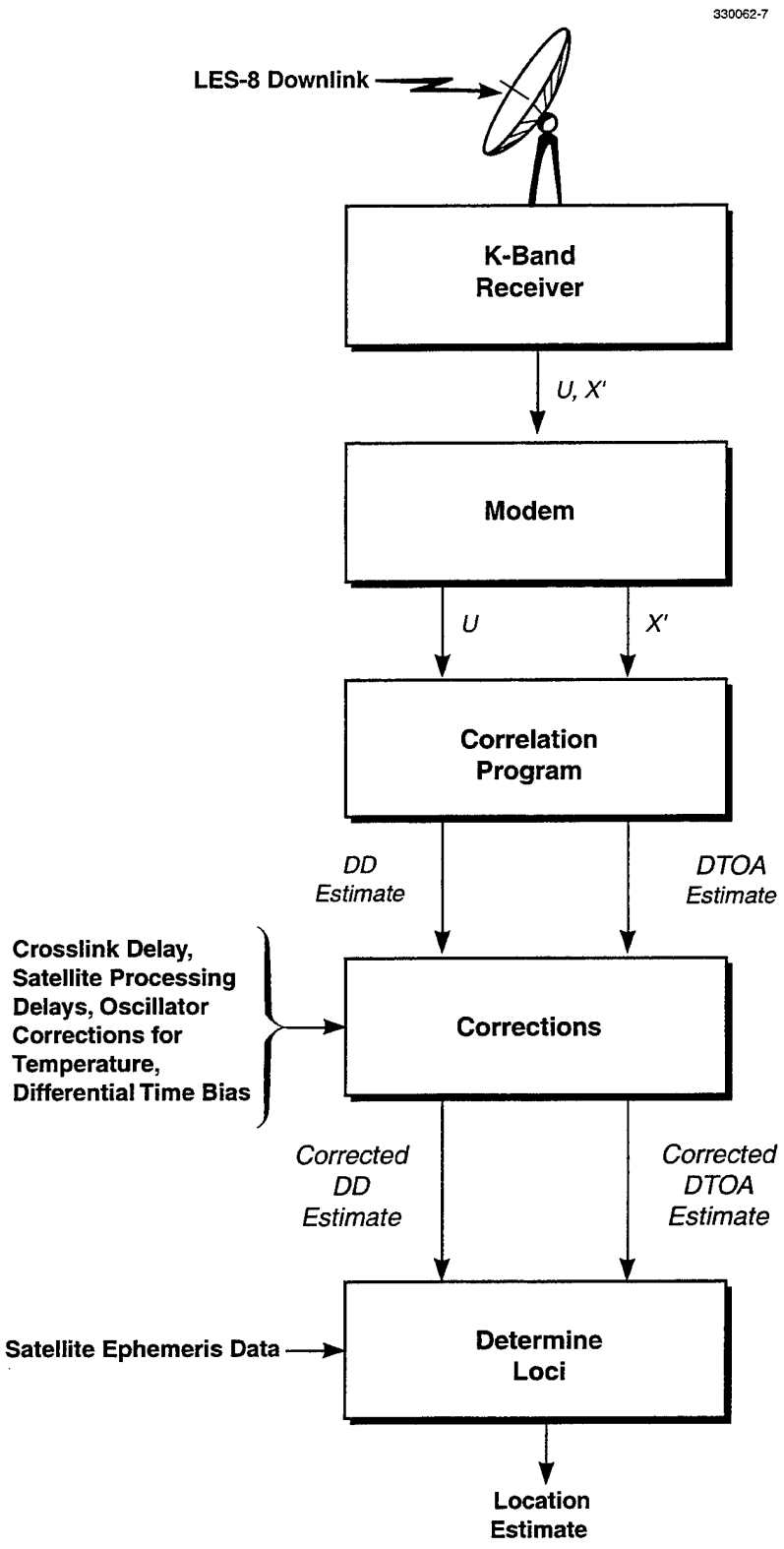

Figure 7. Ground terminal and data processing.

3.3 THREE-STEP CORRELATION/ESTIMATION PROCEDURE

The individual time intervals are each processed independently, one pair of DTOA/DD estimates being extracted from each interval. The problem of estimating these quantities strongly parallels the radar problem of estimating time delay and Doppler shift to obtain range and velocity information about a target. It should be no surprise, therefore, that a correlation estimation procedure similar to that used in radar work is employed here.

The data available for estimating the DTOA/DD consists of discrete-time samples of the hard-limited received-signal waveforms at each satellite. Let u(k) and x(k) represent the k^{th} data samples received from LES-8 and LES-9, respectively, given in the complex-valued form

$$u(k) = I_u(k) + jQ_u(k)$$
$$x(k) = I_x(k) + jQ_x(k) \tag{3.1}$$

where each sample is composed of the I and Q data bits (either 0 or 1) produced at the k^{th} sampling instant.

The correlation processing reproduces the ambiguity function associated with the transmitted signal waveform, albeit a noisy version thereof. The DTOA and DD estimates are given by the values of time and frequency corresponding to the peak of the function, as illustrated in Figure 8.

The estimation procedure is carried out in three stages: (1) computation of "coarse" DTOA/DD estimates, followed by (2) more accurate, "finer-grained" DTOA/DD estimates, and lastly, (3) an interpolation calculation which gives the final DTOA/DD estimates.

The first two steps involve cross-correlating the data sequences obtained from the two satellites using the discrete-time correlation function

$$R(m,n) = \left| \sum_{k=1}^{N} x(k+m)u^*(k)e^{-j\frac{2\pi}{N}nk} \right| \tag{3.2}$$

where m is the time-shift index from DTOA, n is the frequency-shift index for DD, N is the total number of data samples used, and * denotes the complex conjugate. The objective is to find the values of m and n which maximize R(m,n).

At the first step, only a relatively small subset of all the available data samples is used to compute quick, "coarse" estimates by means of Fast Fourier Transform (FFT) techniques. Tentative DTOA/DD estimates are thereby obtained without the need to perform a laborious, time-consuming computation using a large number of (or possibly all) data samples. Let X(p) and U(p) be the FFTs of the sequences x(k) and u(k) respectively, where p is the discrete-frequency index. Then the cross-correlation operation indicated by (3) is carried out by the equivalent calculation

$$R(m,n) = \left| FFT^{-1}[X(p-n)\ U^*(p)] \right| \tag{3.3}$$

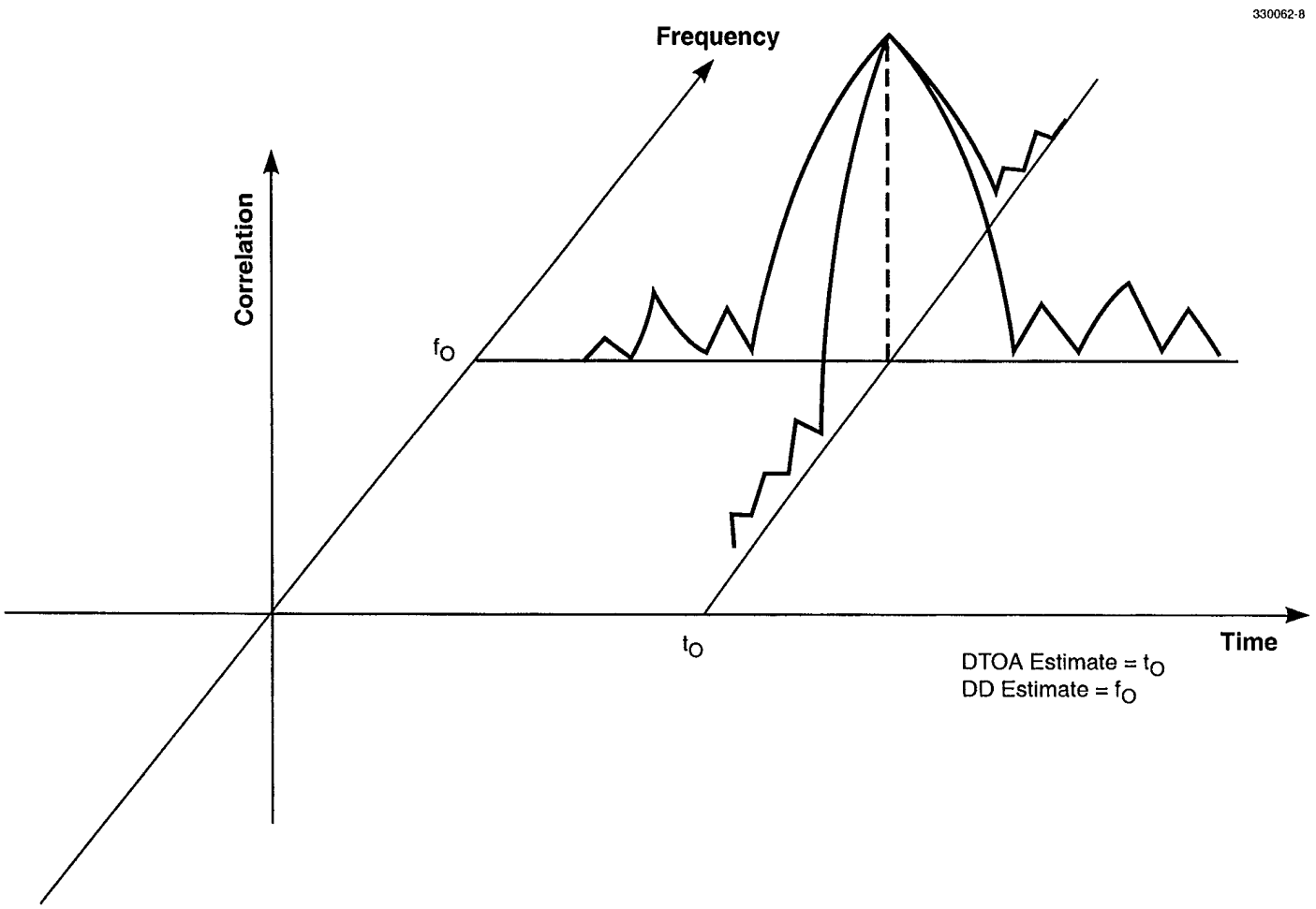

Figure 8. Cross-correlation estimation of DTOA and DD.

where FFT^{-1} denotes inverse FFT. Figure 9 compares the operations (3.2) and (3.3) schematically. The index n which gives the maximum correlation is found by iteration. The time index m corresponding to the peak is read directly from the inverse FFT. 8192-point FFTs are employed in this operation, using data sequences of 4096 x(k) and 4096 u(k) data samples (each padded with 4096 zeros to avoid a "circular" correlation). The time resolution (time-cell size) at this stage is just the sampling time interval: 200 μs in the narrowband mode and 20 μs in wideband. In the frequency domain, the resolution (frequency-cell size) is given by the reciprocal of the time duration of the data segment used for the "coarse" correlation, giving: 0.61 Hz in the narrowband mode and 6.1 Hz in wideband.

After the first step, the search for the correlation peak is narrowed to a neighborhood of several sample points around the tentative DTOA/DD estimate. The correlation procedure in its second step performs a "brute-force" computation of the correlation as given by (3.2) at the candidate DTOA/DD points, using *all* the data samples. The process becomes finer-grained in that each frequency cell from the "coarse' correlation stage is subdivided into smaller cells (by virtue of the time segment used being longer in duration). The time-cell size does not change since it is fixed by the sampling interval. The DD and DTOA resolutions here are: 0.1 Hz and 200 μs (narrowband) or 1.0 Hz and 20 μs (wideband). The accuracy of the DTOA/DD estimates improves at this stage because of the larger number of data samples being employed. A total of N = 50,000 samples each of x(k) and u(k) data is used per observation interval.

The discrete-time correlation given by (3.2) yields estimates only at discrete time and frequency values. An improved DTOA/DD estimate can be obtained by interpolating between sample points of the discrete cross-correlation. Therefore, at the time step, an interpolation procedure, involving a least-squares fit of a paraboloid to several points around the peak found in the second step, is carried out. Figure 10 illustrates the method. An analog reconstruction of the correlation function is thereby generated by the paraboloid, the peak of which gives the DTOA/DD estimates.

3.4 CORRECTIONS TO DTOA/DD ESTIMATES

Corrections to the DTOA/DD estimates must be made to compensate for various fixed, systematic errors or biases, some of which are known *a priori* and some which must be calculated or estimated from various "calibration" data. The first such correction involves the previously mentioned crosslink delay which is simply computed from the satellite ephemerides and subtracted from the DTOA estimate. Processing delays within the satellites themselves, some known and some unknown, are to be determined. The known delays are associated with the so-called "Elastic Shift Register" (ESR) in the crosslink receiver of LES-8[3]. The function of the ESR is to buffer both rate and delay of the received crosslink data. The buffering is needed to assure proper multiplexing of the LES-8/9 data streams in the presence of changing crosslink delays and clock-rate differences between the two satellites. Two buffer clocks are involved. The input clock for rate buffering is derived from the crosslink bit stream while the output clock is synchronized to LES-8's own sampling clock. The amount of buffer storage delay varies but is some number of data samples and is therefore equal to an integral multiple of a sampling period (either 20 or 200 μs). The delay is determined by reading satellite telemetry.

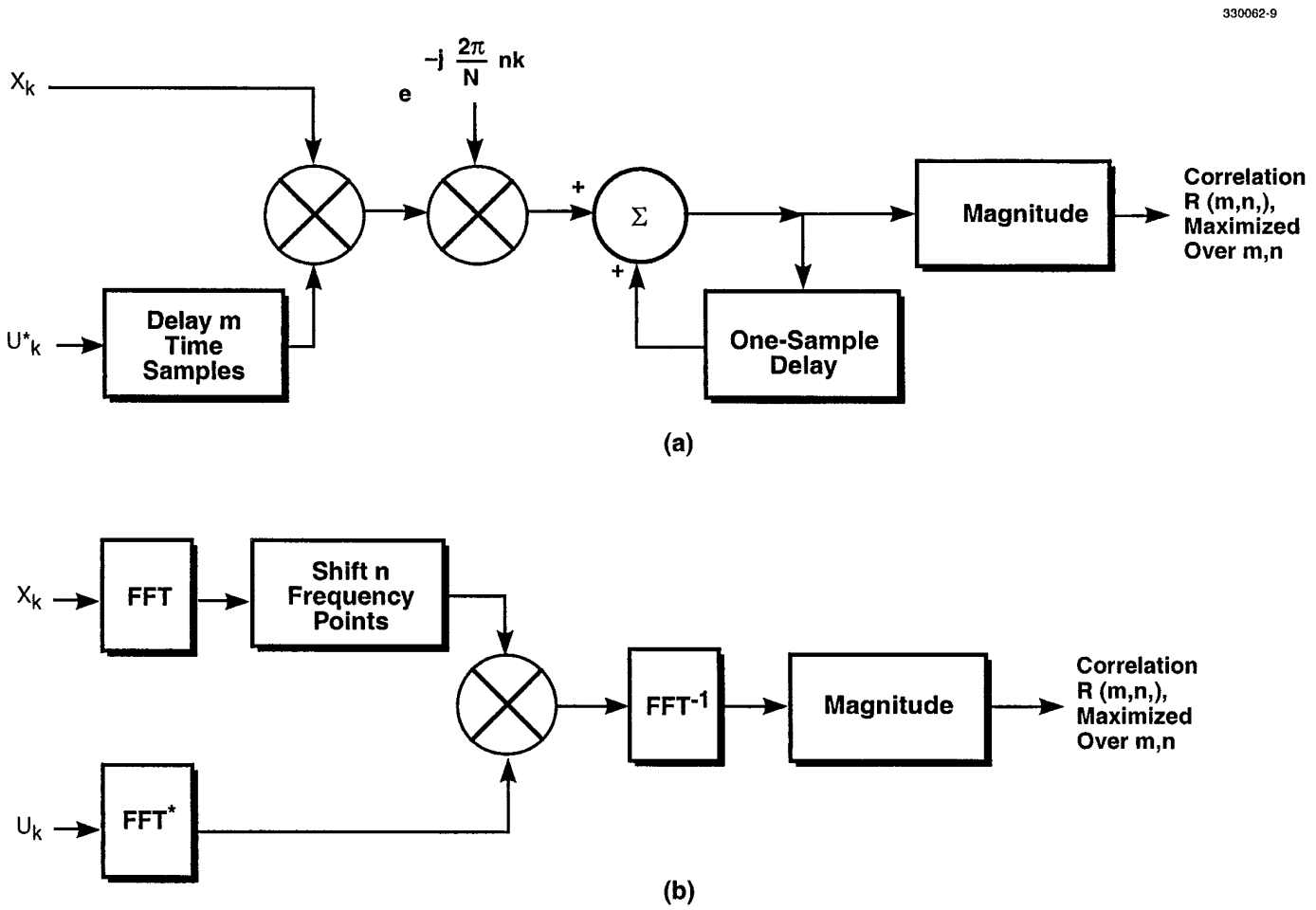

Figure 9. Implementation of DTOA and DD estimation procedures.

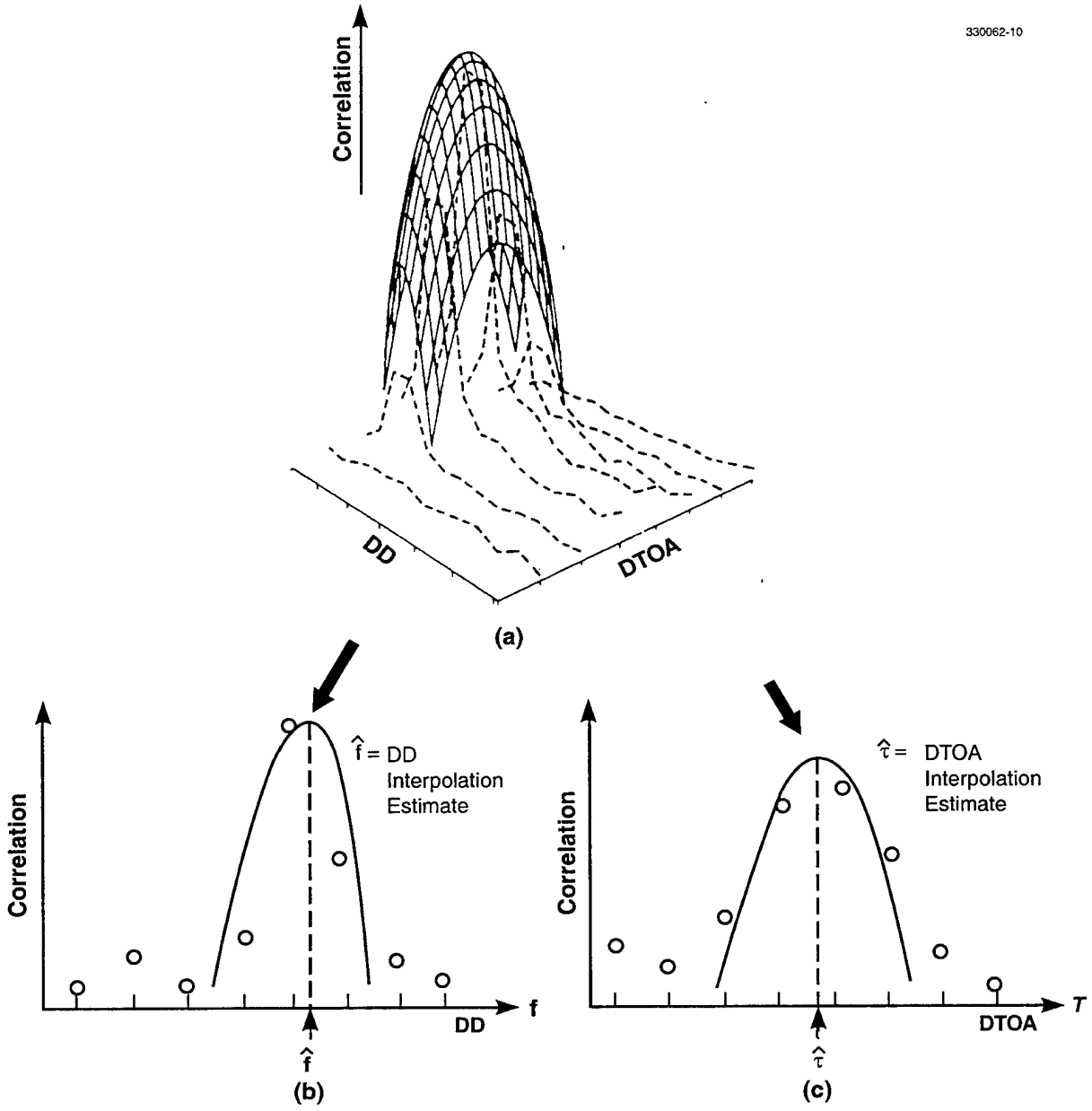

Figure 10. Interpolation estimation of DTOA and DD: (a) Fitting of hyperboloid to discrete correlation function, (b) Cross-section in plane of constant time through peak of hyperboloid, (c) Cross-section in plane of constant frequency through peak of hyperboloid.

An unknown processing delay of a fraction of a sampling interval arises because the sampling times of the received crosslink data (corresponding to the sampling times of the buffer input clock) do not, in general, coincide with the sampling times of the buffer output clock. This sampling delay is then equal to the difference between the time of a sampling instant of the buffer output clock and the arrival time of the next crosslink data bit. The amount of this delay is some fraction of one sample period. The operation of the ESR and the origins of the sampling delay are illustrated in Figure 11. Because the ESR telemetry data provides only buffer delay information which is equal to an integral multiple of a sampling period, the fractional sampling delay is not accounted for and must, therefore, be found by other means.

The unknown delays are estimated by using special "calibration" transmissions from a known site (usually Lincoln Laboratory in Lexington). A DTOA estimate for one such transmission is obtained and the known delays are subtracted out. The difference between the resulting measured value and that predicted for the site based on satellite ephemerides is attributed to the unknown delay. BPSK transmissions using maximal-length shift-register modulation sequences are employed for calibration because of their good correlation properties. For improved accuracy the final estimate of the unknown delay is obtained by averaging the delay estimates for a number of these transmissions (typically 10 or so). To confine most of the signal power to the receiver passband, a bit rate of 2 kHz is used to calibrate the narrowband link, and 20 kHz is employed for wideband.

Finally, the DD data must be corrected for slight temperature-induced frequency shifts in the satellite oscillators. This correction can be computed after observing the drifts over time of each satellite's oscillators at K-band as received on the downlink. The temperature is also monitored via telemetry, and a deterministic frequency versus temperature offset plot is generated. This plot typically exhibits hysteresis, as shown in Figure 12, indicating that one must determine whether the oscillator is operating on a rising or falling portion of the curve. To predict frequency offsets at any time thereafter, it is only necessary to obtain satellite temperature data from telemetry for the time of interest and then refer to the offset curve for the frequency correction. LES-8 generally experiences larger excursions in temperature, and therefore, larger offsets. The differential offset (the difference between the offsets of LES-9 and LES-8) is typically on the order of 0.1 Hz but can be as large as 0.5 Hz. It is added or subtracted, as appropriate, to the DD estimate.

3.5 LOCI DETERMINATION

From the equations of position, (2.1) and (2.3), emitter-position loci may be determined. A computer search algorithm finds a set of solutions to each equation, thereby generating a LOP for each DD or DTOA estimate. With the aid of a computer-based map-plotting package, the loci may be plotted on computer-generated earth maps, with a range of displayed longitude and latitude which can be selected by the user.

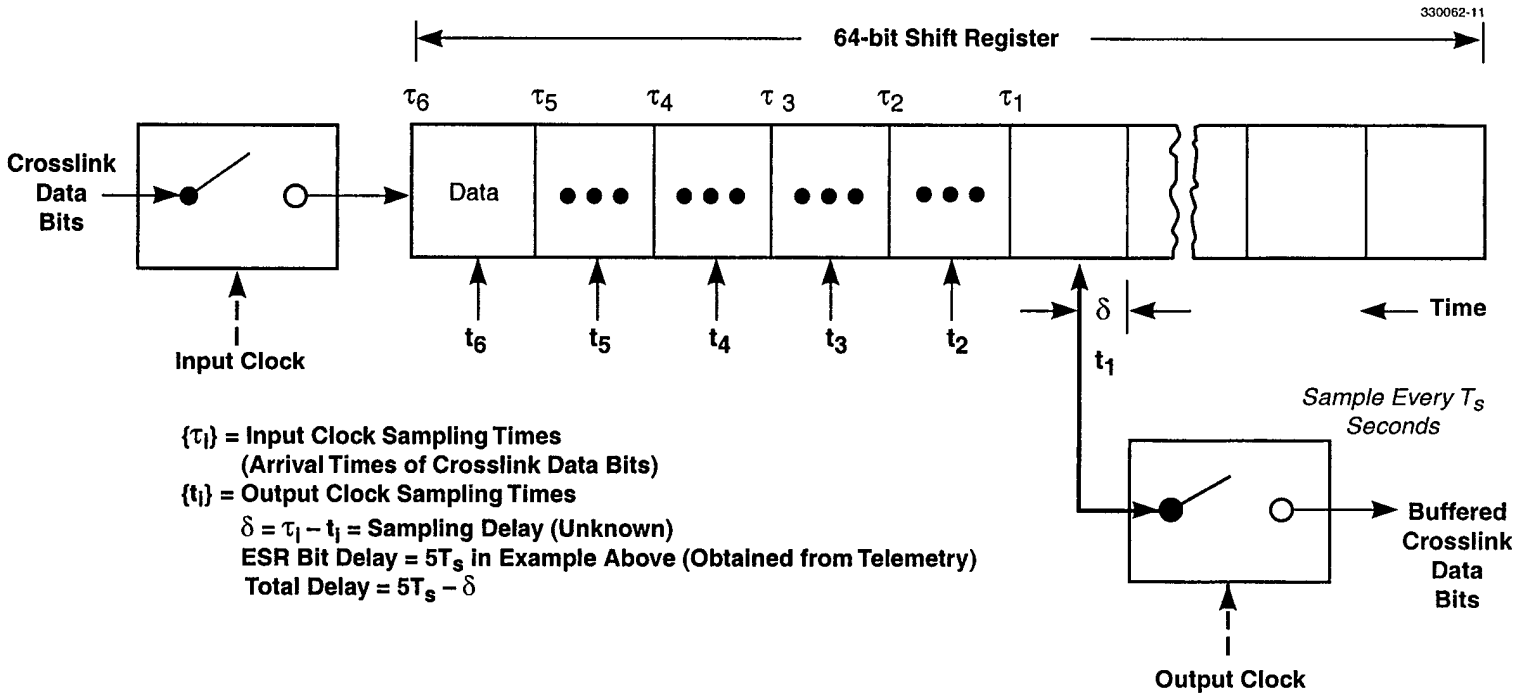

Figure 11. Operation of LES-8/9 elastic shift register.

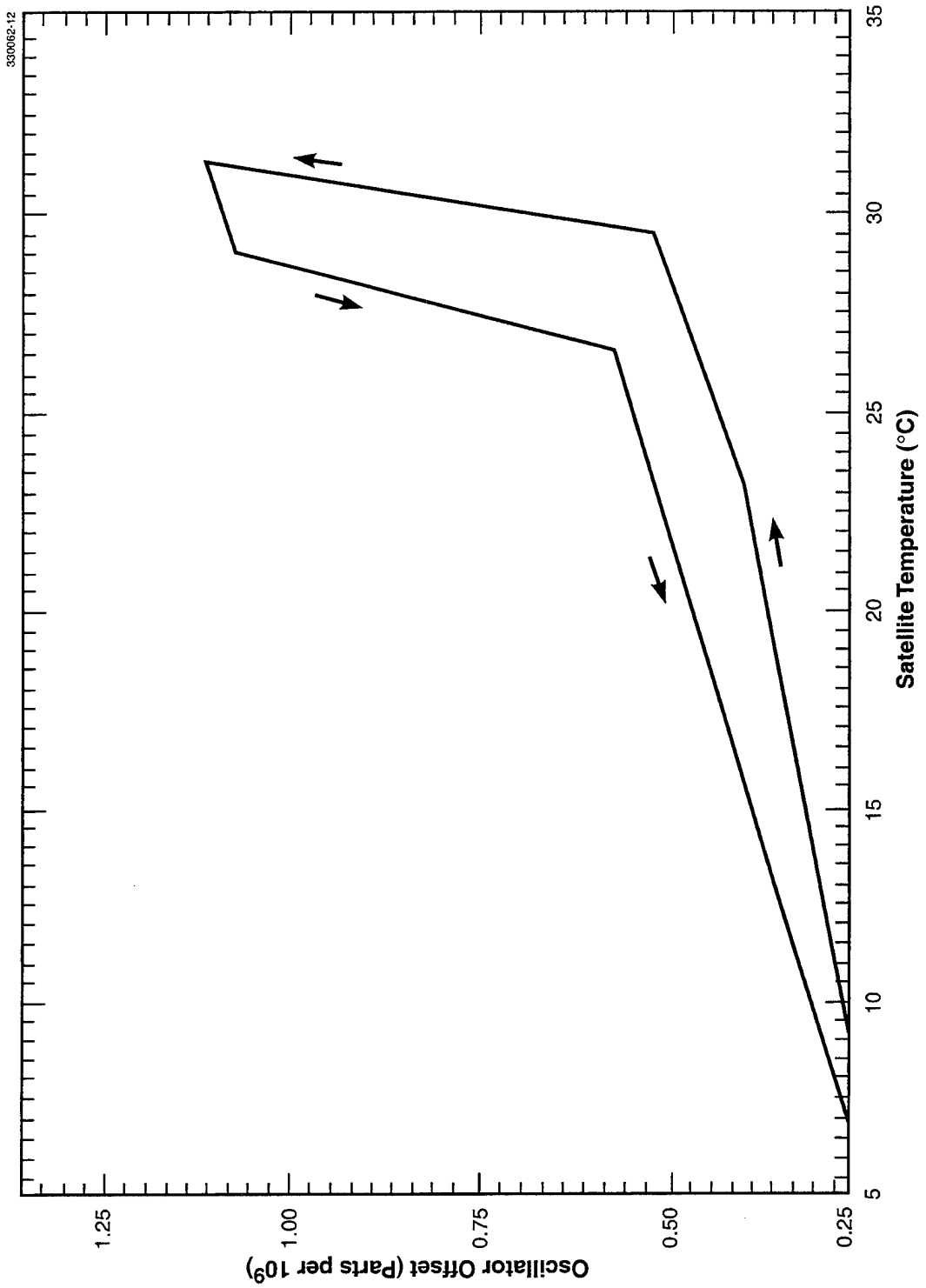

Figure 12. Typical satellite oscillator offset characteristics.

3.6 MULTIPLE-MEASUREMENT COMBINING

While an estimate of emitter location can be made on the basis of a single observation, multiple observations can be used to improve the location accuracy. One procedure for doing so is described here.

Assume N observations are made at time intervals centered at times $\{t_i\}_{i=1}^{N}$, from which are obtained N DTOA/DD estimates $\{\tau_i, f_i\}_{i=1}^{N}$. The problem of estimating the source location can then be posed as one of the finding the location which, in some sense, best "fits" the DTOA/DD data. To every location $\underline{r}_T$ on earth corresponds the data set $\{\tau_i(\underline{r}_T), f_i(\underline{r}_T)\}_{i=1}^{N}$ for the observation times $\{t_i\}_{i=1}^{N}$, giving the DTOA/DD data which would be obtained for $\underline{r}_T$ from perfect measurements with the satellites. This information can be computed from equations (2.1)–(2.3). The location estimate $\hat{\underline{r}}_T$ is then chosen to be the $\underline{r}_T$ which gives a least-squared-error fit,

$$\hat{\underline{r}}_T = \left\{\underline{r}_T : \varepsilon(\underline{r}_T) = \min_{\underline{r}_T} \varepsilon(\underline{r}_T)\right\}$$

$$\varepsilon(\underline{r}_T) = \sum_{i=1}^{N}\left\{w_{1,i}\left[\tau_i(\underline{r}_T) - \tau_i\right]^2 + w_{2,i}\left[f_i(\underline{r}_T) - f_i\right]^2\right\}$$

$w_{1,i}$ and $w_{2,i}$ are weighting factors. When the DTOA and DD estimation errors are independent, zero-mean Gaussian random variables, it can be shown that the choice

$$w_{1,i} = \left[\sigma_{DTOA}(i)\right]^{-2}$$

$$w_{2,i} = \left[\sigma_{DD}(i)\right]^{-2}$$

where $[\sigma_{DTOA}(i)]^2$ and $[\sigma_{DD}(i)]^2$ are the DTOA and DD estimation variances at times t_i, results in the maximum-likelihood estimate for $\underline{r}_T$.

4. LIMITATIONS ON LOCATION-ESTIMATION ACCURACY

In the absence of systematic errors or biases, the accuracy with which an emitter can be located is limited ultimately by inevitable noise-induced errors in estimating DTOA and DD. Therefore it is of interest to know how accurately these quantities can be estimated. Some statistical estimation results are given here. In practical systems, however, other errors are incurred, including those due to imperfections in the satellite receivers, disturbances on the various links, inaccuracies in knowledge of satellite ephemerides, and any emitter motion. The effects of these errors are discussed here. Finally, consideration is given to the role of the satellite/emitter geometry in location accuracy.

4.1 DTOA/DD ESTIMATION

The fundamental limitation on DTOA/DD estimation accuracy is receiver and/or background noise, which can usually be modeled as additive white Gaussian noise (AWGN). Cramer-Rao bounds on the standard deviation of the estimation errors can be found in Reference 4.

$$\sigma_{DTOA} \geq \frac{1}{\beta\sqrt{BT\rho}}$$

$$\sigma_{DD} \geq \frac{1}{T_o\sqrt{BT\rho}} \tag{4.1}$$

where B is the receiver noise bandwidth (which is assumed to be the same for both receivers), β is the rms bandwidth of the signal, T is the observation-interval length, T_o is the rms duration of the signal, and ρ is the effective signal-to-noise ratio (SNR) at the receiver inputs. The various parameters are defined as

$$\beta = 2\pi\left[\frac{\int_{-\infty}^{\infty} f^2 S(f)df}{\int_{-\infty}^{\infty} S(f)df}\right]^{1/2} \tag{4.2}$$

where S(f) is the signal power-density spectrum which is assumed to have zero centroid, and

$$T_o = 2\pi\left[\frac{\int_{-\infty}^{\infty} t^2|s(t)|^2 dt}{\int_{-\infty}^{\infty}|s(t)|dt}\right]^{1/2} \tag{4.3}$$

for the signal s(t) where $|s(t)|^2$ is assumed to have zero centroid, and

$$\frac{1}{\rho} = \frac{1}{2}\left[\frac{1}{\rho_8} + \frac{1}{\rho_9} + \frac{1}{\rho_8\rho_9}\right] \tag{4.4}$$

where ρ_8 and ρ_9 are the SNRs in each receiver in the noise bandwidth B. In practice, the performance given by these lower bounds is approached only when the SNR is large and/or the signal time-bandwidth product is large.

It is evident from (4.1) that signals with large bandwidth can be expected to yield the most accurate DTOA estimates, while those of long time duration should give the best DD estimates. (The same time-bandwidth considerations apply, of course, in radar work where time delay and Doppler estimation accuracies depend upon the choice of transmitting waveforms.) Also indicated by the bounds is the fact that very narrowband emitters, e.g. CW, will give poor DTOA accuracy, so that one may be forced to employ an emitter-location approach which ignores the DTOA data and uses only DD information. The DD accuracy in this case is likely to be good, however, since the signal will, of necessity, be of relatively long time duration. Narrowband sources are usually recognized by the width of the cross-correlation function being large in the time domain. Similarly, very short-pulse emitters may yield poor DD but good DTOA accuracy, so that a DTOA-only method must be pursued. In the latter case, the cross-correlation will be broad in frequency, but relatively narrow in the time domain. Those emitters with sufficiently large bandwidth and effective time duration may be located by use of both DTOA and DD.

In the event that a DTOA-only or DD-only approach is used, at least two measurements of the one observable at two *different* times by both satellites are required to generate at least two different loci of possible locations. The intersection of the pair of DTOA or DD loci gives the "fix." Because of the need for different observation times, a near-instantaneous location estimate is not possible. In fact, obtaining loci which intersect nearly orthogonal to one another for best location accuracy requires a substantial change in the satellite/emitter geometry between observations. With LES-8/9 an inter-observation wait is typically several hours, but in practice the DTOA loci are never found to be close to orthogonal because the satellites always remain relatively close together in their present stations. Therefore, use of both DTOA and DD data from the same observation is the preferred approach whenever possible.

Certain types of signals will yield estimation ambiguities, resulting from multiple peaks in the cross-correlation and thus multiple location possibilities. An example occurs in DTOA for signals with repetitive modulation occurring at sufficiently high repetition rates. Additional observations taken at later times may resolve the ambiguities.

The Cramer-Rao bounds can be quantified to provide benchmark performance limits for LES-8/9. For simplicity, assume that the received signal has a flat spectrum over the receiver passband and a constant-amplitude envelope over the duration of one observation interval. The bounds then reduce to

$$\sigma_{DTOA} \geq \frac{0.55}{B} \frac{1}{\sqrt{BT\rho}}$$

$$\sigma_{DD} \geq \frac{0.55}{T} \frac{1}{\sqrt{BT\rho}} \qquad (4.5)$$

If it is assumed that the –3 dB receiver bandwidth equals the receiver noise bandwidth (B = 35 kHz in wideband and 3.5 kHz in narrowband), one obtains the DTOA error performance plotted in Figure 13 for both modes. (The narrowband mode gives poorer DTOA accuracy.) The results for DD estimation accuracy are given in Figure 14, with the narrowband mode giving better performance.

In examining Figures 13 and 14, a fundamental difficulty with use of LES-8/9 for DTOA/DD measurement comes to light. Recalling that the received signals are hard-limited and sampled, attaining the DTOA estimation performance given in Figure 13 with a sampling interval of 20 μs becomes a non-trivial problem. Accuracy of DTOA estimates obtained from noisy, sampled, clipped data has been studied by Berger (Reference 5) and some of the key findings are summarized here. Expressions for bias and variance are developed in Reference 5. Plots based on those results are given in Figures 15 and 16 (the exact expressions are too complicated to give much insight into the problem and will not be given here). The bias and variance depend upon the sampling interval T_s, and the parameters $a^2 = \rho_8/\beta T$ and $b^2 = \rho_9/\beta T$, where ρ_8 and ρ_9 and β are as defined earlier, and $\overline{C} = 2NT_s\beta$, with N being the total number of data samples ($\overline{C}$ is the expected number of zero-crossings which occur in NT_s seconds for a Gaussian signal of statistical rms bandwidth β, Δ is the DTOA modulo T_s and $\hat{\Delta}$ is the estimate of Δ). The results assume the differential Doppler shift at each receiver is zero, the received signal itself is Gaussian and the final DTOA estimates are obtained by a quadratic interpolation procedure like that used with LES-8/9.

What is indicated in Figures 15 and 16 is that the bias depends upon the value of DTOA itself and is non-zero even when the receiver SNR is infinite. The variance, in the range $|\Delta| \leq 0.4\ T_s$, decreases with increasing SNR but is never zero for finite N unless $\Delta = 0$. However, variance does tend to zero as N becomes large. (Bias and variance are given only for the range $|\Delta| \leq 0.5\ T_s$ since it is assumed the estimation accuracy is good enough so that the error is smaller in magnitude than the size of a sampling interval.) A fundamental limitation arising from clipping and sampling is the bias, which, unlike the variance, is not reduced by using a longer data segment. Performance is not readily compared to that given by the Cramer-Rao bounds in (4.1) except on a scenario-by-scenario basis. In selected situations, however, the degradation in rms error from clipping and sampling is found to range from almost none to more than an order of magnitude. All other things being equal, the best accuracy is obtained by decreasing the sampling interval (i.e., using the wideband LES-8/9 mode of operation). The effects on DD estimation accuracy have not been studied.

4.2 EFFECTS OF SATELLITE-RECEIVER IMPERFECTIONS

DTOA and DD estimation accuracies are affected by the extent to which the satellite receivers distort the received signals (outside of clipping and sampling) because of receiver characteristics which are deficiencies from the standpoint of emitter location. (The receivers were not designed with emitter location as a consideration.) No attempt is made to quantify all the various effects. They will simply be described here.

Some obvious receiver imperfections, which would also affect the normal communications system performance, include oscillator phase noise and unwanted AM/PM conversion which can affect DD

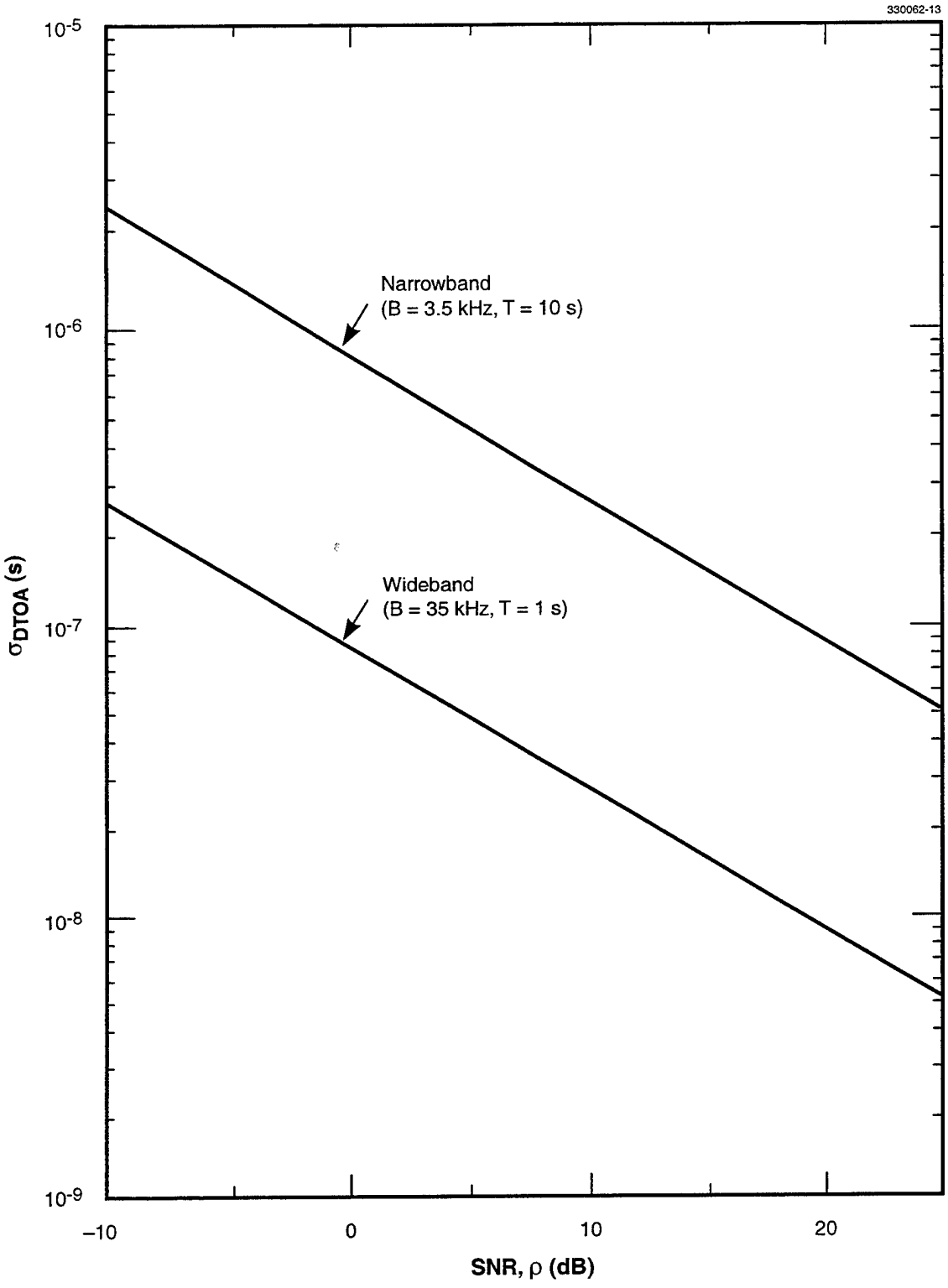

Figure 13. Standard deviation of DTOA estimation error from Cramer-Rao bound.

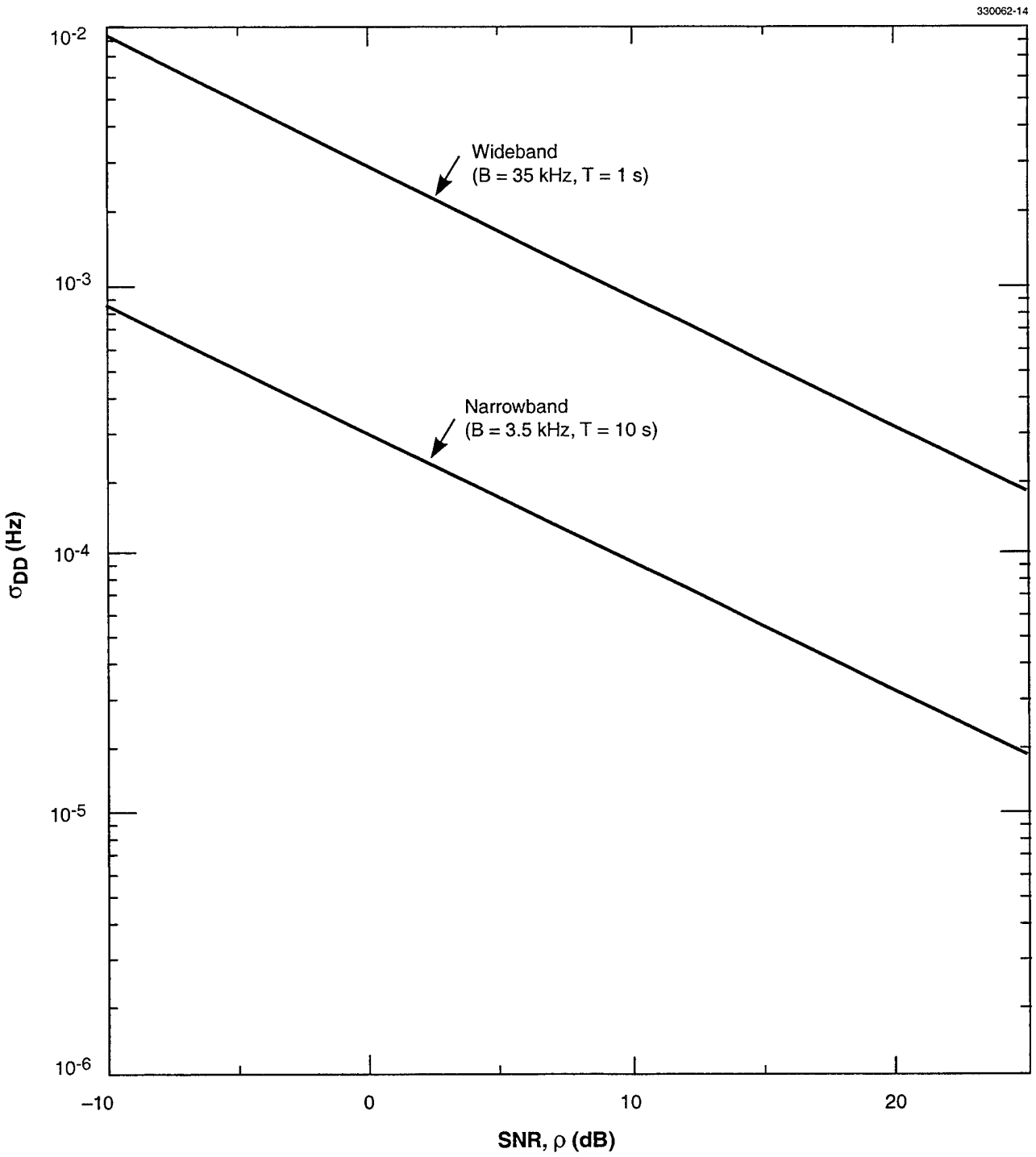

Figure 14. Standard deviation of DD estimation error from Cramer-Rao bound.

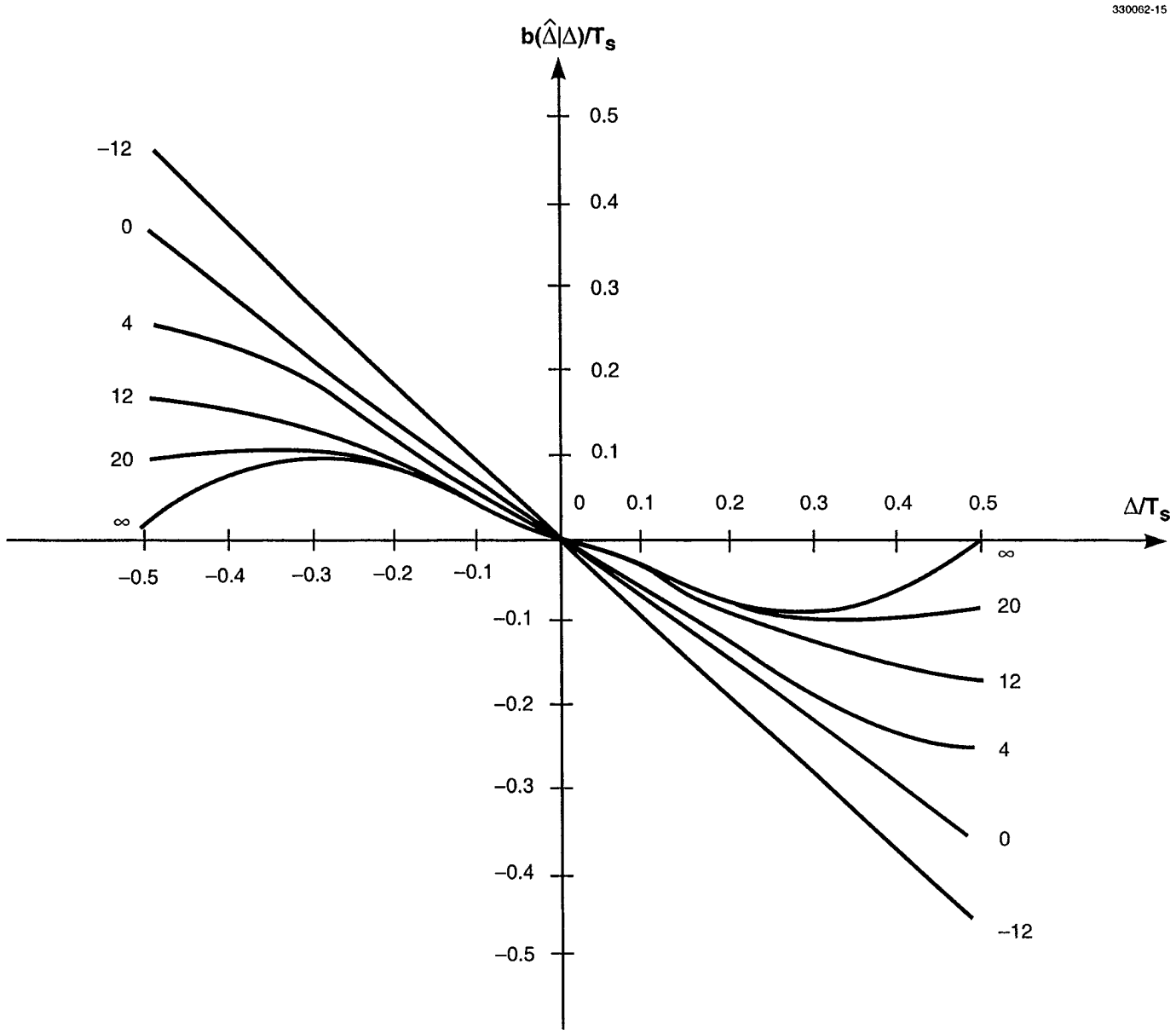

Figure 15. Normalized DTOA interpolation-estimation bias with $-10 \log a^2 = -10 \log b^2$ as a parameter.

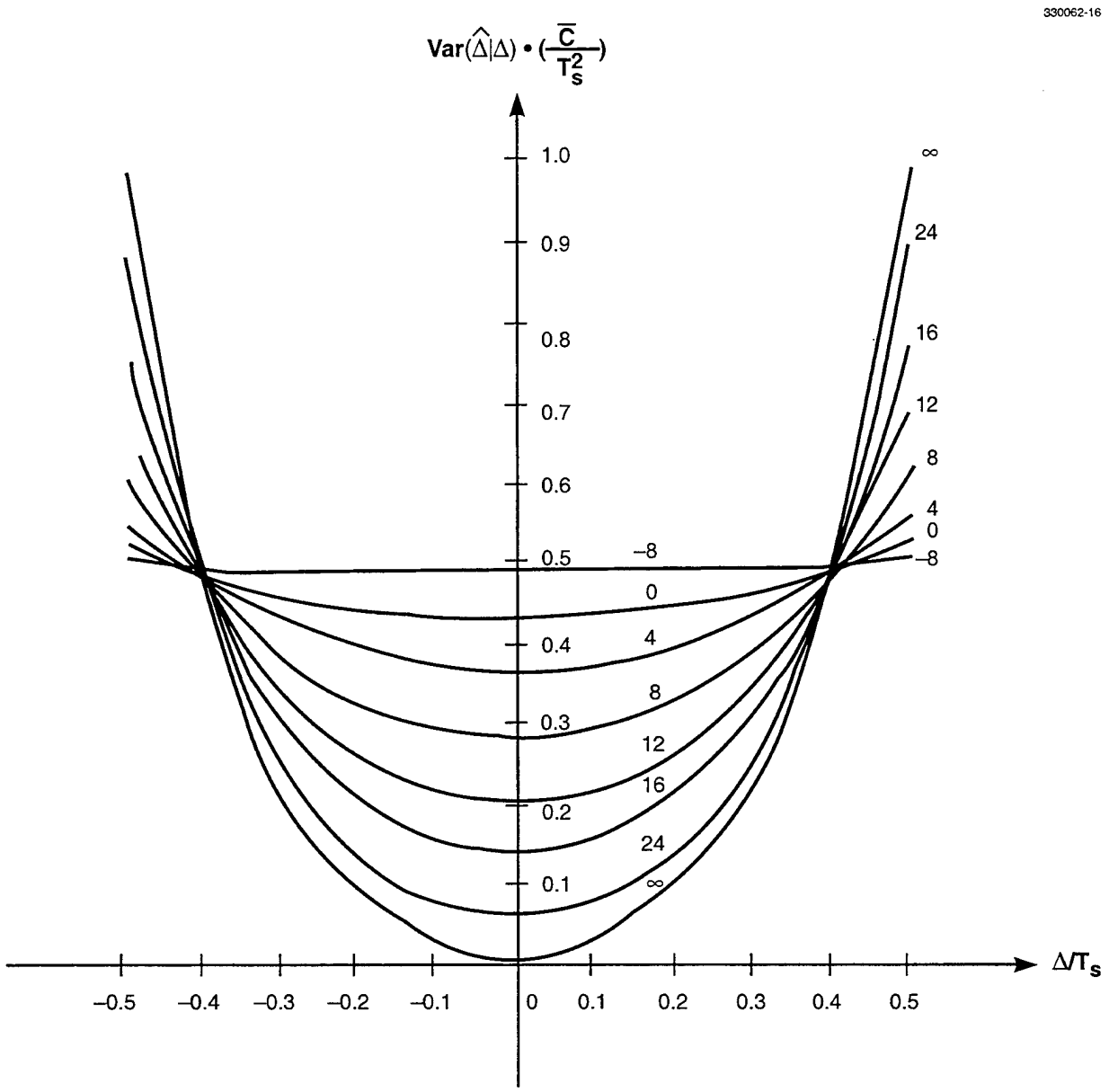

Figure 16. Normalized DTOA interpolation-estimation variance with $-10 \log a^2 = -10 \log b^2$ as a parameter.

estimation accuracy, and any non-linearities which give rise to intermodulation distortions or other spurious responses that interfere with the desired signal.

Various filters in the receivers exhibit unavoidable phase shifts which, in general, will vary across their passbands. The resultant group-delay characteristics can contribute to the DTOA error to the extent that the group-delay characteristics in the two satellite receivers are not exactly matched to each other. No information is available on the amount of mismatch. The overall group delays in the individual receiver are[6] 300 μs in the narrowband mode and 55 μs in wideband. If the group-delay characteristics in the two satellites can be assumed to be matched within 10%, then the differential group delays can be as large as 30 μs and 5.5 μs in the narrowband and wideband modes, respectively. The mismatch can be expected to be largest at the edges of the filter passbands. The effect on DTOA estimation accuracy will depend upon the signal being received. Narrowband signals near the edges of the receiver passband will likely be most affected. DD estimates for signals with frequency modulations can also be degraded since the differential phase response in the receivers can induce spurious phase modulation in the signal. The group delay-effects are also temperature dependent and thus can vary over time.

Other systematic errors which are estimated and factored out include satellite oscillator drifts with temperature (which were discussed in Section 3) and the unknown faction-of-a-sample time delay (also described in Section 3). To some extent, the unknown differential group delay between the two satellite receivers is also accounted for by the time-delay "calibration" procedure using test transmissions from a known site. Because the differential group delay will vary with frequency, the correction obtained from the wideband "calibration" signal really represents an averaging of the effects over the passband of the receivers. The actual DTOA error in a given situation will depend upon the spectrum of the particular signal being received. The procedures for estimating systematic errors, being imperfect, do not completely eliminate the systematic effects. However, the temperature-related oscillator errors after correction have been calculated as contributing no more than 0.05 Hz to the DD error. The various time-delay biases can be estimated to an accuracy of one-fourth of a sampling period, resulting in an additional error of up to 50 μs in the narrowband mode and 5 μs in wideband.

Finally, the DTOA/DD estimates will be slightly degraded by the loss of received-signal information bits to the overwrite bits (as discussed in Section 3).

4.3 LINK EFFECTS

The ability to locate a source can be degraded by the presence of other uplink signals in the passbands of the receivers. If the multiple emitters can be resolved in their DTOA and DD, their locations can all be estimated simultaneously. If they are not resolvable, substantial errors may be incurred in attempting to locate any one emitter. Although this issue can be important in some applications, it is typically not a problem with LES-8/9 since an RFI source under investigation is typically an isolated, strong signal and is received in a relatively narrow receiver bandwidth.

Ionospheric refractivity effects will create additional time delays and frequency shifts in the uplink signals, possibly affecting the DTOA and DD data. Such ionospheric effects are under continuing study by a number of researchers. At UHF, however, the effects are relatively small compared to other sources

of error and no attempt has been made to compensate for them when using LES-8/9 for source location. In fact, in one test, data taken during a period of ionospheric disturbance yielded no apparent increase in error compared to that from other times.

Also, of course, any errors in relay of satellite data via the crosslink or downlink will contribute to additional errors in the DTOA/DD estimates. This effect is small in comparison to other sources of error, however. The crosslink is essential error-free in normal operation while the downlink operates with a bit-error rate typically in the range of 10^{-2}.

4.4 ACCURACY OF SATELLITE EPHEMERIDES INFORMATION

Computation of emitter LOPs requires knowledge of the satellite positions and velocities. Therefore, errors in that knowledge will affect location-estimation accuracy. As discussed in Chapter 1, orbit-fitting is accomplished by the Laboratory's Planetary Ephemeris Program (PEP) which uses ranging data, taken periodically, to generate orbital-parameter estimates. These estimates can be extrapolated backward or forward in time. Orbital predictions are updated approximately bimonthly when ranging data is taken, and they are most accurate for the time around the update. Their accuracy degrades with time.

A study of orbit-fitting errors indicates that at any one time, the magnitudes of X-Y-Z components of the velocities $\underline{v}_8$ and $\underline{v}_9$ are known to within approximately 10^{-4} km/s, while the magnitudes of the X-Y-Z components of positions $\underline{r}_8$ and $\underline{r}_9$ are accurate to 10 km or so. The contribution to the location-estimation error is discussed in Section 4.6, Geometric Considerations. (See Appendix A for more details on orbit-fitting errors.)

4.5 SOURCE MOTION

The DTOA/DD technique assumes the transmitting source is stationary. A moving source generates a different DD than a stationary one and, in general, will induce location-estimation errors. The DD equation (2.3) can be modified to take the motion into account. If $\underline{v}_T$ is the source velocity vector, $\underline{v}_8$ is replaced by $\underline{v}_8 - \underline{v}_T$, and $\underline{v}_9$ by $\underline{v}_9 - \underline{v}_T$, resulting in

$$f = \left[\left(\underline{v}_9 - \underline{v}_T\right)\cdot \underline{i}_9 - \left(\underline{v}_8 - \underline{v}_T\right)\cdot \underline{i}_8\right]\frac{f_o}{c} \tag{4.6}$$

The DTOA estimate is not affected by the motion to the extent that the change in $\underline{r}_T$ is small over an observation interval.

Knowing $\underline{v}_T$ permits proper determination of location from the DD information. However, for sources of unknown origin, $\underline{v}_T$ will not be known and ideally should be estimated simultaneously with the DTOA and DD. A single observation by the two satellites with the three resultant location equations (2.1), (2.2) and (2.3) is insufficient for unique determination of both $\underline{r}_T$ and $\underline{v}_T$. More receivers are required to provide the additional information needed if location is to be estimated from one observation. Since only two receivers are available with LES-8/9, using multiple observations at different times might suffice, provided $\underline{v}_T$ is known to be the same over the entire period of data-taking and the change in $\underline{r}_T$

is negligible between observations. From a practical standpoint, however, nothing can be assumed a *priori* about $\underline{v}_T$ for an unknown source and estimating $\underline{v}_T$ (and consequently the location rT) is realistically infeasible with LES-8/9.

An alternative to dealing with a moving emitter is to ignore the DD data altogether and estimate its position from DTOA data only, provided the emitter is in fact known to be nonstationary. The existence of substantial emitter velocity (aircraft speeds, typically) may be inferred from DD data whose magnitude or rate-of-change is outside the range possible for a fixed emitter. With LES-8/9, DD for fixed sources is usually no greater than ±15 Hz, with up to ±0.1 Hz/min rate-of-change, depending upon the emitter location and the satellite positions and velocities. DTOA estimates from the two receivers at two different times (typically several hours apart for LES-8/9) can be used, provided the change in $\underline{r}_T$ is small between observations.

Roughly speaking, the effects of emitter motion can be considered negligible only if its velocity is very much smaller in magnitude than the satellite velocities with respect to the earth. It is possible in some situations that antenna movement, caused by wind, for example, can affect the DD data and therefore the location accuracy, even though the transmitter itself is actually stationary.

Results of tests on DD location accuracy conducted with a cooperating airborne emitter are discussed in detail in Section 5.

4.6 GEOMETRIC CONSIDERATIONS

Emitter-location accuracy can be strongly dependent upon the positions and velocities of the satellites with respect to the emitter. Some geometries are more favorable than others in that they yield greater location accuracy for given DTOA/DD estimation errors.

A qualitative argument can be made to distinguish "good" from "bad" geometries. Assume (ideally) that emitter-location errors arise only from the DTOA/DD estimation errors, i.e., the system errors not related to DTOA/DD estimation are negligible, and that the DTOA/DD errors are geometry-independent. The desirable geometries are those that result in emitter-position loci which are least sensitive to changes in the values of the DTOA and DD, and therefore to errors in those quantities. It follows necessarily, then, that in those situations, the *a priori* uncertainty in location (usually the entire visible earth) corresponds to a large range of possible values of DTOA and DD for the emitter in question. Therefore, satellite positions and velocities should be such that large values of DTOA and DD can be generated for a wide range of locations on the earth. The geometries which give the largest DTOA are those in which the satellites tend to be spatially separated by large distances. The largest DD values arise when the differential velocity of the satellites is large, which implies that the individual satellite velocity vectors are large in magnitude and/or point in widely different directions relative to the emitter.

An analysis giving explicit formulas relating location accuracy to geometry has been reported in a 1982 paper[7] and confirms these qualitative notions. The results from that paper are summarized here and used to give an indication of the location-estimation accuracies achievable from LES-8/9. The expressions for location accuracy are of the form

$$\sigma = MG \tag{4.7}$$

where σ is the standard deviation of the location area, M is a measurement factor, and G is a geometric factor. M depends only on the accuracy of the DTOA or DD estimates and the accuracy of the satellite position/velocity information. Other sources of error are not considered. G is a function of the actual positions and velocities of the satellites with respect to the emitter.

In the case of location accuracy (σ_1) from DTOA, the measurement and geometric factors are given by [18]

$$M_1 = \left(\sigma_{DTOA}^2 + 2\sigma_p^2 / c^2\right)^{1/2}$$

$$G_1 = c / \left[4\sin^2(\theta/2) - \left(\cos\phi_8 - \cos\phi_9\right)^2\right]^{1/2} \tag{4.8}$$

σ_p is the standard deviation of the error in the estimates of each of the satellite's X-Y-Z position coordinates, with that error assumed to be the same along each coordinate. c is the speed of light and σ_{TOA} the standard deviation of the DTOA-estimation error. The various terms in the geometric factor can be explained by referring to Figure 3. θ is the angle subtended at the transmitter by the two satellites, ϕ_8 is the angle between $\underline{r}_8 - \underline{r}_T$ (note the reversal with respect to Figure 3) and $\underline{r}_T$, and ϕ_9, the angle between $\underline{r}_9 - \underline{r}_T$ and $\underline{r}_T$.

Since G_1 is scenario-dependent, no single value can be applied for all possible emitter locations. To give an indication of the kind of accuracy achievable with LES-8/9, assume the emitter is located at the midpoint between the subsatellite points on earth. Then $\phi_8 = \phi_9$ and G_1 reduces to

$$G_1 = \frac{c}{2\left|\sin(\theta/2)\right|} \tag{4.9}$$

To relate G_1 to the results to be described in the following chapter, it is noted that the intersatellite separation for that work was rather small, with $\theta \approx 3°$. Thus one finds that G_1 gives 5.7 km per μs of measurement error.

In the wideband receiving mode of the satellite, σ_{DTOA} is estimated to be 5 μs at best, based on knowledge of the various factors contributing to the DTOA estimation error. σ_p is estimated to be typically 5 km, although this value will vary over time, depending upon the quality of a given day's orbit fit. Then the measurement factor using the aforementioned values of σ_{DTOA} and σ_p is M_1 = 24 μs, where it is noted that the σ_p error dominates σ_{DTOA} error. The location error σ_1 from the DTOA data is then about 137 km.

In the narrowband receiving mode, σ_{DTOA} can be expected to increase by a factor of ten to 50 μs, giving M_1 = 55 μs, where now the DTOA estimation error is more significant that the orbit-fitting error. The location error increases to 314 km.

Although the preceding numbers were calculated for an emitter situated between the subsatellite points, they should be indicative of the kind of accuracy to be expected for other locations because of

the relative closeness of LES-8 and LES-9 to each other at all times. The largest deviation from the calculated figures will occur for emitters around the edges of the visible earth. The accuracy can be improved by increasing the separation between satellites so as to increase the angle θ and thereby reducing the geometric sensitivity G_1.

The formulas for M and G as they relate to the accuracy (σ_2) from DD are [18]

$$M_2 = \left[\sigma_{DD}^2 + 2\sigma_v^2/\lambda^2 + \left(\dot{\alpha}_8^2 + \dot{\alpha}_9^2\right)\alpha_\pi^2/(2\lambda)^2\right]^{1/2}$$

$$G_2 = \left[\dot{\alpha}_9^2 + \dot{\alpha}_8^2 - 2\dot{\alpha}_8\dot{\alpha}_9\cos\gamma - \left(\dot{\alpha}_9\cos\beta_9 - \dot{\alpha}_8\cos\beta_8\right)^2\right]^{-1/2} \qquad (4.10)$$

λ is the emitter wavelength, σ_{DD} is the standard deviation of the DD estimating error, and σ_v is the standard deviation of the error in estimating the value of each component of $\underline{v}_8$ and $\underline{v}_9$, assuming the error to be the same for each coordinate of both satellites. $\dot{\alpha}_8$ and $\dot{\alpha}_9$ are the angular velocities of LES-8 and LES-9, respectively, as seen from the emitter. γ is the angle between the components of the velocity vectors $\underline{v}_8$ and $\underline{v}_9$ which are perpendicular to $\underline{r}_T - \underline{r}_8$ and $\underline{r}_T - \underline{r}_9$, respectively. β_i (i = 8, 9) is the angle between $\underline{r}_T$ and the component of $\underline{v}_i$ which is perpendicular to $\underline{r}_T - \underline{r}_i$.

A strong scenario dependence is evident in (4.10), more so than in the case of DTOA (4.8) because of the number of parameters involved with M_2 and G_2. To quantify the location accuracy with LES-8/9, it is assumed, as before, that the emitter is located between the subsatellite points. Because of the high degree of similarity in the orbital behaviors of the two satellites, it is reasonable to assume $\alpha_8 = \alpha_9 = \alpha$. A simple calculation based on PEP data reveals that α varies between 3.5×10^{-5} rad/s to 7.3×10^{-6} rad/s, depending upon where the satellites are in their orbits. DD location accuracy will therefore be calculated for the geometric mean of $\alpha = 1.6 \times 10^{-5}$ rad/s, recognizing that the actual value in any given situation can be as much a factor of two larger or smaller. The exact value of the angle γ depends upon specifics of the satellite orbits but is typical comparable to the angle θ. Therefore, the value $\gamma = \theta = 3°$ will be used. For an emitter located around the subsatellite points, $\beta_8 \approx \beta_9 \approx \pi/2$ and $\cos\beta_8 \approx \cos\beta_9$. $\lambda = 1$ is a good approximation for the portion of UHF band where LES-8/9 can tune. Under these various assumptions, G_2 simplifies to

$$G_2 = \frac{\lambda}{\dot{\alpha}} \frac{1}{2\sin\frac{\lambda}{2}}$$

$$= 1.19 \times 10^3 \text{ km/Hz} \; . \qquad (4.11)$$

Because of the wide range of possible values of the various parameters on which G_2 depends, the numerical result given in (4.11) should be regarded only as an order-of-magnitude estimate.

To calculate the measurement error, assume $\sigma_v = 0.1$ m/s as a typical velocity-estimate error. In the narrowband receiving mode, σ_{DD} is about 0.025 Hz at best, and thus $M_2 = 0.16$ Hz. The DD-location estimation error $\sigma_2 = M_2 G_2$ is then found to be 190 km, using the value of G_2 found above. In the narrowband mode, the orbit-fitting errors σ_p and σ_v dominate the DD estimation error in determining M_2. On the other hand, in the wideband case $\sigma_{DD} = 0.25$ Hz is the best expected performance, and $M_2 = 0.30$ Hz. Here the main source of error is the DD estimate, and the resultant error in the location estimate is 357 km.

The geometric factor G_2 can be reduced and location accuracy improved by increasing the inter-satellite separation. As LES-8 and LES-9 are moved further apart, orbital mechanics dictates that they will become more out of phase with respect to each other in their orbital paths. The result is that the velocity vectors $\underline{v}_8$ and $\underline{v}_9$ will tend to differ more from each other in their direction and larger values of DD will be generated, thereby improving location accuracy. In terms of the expression (4.10) for G_2, the angle γ will be increased, and G_2 decreased. Taking DD data over the parts of the satellite orbits with the largest angular velocities α_8 and α_9 with respect to the emitter also reduces G_2, all other things being equal.

It is then straightforward to show that the standard deviation σ of the error in locating the emitter from a DTOA/DD loci pair is given by

$$\sigma = \sqrt{\frac{\sigma_1^2 + \sigma_2^2}{\sin\psi}} \qquad (4.12)$$

where ψ is the angle between the DTOA and DD loci at their intersection. It is assumed that other errors, not accounted for by σ_{DD}, σ_{DTOA}, σ_p and σ_V, are zero. Using the values for σ_1 and σ_2 obtained in the preceding examples of DTOA data taken in the wideband mode and DD data in the narrowband mode, and assuming $\psi = 90°$, which is very nearly the case in many observed situations, one obtains the location error as $\sigma = 234$ km. Once again, it is emphasized that this number should be regarded as only an indication of the accuracy attainable from one observation. The actual accuracy to be had in a given situation depends upon many factors, including the signal waveforms being received, the satellite receivers SNRs, the satellite orbital parameters at the time of reception, the accuracy of the satellite orbit-fitting data, the location of the emitter itself, and the contributions of the various other errors discussed earlier in this chapter. Variations in these parameters can cause substantial variation in location estimation accuracy from one emitter to another.

If N observations are made of the source, and the satellite position errors from all observations are independent, the location error becomes

$$\sigma = \sqrt{\frac{\left(\sigma_1^2 + \sigma_2^2\right)/N}{\sin\psi}} \qquad (4.13)$$

In practice, the position errors will be correlated from one observation to the next because the error contributions from the satellite orbit-fitting data and from some of the other sources are themselves correlated. Therefore, the actual location-estimation accuracy will fall between that predicted by equations (4.12) and (4.13).

5. TEST RESULTS

A series of tests was conducted with LES-8/9 using transmissions from Lincoln Laboratory, Lexington, to determine what kind of location accuracy could actually be achieved in practice, albeit under carefully controlled conditions. A second group of tests was carried out with a known, but non-cooperating transmitter at Hall Beach, Canada. Finally, an emitter-location experiment involving a cooperative airborne transmitter was conducted to examine the moving-emitter problem. Results of these tests are given here.

5.1 LINCOLN LABORATORY TESTS

A large number of emitter-location tests were made with a Lincoln Laboratory transmitter on 303.4 MHz as a simulated RFI source to verify proper operation of all aspects of the system, particularly the various software packages. In the course of testing, a number of problem areas were identified, resulting in corrections or improvements. The results presented here are those obtained at the final stages of testing, at which point the system had been essentially "debugged" completely.

For these tests a pseudonoise-type signal was transmitted by using binary maximal-length shift-register (MLSR) sequences to modulate the BPSK transmitter. This signaling choice was made on the basis of the time-domain correlation properties of MLSR sequences. The chip rate was varied for the different tests, but it was kept in the kilohertz range so that most of the signal power would be confined to the passbands of the satellite receivers. A sequence length of 2^{18}-1 bits was employed so as to avoid time-domain correlation ambiguities. The constant-envelope BPSK signals also ensured favorable correlation-estimation accuracy in the frequency domain. The power of the signals as actually received in each satellite was obtained from received-power-monitor data available via telemetry. This information permitted estimation of the actual SNR within the passband of each receiver.

It was determined early on that the quality of the data obtained in the wideband receiving mode in LES-8/9 was quite poor. The problem did not originate in reception of the uplink but rather of the downlink from LES-8 to Lexington. The received-signal power at the ground terminal was insufficient to demodulate the high-rate (200 kbps) DPSK downlink with a sufficiently low bit-error rate. The cause was a combination of a modest receiving-antenna aperture (4-foot dish) and ground terminal receiver noise figure (5.5 dB). As a result of the high bit-error rates, the reconstructed received-signal information was effectively noisy and yielded poor DTOA/DD correlation estimation performance. On the other hand, the received downlink signal power was usually more than adequate to obtain low bit-error rate (10^{-2} or less) in the narrowband receiving mode with its low-rate (20 kbps) downlink. Therefore, almost all the Lincoln Laboratory test transmissions were received in the narrowband satellite channels.

The outcome of one series of tests is reported here, being representative of the quality of results obtained at other times after the system was made fully operational. The spectrum of the test signals as received in the satellites is obtained from the baseband x(k) and u(k) clipped and sampled data recovered on the ground. A typical FFT of that data is shown in Figure 17. It appears to exhibit the $|\sin x/x|$ spectral-envelope shape expected for MLSR sequence modulation. (The transmitter chip rate in this example was

1 kHz.) The "noiseness" of the FFT is due, in part, to satellite receiver noise, and to the fact that the interval of data being analyzed here is only 1.64 s in duration, which is considerably less than the MLSR sequence length. Averaging over a considerably longer interval would produce a smoother looking FFT, but this is not an issue of concern since the problem at hand is not one of spectral estimation. The main point of Figure 17 is verification of reception of the test signals in both satellites.

Figures 18 and 20 show typical cross-correlations for DTOA and DD obtained by FFT at the "coarse" correlation stage (by the method explained in Section 3.3, Three-Step Correlation/Estimation Procedure). Each FFT correlation employes a 8192-point transform. The first 0.82 s segment of each 10 s observation from LES-8/9 in the narrowband receiving mode is used to obtain the results shown. (Recall that the *entire* 10 s interval is used at the second stage of the correlation estimation operation.) Figure 18 is the cross-correlation in the time domain for constant DD obtained after searching out the value of DD which gives the highest correlation peak. This peak is clearly visible at the approximate center of the plot, as the DTOA plus crosslink delay is only a few ms. An expanded view of the correlation for DTOA in the immediate neighborhood of the peak is given in Figure 19, where the indicated delay is approximately 8 ms, most of which is the crosslink delay. The width and the triangular shape of the correlation function around the peak are precisely that expected for the pseudonoise-type modulation which was used for the test. The result of a separate calculation for the DD spectrum is shown in Figure 20. This spectrum actually represents a two-dimensional cross-sectional view of the reproduced signal ambiguity function in a plane of constant DTOA, namely that corresponding to the best DTOA estimate. The peak of the spectrum, which gives the DD estimate, happens to be at about 0 Hz, although non-zero values are, in general, observed at other times. The width of the peak is approximately the reciprocal of the signal duration, or about 0.6 Hz in this case.

The importance of estimating DTOA and DD *jointly* is illustrated in Figure 21. Shown here is the time-domain cross correlation obtained when the correct DD estimate has not been found, using exactly the same signal data as in Figure 19. No correlation peak is evident at all since what has happened is that the ambiguity function is, in effect, being viewed in a plane of constant DD sufficiently far removed from the actual peak that it does not intersect any portion of that peak. Until an estimate of DD which is close to the correct value is found, no peak will be found in the time domain.

The "fine" correlation and interpolation operations were then performed, based on the DTOA/DD estimates obtained from the FFT correlations. (The final estimates for the DTOA and DD for the data set examined here turned out to be 7995.5 μs and 0.282 Hz, respectively. See Appendix B for details on the calculations of these estimates.)

After obtaining the LES-8/9 orbital parameters from PEP for the time of reception and calculating or estimating the various time-delay and frequency corrections (as explained in Section 3.4, Corrections to DTOA/DD Estimates), the DTOA and DD loci were plotted. Figures 22 and 23 show two different views of the results. The indicated "fix" for this particular observation was within 25 km of Lexington. A number of other observations taken at slightly later times yielded similar results, with a spread of location estimates around Lexington. The satellite orbit-fitting errors at the time were known to be small since the PEP data was obtained from a relatively "fresh" orbit fit. It should be pointed out, however, that the satellite processing delay corrections which were estimated for the DTOA data were obtained by

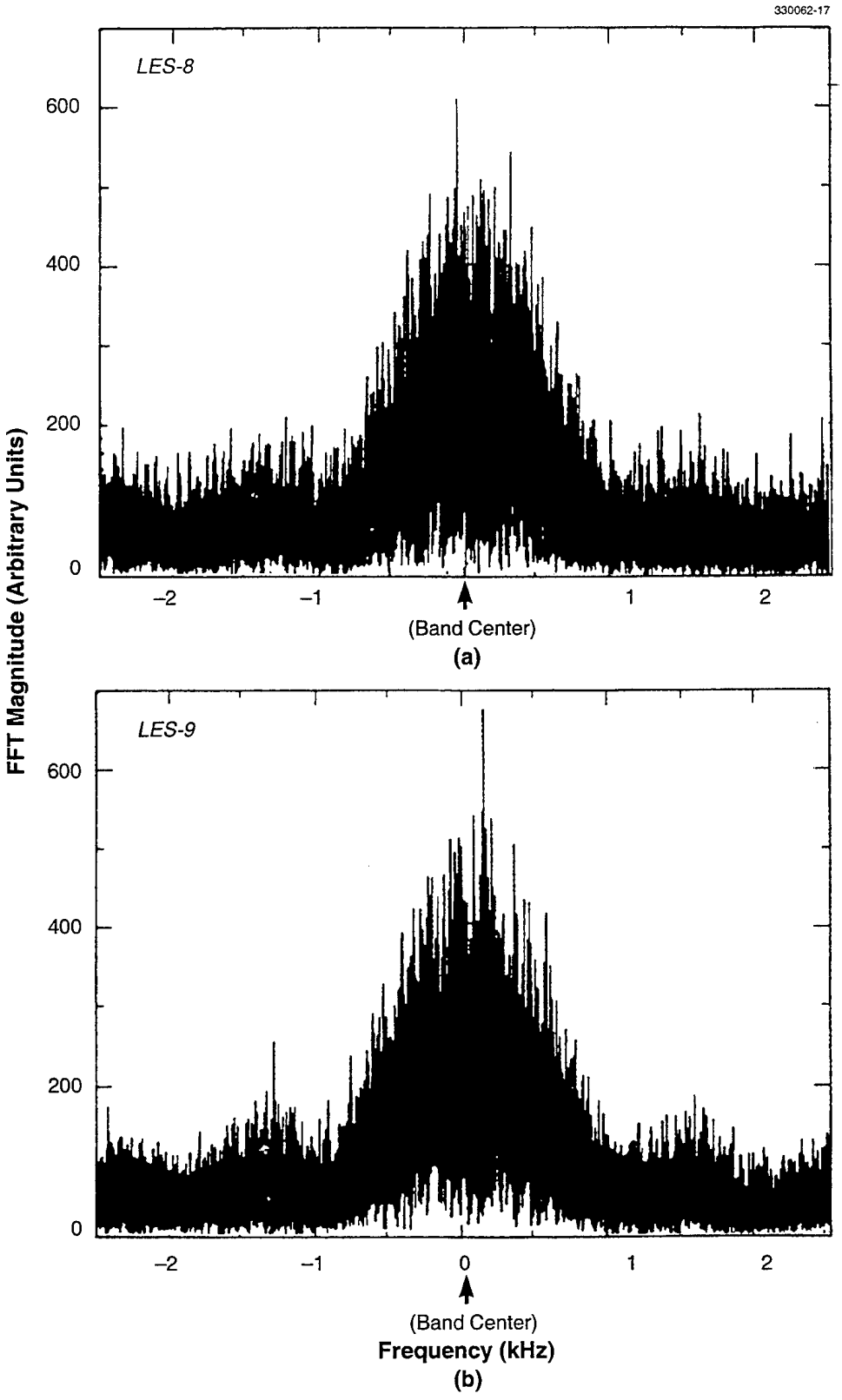

Figure 17. Spectra of pseudonoise test signals as received in (a) LES-8, and (b) LES-9.

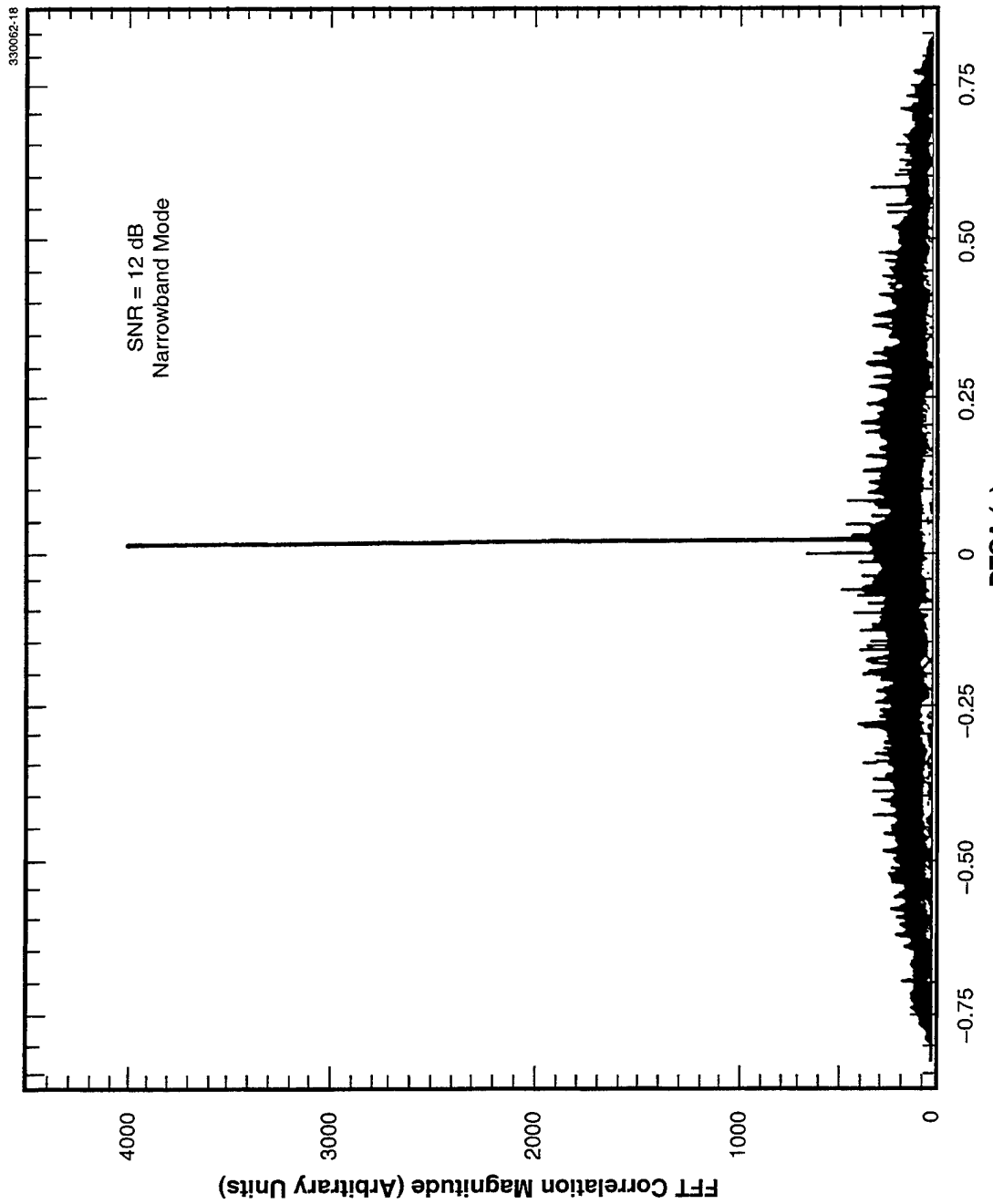

Figure 18. Cross-correlation for DTOA with pseudonoise signals.

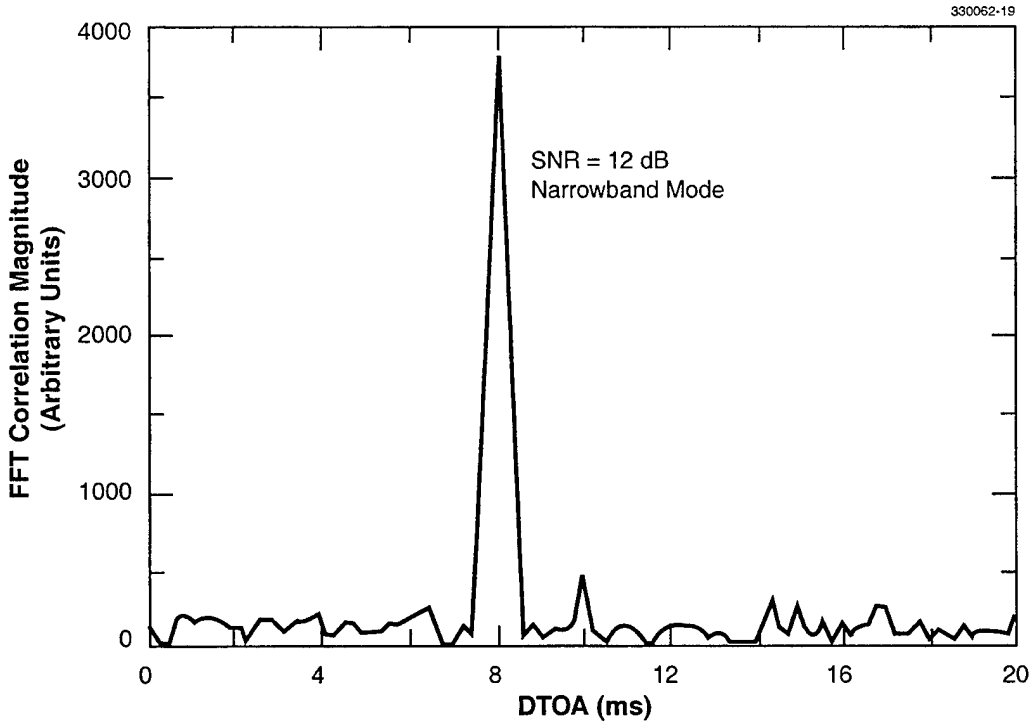

Figure 19. Expanded view of Figure 18 of cross-correlation for DTOA.

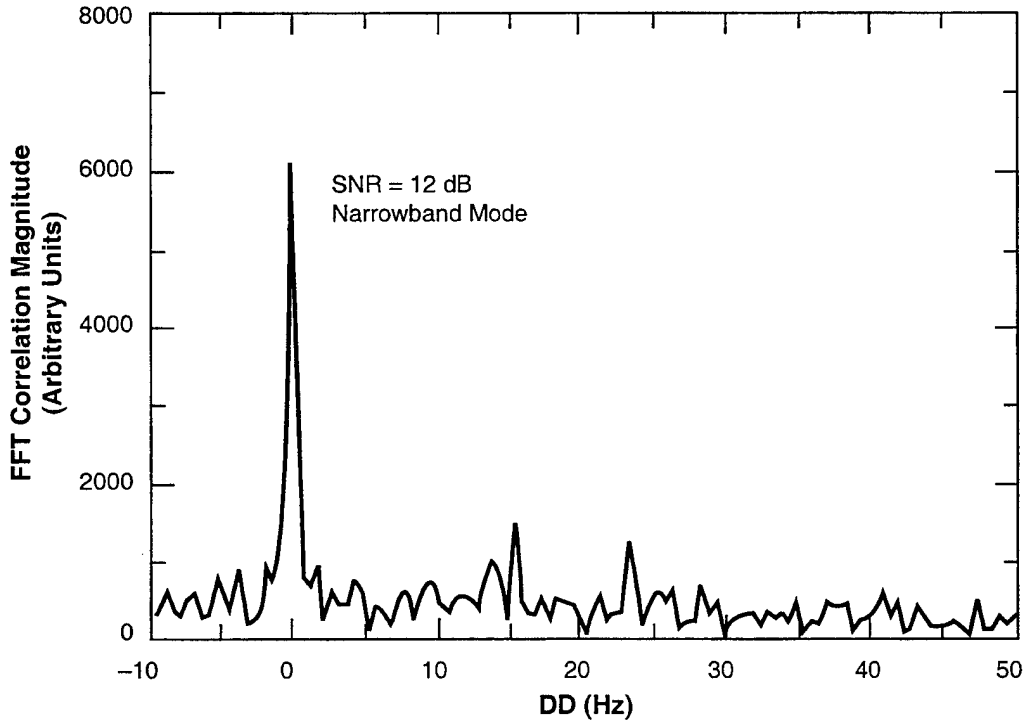

Figure 20. DD spectrum with pseudonoise signals.

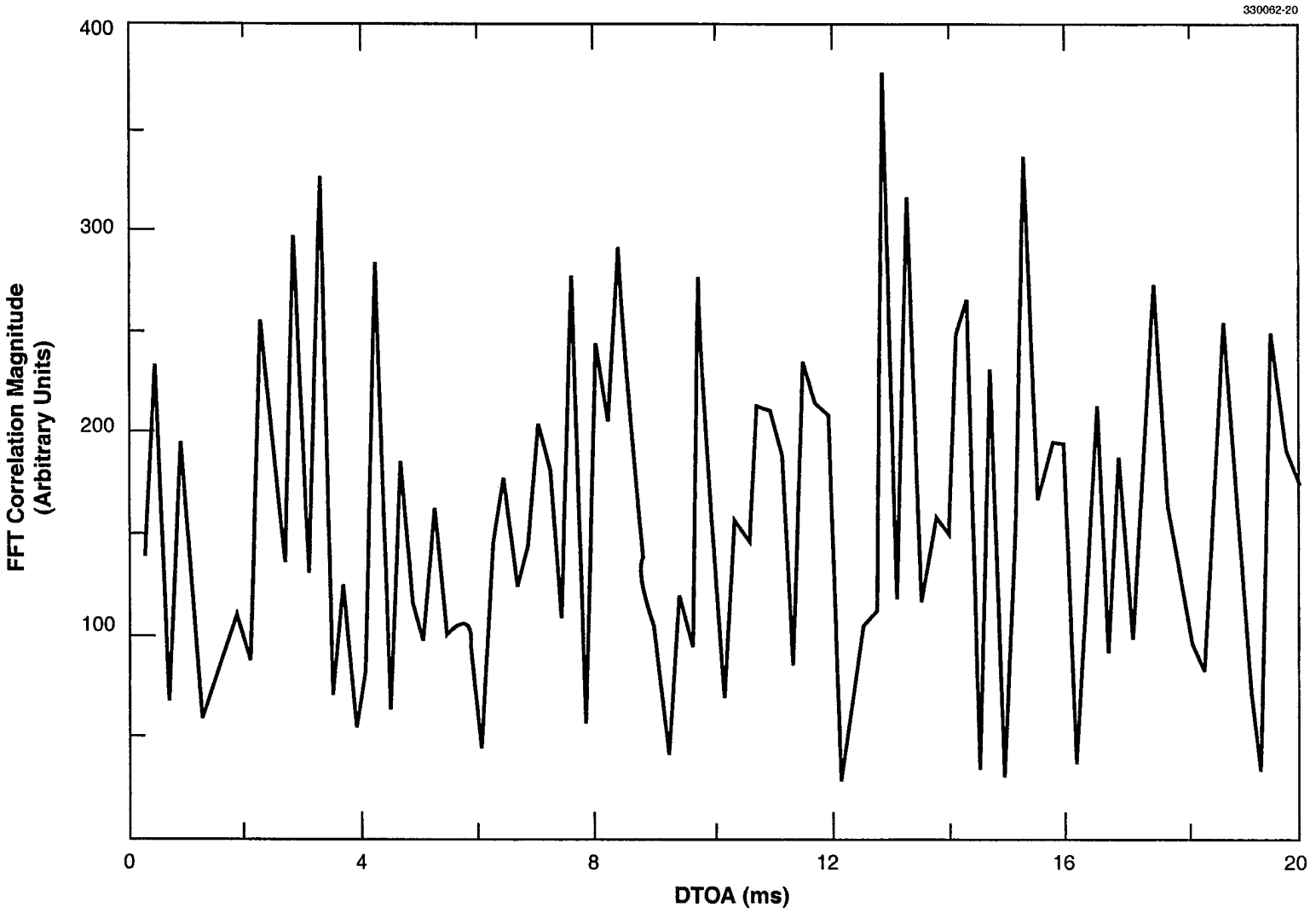

Figure 21. Cross-correlation for DTOA with large error in DD estimate.

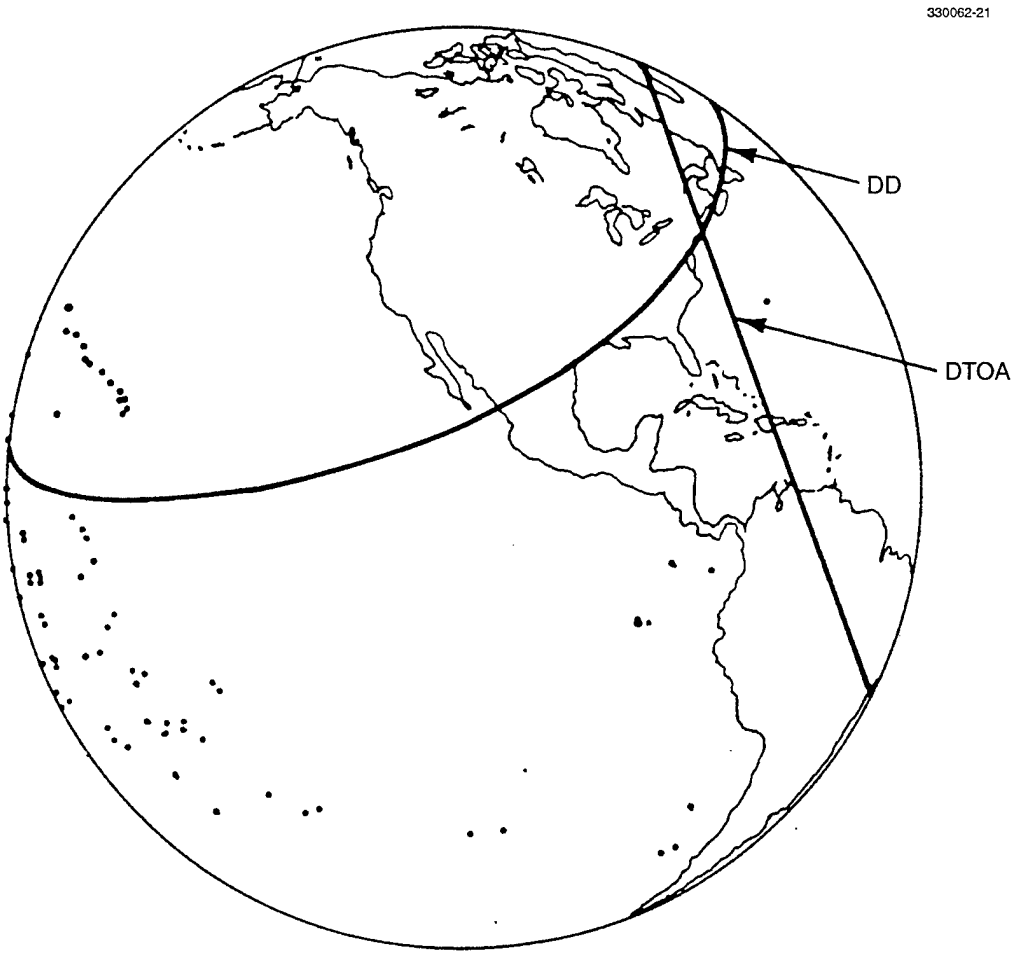

Figure 22. Typical DTOA and DD loci from Lincoln Laboratory test transmission, 1 July 1981.

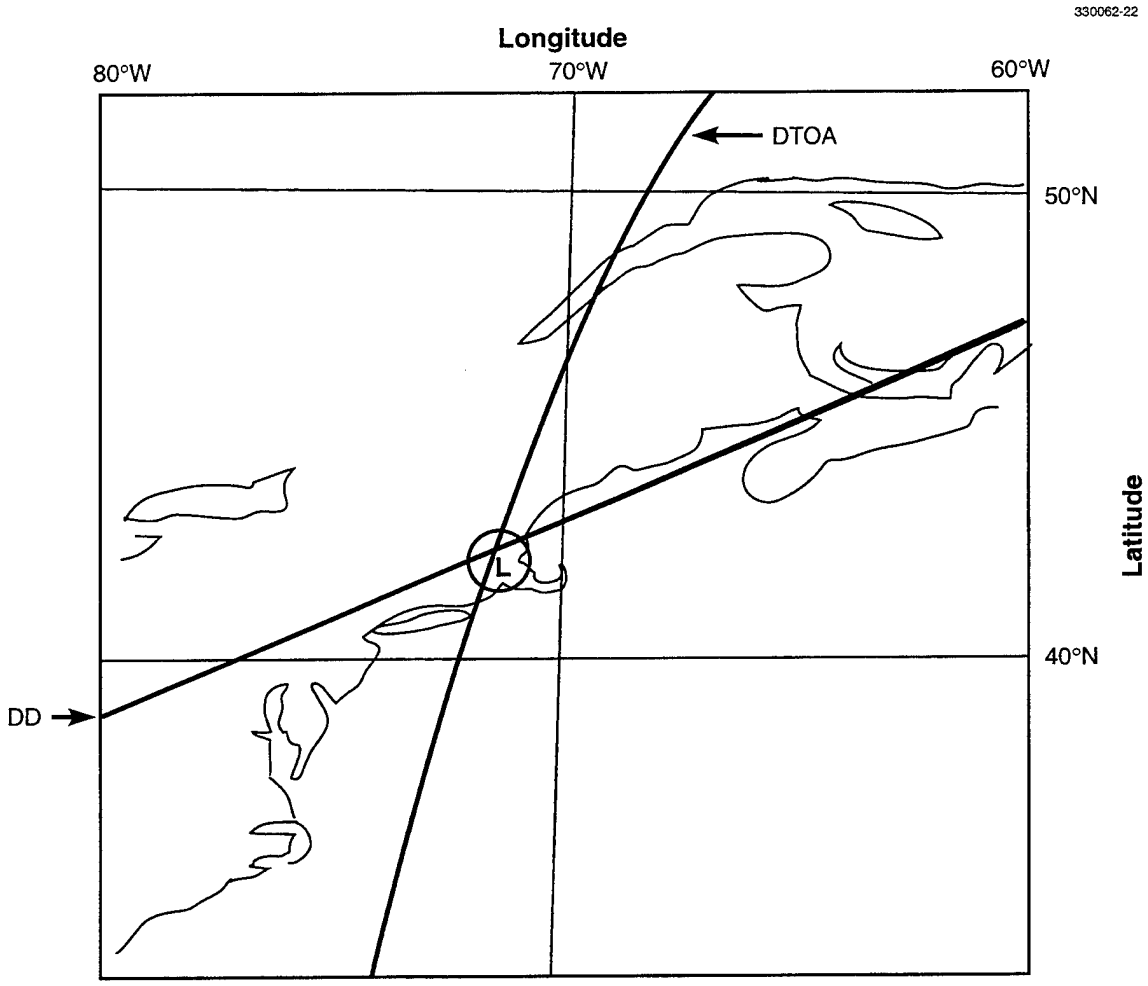

Figure 23. Expanded view of DTOA and DD loci intersection from Lincoln Laboratory test transmission, 1 July 1981.

"calibrating" on Lexington itself, and therefore, it should not be surprising that the DTOA loci ran close to Lincoln Laboratory. However, the same single correction was applied to *all* the DTOA data. There were variations between the individual DTOA loci due to random estimation errors but the loci were consistent in that the variations were not large. It was found during other tests that when the orbit-fit quality was not as good, the DD loci would exhibit apparent biases, being shifted as much as 200 km off Lexington with little variation from one locus to the next.

Limitations on manpower and time prevented the implementation of the multiple-measurement-combining scheme described in Section 3.6, Multiple-Measurement Combining. However, one simple *ad hoc* procedure employed in its place is to pick as the "best" estimate the location at the centroid of the geographic region enclosing the spread of "fixes" from the collection of single-shot observations. All things considered, it is felt that this *ad hoc* method would not give greatly different results from those for an "optimum" approach.

Testing continued with the Lincoln Laboratory transmitter operating at reduced power to determine the degradation in accuracy with weaker signals and the minimum "usable" SNR for which reliable estimates could still be obtained. First, the satellite-receiver SNRs were estimated at the different transmitting powers from the received-power information recovered from the LES-8/9 telemetry. The transmitted signal was modulated by pseudonoise at 2 kHz chip rate while the transmitter power was cut in 10-dB steps, starting at 80 watts output (284 watts EIRP, after accounting for feedline loss and antenna gain) and eventually reducing to 0.08 watts (0.28 watts EIRP). Figure 24 gives an example of received signal-plus-noise power data from telemetry taken over the course of one test period, indicating the transmitter powers for the different times. The data is for the narrowband receiving mode and the receiver noise power in that mode is what is indicated during the "off" interval. Comparing the noise power to the total received power during the 80-watt transmitting period, the receiver SNR (in this case for LES-9) is estimated to be 12 dB. A similar plot of data was also obtained for LES-8. At the other transmitter powers, the SNRs were then 2 dB at 8 watts, –8 dB at 0.8 watts, and –18 dB at 0.08 watts.

From the FFT correlations computed from the signal data at the different power levels, it was determined that correlation peaks which could be consistently identified with the received signal were observed down to the –8 dB SNR level. Figure 25 gives an example of the DTOA and DD correlations obtained at this SNR. One difference between Figures 19 and 20 and Figure 25 is the reduction in peak height (as expected) of the correlation peak. At the SNR of 2 dB, the amplitude of the peak assumed a value intermediate to those at the higher and lower powers. At the lowest power, the signal was completely lost, with no correlation peak to be found. Therefore, it was estimated that –12 to –13 dB was the lowest SNR for which any peak would be visible, although no tests were actually run at the level. However, it should be noted that different conclusions about usable SNR may hold for different signal waveforms. The results obtained here can be regarded as optimistic because of the choice of the transmitted signal waveforms.

In terms of the accuracy with which Lexington was actually "located," it was found that the data taken at the SNR of 2 dB yielded essentially as good performance as that taken at 12 dB. The spread in DTOA and DD loci over nine different observations at a SNR of 12 dB is shown in Figure 26. At –8 dB SNR, the errors increased noticeably, by as much as a factor of 2 to 3 in terms of the distance

between

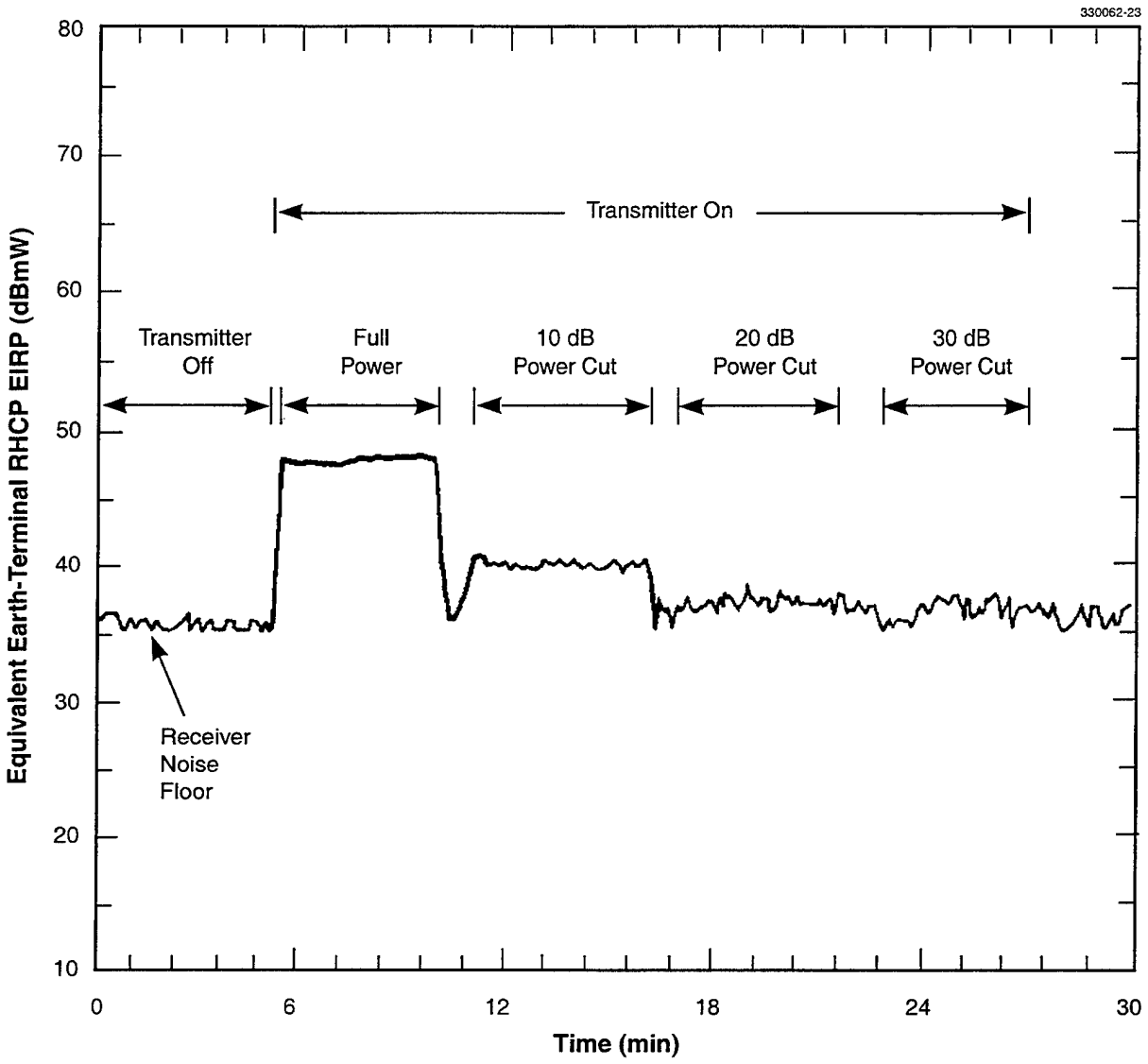

Figure 24. Received-signal power in LES-9 during test transmissions.

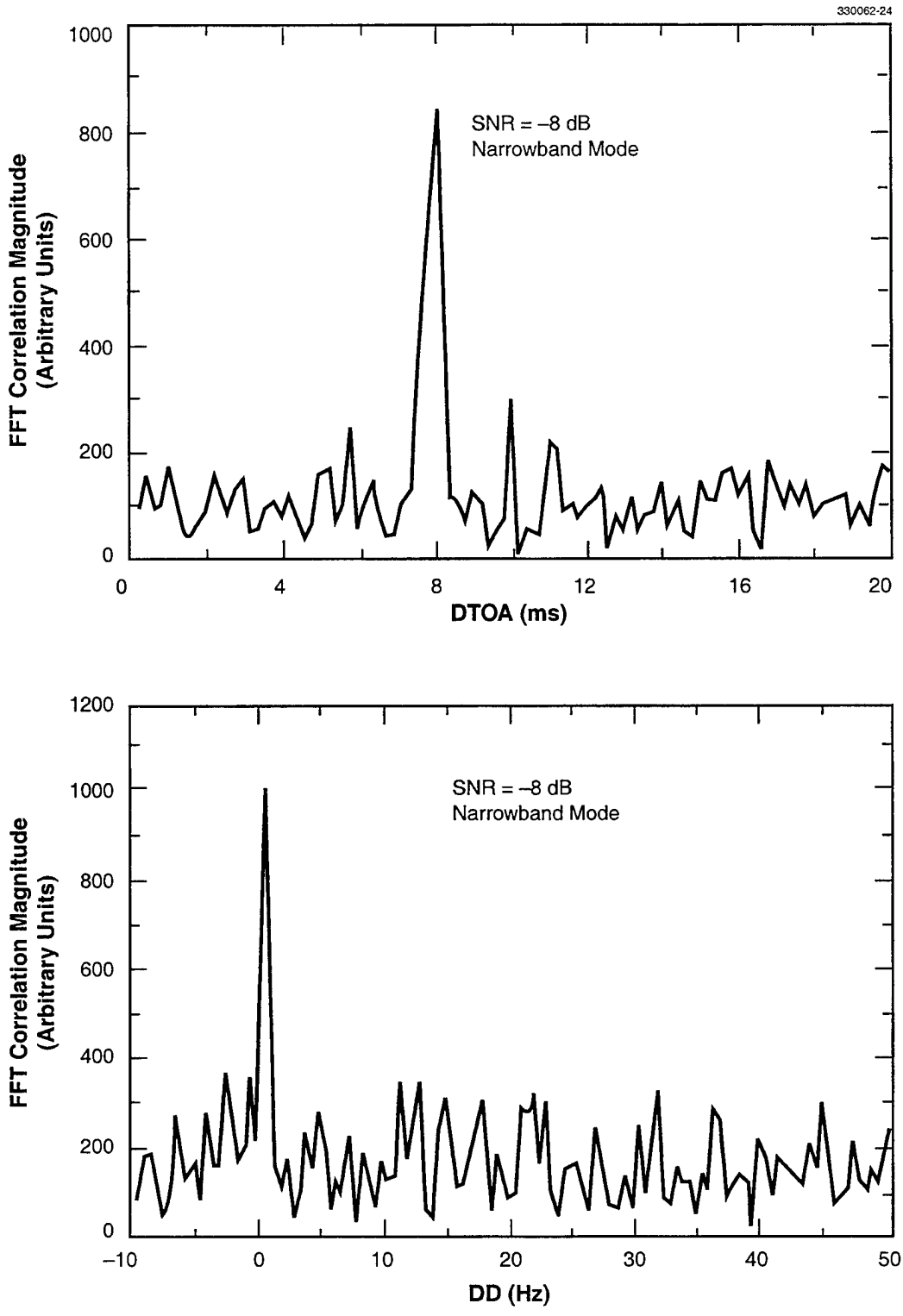

Figure 25. Cross-correlation for DTOA and DD at low SNR from Lincoln Laboratory test transmission.

the position estimates and Lexington. Figure 27 shows the spread in the DTOA and DD loci in the latter case. What is evident in the figure and was found to be true in general is that the variance in the DTOA loci was greater than that of the DD loci. This is a consequence of using the narrowband receiving mode of LES-8/9. The worst-case "fixes" were still within 350 km of Lexington, however.

The conclusion from the tests at reduced transmitter power is that the location of sources whose received signal power is perhaps as much as 10 dB less than the noise power in the receiver passband may still be estimated with fairly good accuracy. An interesting implication of this finding is that sources which cannot even be detected on the basis of the received-power information from telemetry may be located provided their presence under the noise in the passbands of the receivers is known by other means. The fact that the errors in the location estimates did not increase greatly at the lower transmitter powers appears to indicate that significant sources of error other than those related to receiver SNR exist. The various possible sources were discussed in detail in the preceding chapter.

To demonstrate the use of only DD or only DTOA, a number of test transmissions suitable for each method (at full power) were made. Location estimation results for the DD technique based on several CW transmissions were approximately one hour apart are shown in Figure 28. The indicated accuracy is fairly good, with the best location estimate, based on "averaging" the results of the various observations, falling within 150 km of Lexington. Because of the relative closeness of the groups of observations in time, the DD loci do not intersect one another nearly as orthogonally to one another as do those for DTOA/DD seen in previous figures.

The DTOA-only method was found to be essentially useless (in the narrowband mode) for transmissions one hour apart because the resultant DTOA loci were always found to be nearly parallel to one another and exhibited much larger position variation than DD loci. No data was taken in the wideband mode, although different results might have been obtained if the wideband mode had been usable. It is concluded that in the narrowband mode, the DD method can be a satisfactory alternative to the combined DTOA/DD approach, whereas the DTOA method is not, unless widely spaced observations (to obtain a substantial emitter/satellite geometry change) are made.

5.2 HALL BEACH TESTS

The tests run from Lexington indicated that under carefully controlled circumstances, positive results could be obtained. However, a more realistic test situation was sought where, in particular, the transmitting source's modulation waveform was not subject to prior selection. For this purpose, the Fox-Main USAF transmitting station located at Hall Beach in northern Canada (81.25° west longitude and 68.75° north latitude) was chosen as another simulated RFI source in a non-cooperating situation. No prior arrangements were made with Hall Beach for the test; the satellites were simply commanded to tune to the Hall Beach frequencies at randomly chosen times for data-taking.

The selection of this source was based on a previous experience in which an unknown RFI source, found by use of the terminator-motion technique, turned out to be the Fox-Main transmitter at Hall Beach. It was learned later that Hall Beach operates a 950 km troposcatter link to Thule, Greenland, on two frequencies, 356.5 MHz and 379.5 MHz, 24 hours a day. The transmitter output of 100 kilowatts feeds a 41.7-dB gain antenna aimed at Thule. However, because of the directionality of the antenna, the EIRP

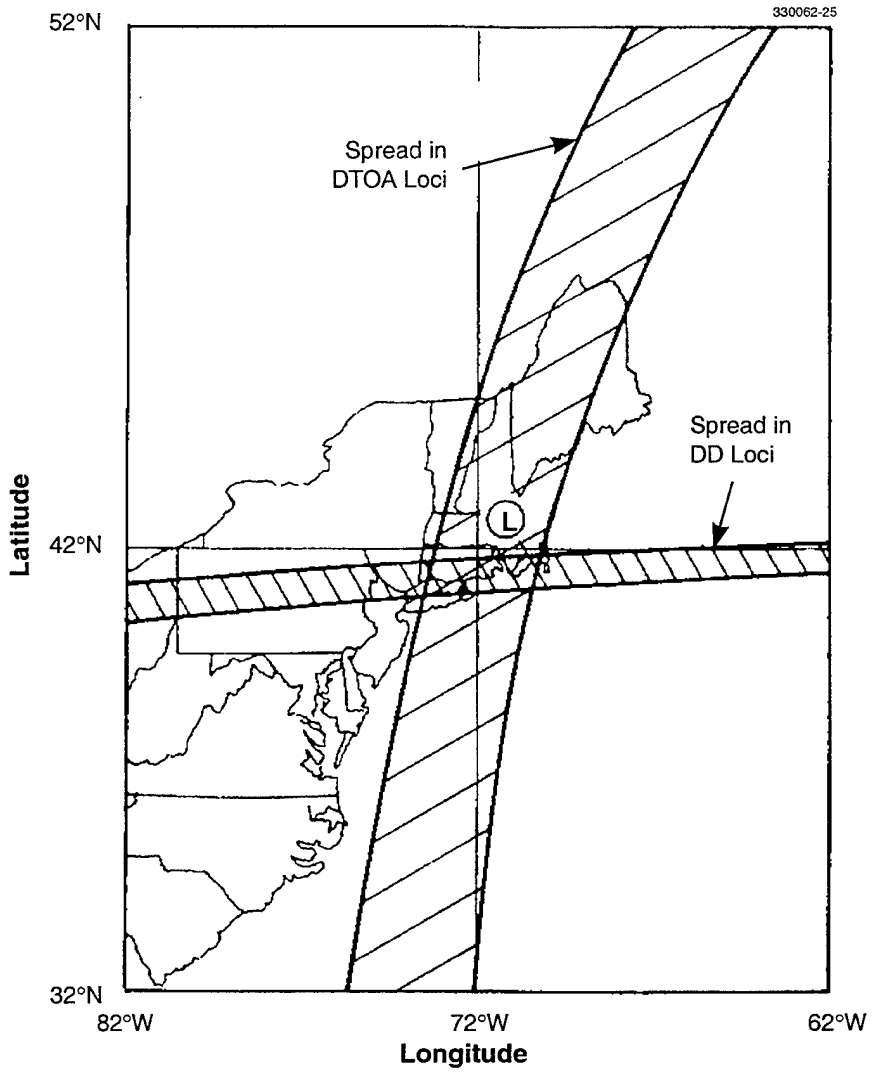

Figure 26. Spread in DTOA/DD loci from nine observations in narrowband mode of Lincoln Laboratory test transmissions, SNR = 12 dB, 28 October 1981.

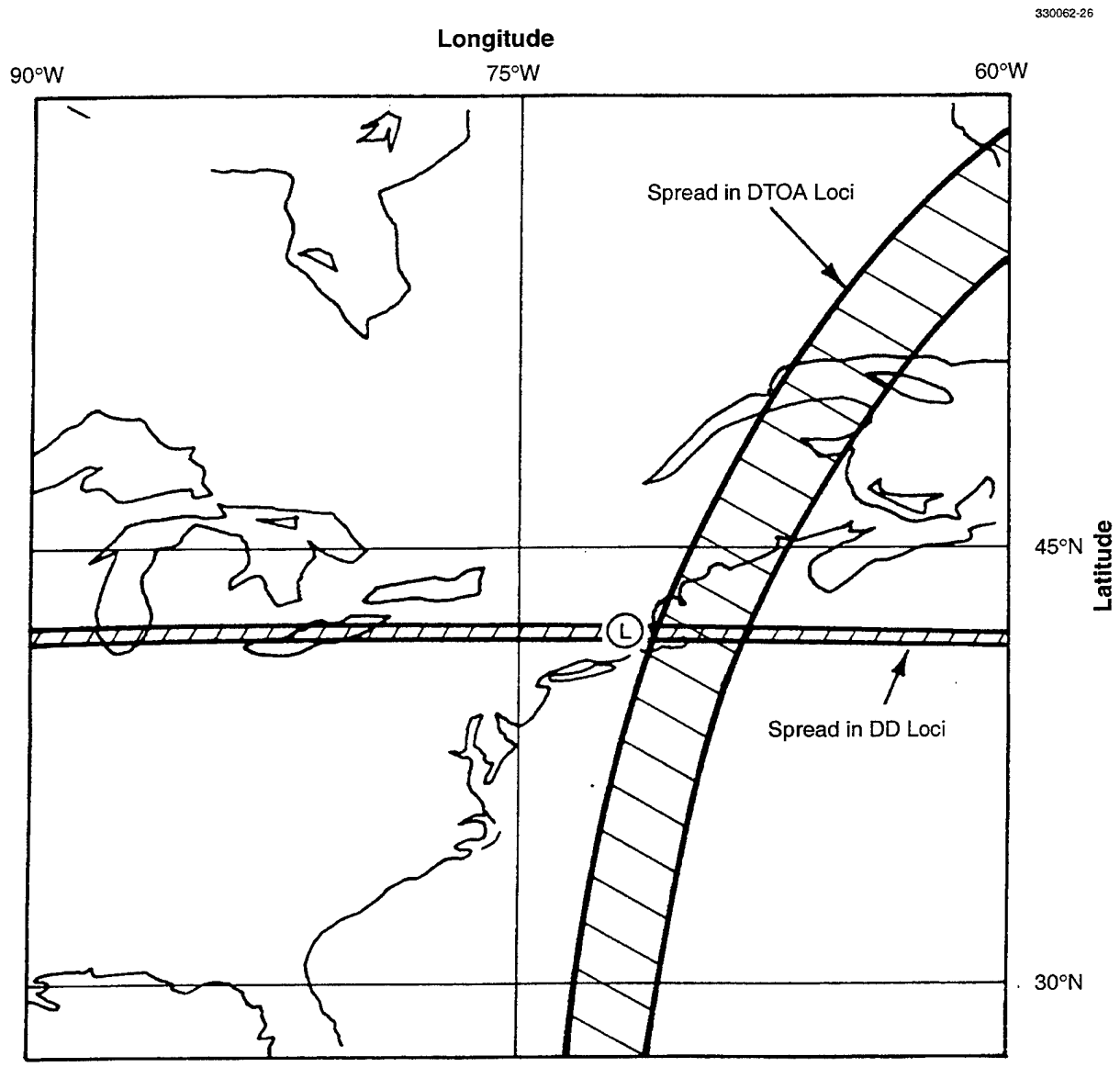

Figure 27. Spread in DTOA/DD loci from four observations in narrowband mode of Lincoln Laboratory test transmissions, SNR = –8 dB, 28 October 1981.

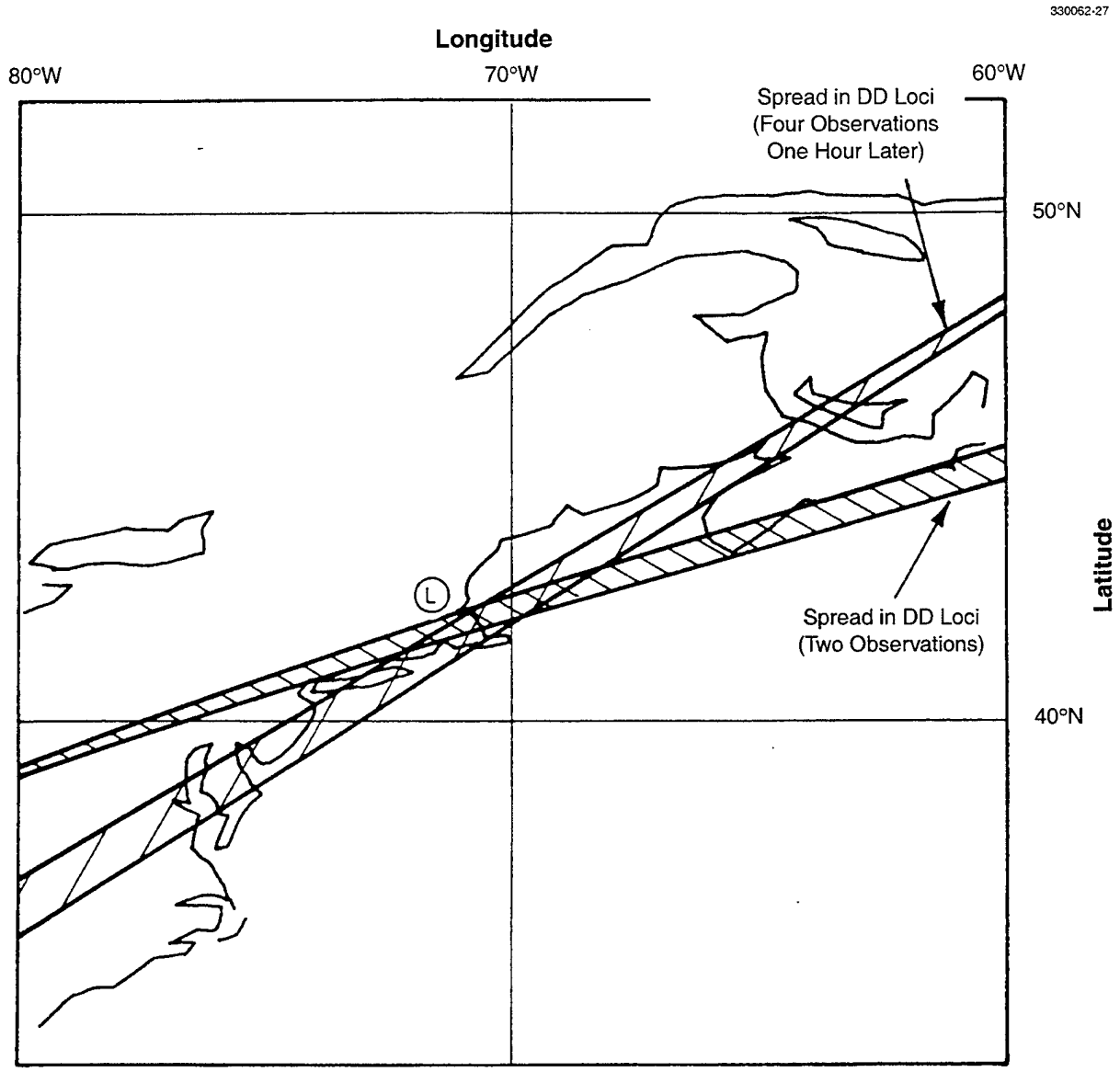

Figure 28. DD loci for Lincoln Laboratory CW test transmission.

radiated toward LES-8/9 is estimated to be about only 100 watts. Twelve FM channels are operated, each with 22.5 kHz deviation. (More details about the modulation are not known.)

The signal spectrum at 356.5 MHz in the narrowband mode, as recovered from the clipped, sampled data from LES-9, is shown in Figure 29. A very similar looking spectrum was obtained from LES-8. Multiple tones appear to be present.

The FFT correlation yielded multiple peaks in the time domain, as would be expected for a multi-tone type of signal. A typical result is shown in Figure 30. The DD spectrum has a single, clearly pronounced peak. The possible ambiguity in DTOA was resolved by the fact that all but one peak occurred outside the range possible for an earth-bound emitter. The single legitimate peak, appearing between 14 and 15 ms, also has slightly greater magnitude than the others.

The results for location estimating after correcting for the various system errors are given in the earth plot of Figure 31, showing the region covered by the spread in DTOA and DD loci. The worst-case single-shot "fix" was in error by 450 km, while the final location estimate, at the center of the region, was within 300 km of Hall Beach. The accuracy, while not as good as that obtained for Lincoln Laboratory's own transmitter, indicates that the emitter-location system does work for sites other than Lexington. The Hall Beach results might also be regarded as being more typical of what can be achieved in a real-world situation.

One of the periods during which the Fox-Main transmitter was being observed provided a rare opportunity for use of LES-8/9's wideband receiving mode. The quality of the high-rate downlink associated with the wideband mode was much better than usual due to favorable orientation of the LES-8 downlink antenna with respect to the receiving station at Lexington and good atmospheric conditions. The Hall Beach signal spectrum as reconstructed from LES-8 data for that time is shown in Figure 32 (essentially the same thing was observed in LES-9). A typical FFT correlation for DTOA and DD is shown in Figure 33. The "noisiness" around the DTOA correlation peak is due at least in part to the downlink quality, which still does not match that of the low-rate narrowband mode. Also, the signal appears to be relatively narrowband compared to the receiver passband, which is evident from the spectrum in Figure 32 and the relative broadness of the DTOA correlation peak in Figure 33. The DD spectrum in Figure 33 appears quite "clean," however.

Figure 34 shows the spread in DTOA loci is significantly less than that observed in the narrowband mode on other occasions. However, not surprisingly, the DD accuracy is substantially poorer. No time or frequency "calibration" data was available on this occasion, so that biases in the source location estimates are probably present. Overall location estimation accuracy, based on this limited use of the wideband mode, appears roughly comparable to that obtained from the narrowband mode.

5.3 AIRBORNE EMITTER EXPERIMENT

Section 4.5, Source Motion, discussed the limitations of the DTOA/DD method with moving emitters. Interest in this problem arose in connection with an actual effort to locate a particular RFI source using LES-8/9. The source in question was CW, rendering the DTOA technique useless. However, its DD loci exhibited a very large geographic spread with no indication of a well-defined fix. The signal was very strong and from the DD data it was concluded that the source had to be moving with substantial velocity

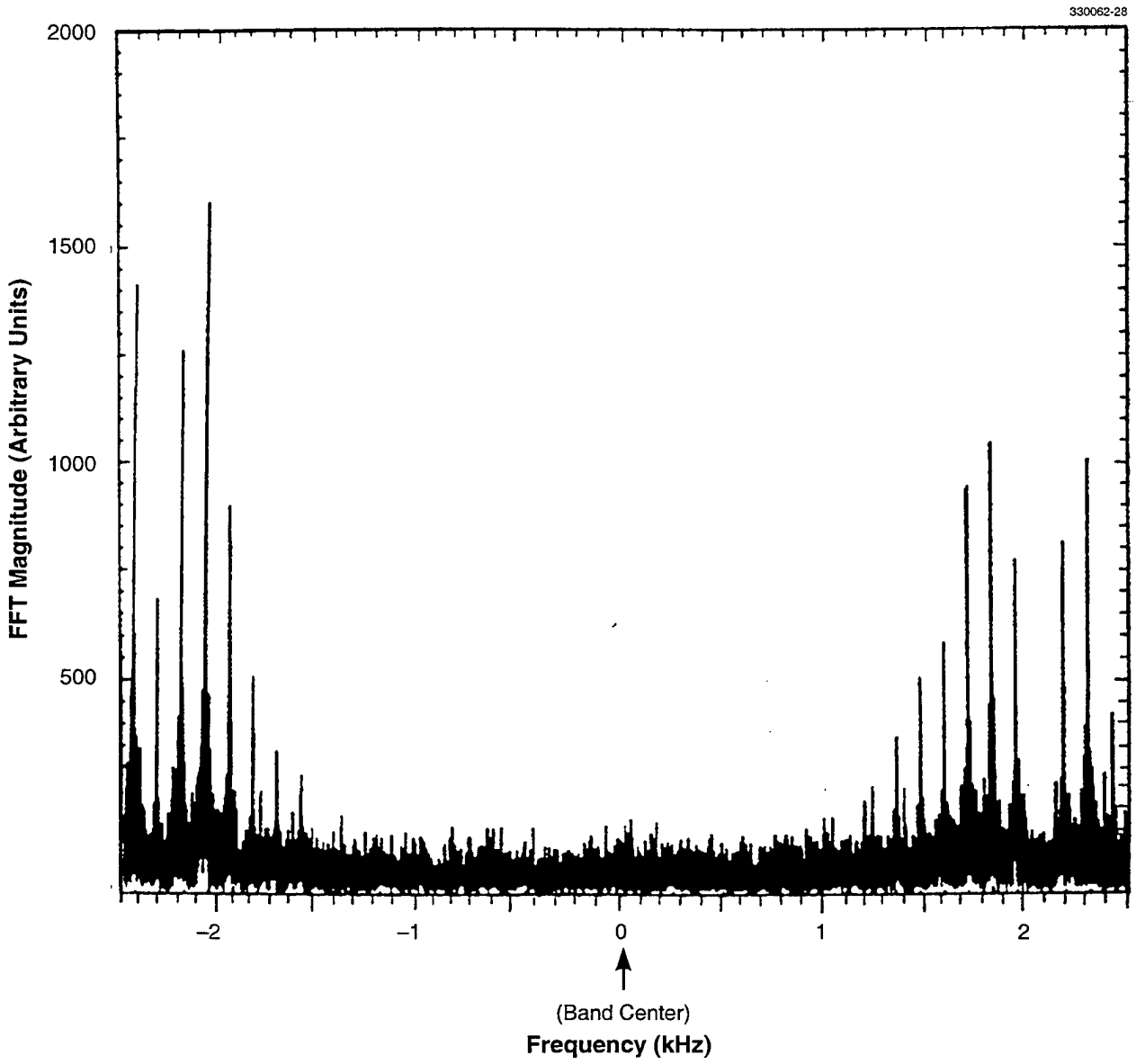

Figure 29. Hall Beach spectrum on 356.5 MHz as received in narrowband mode in LES-9, 1 July 1981.

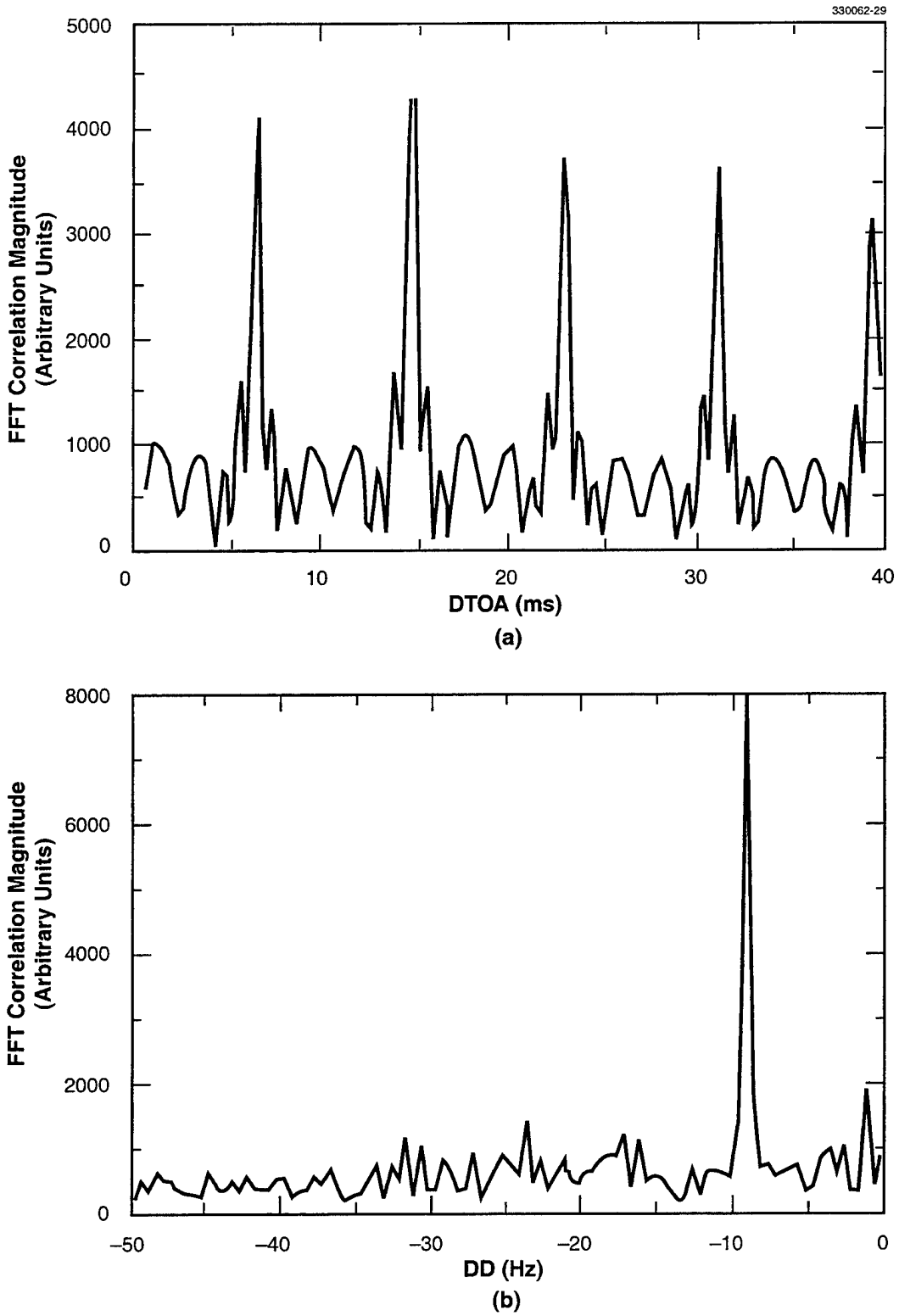

Figure 30. Typical cross-correlation for (a) DTOA, and (b) DD for Hall Beach on 356.5 MHz in narrowband mode.

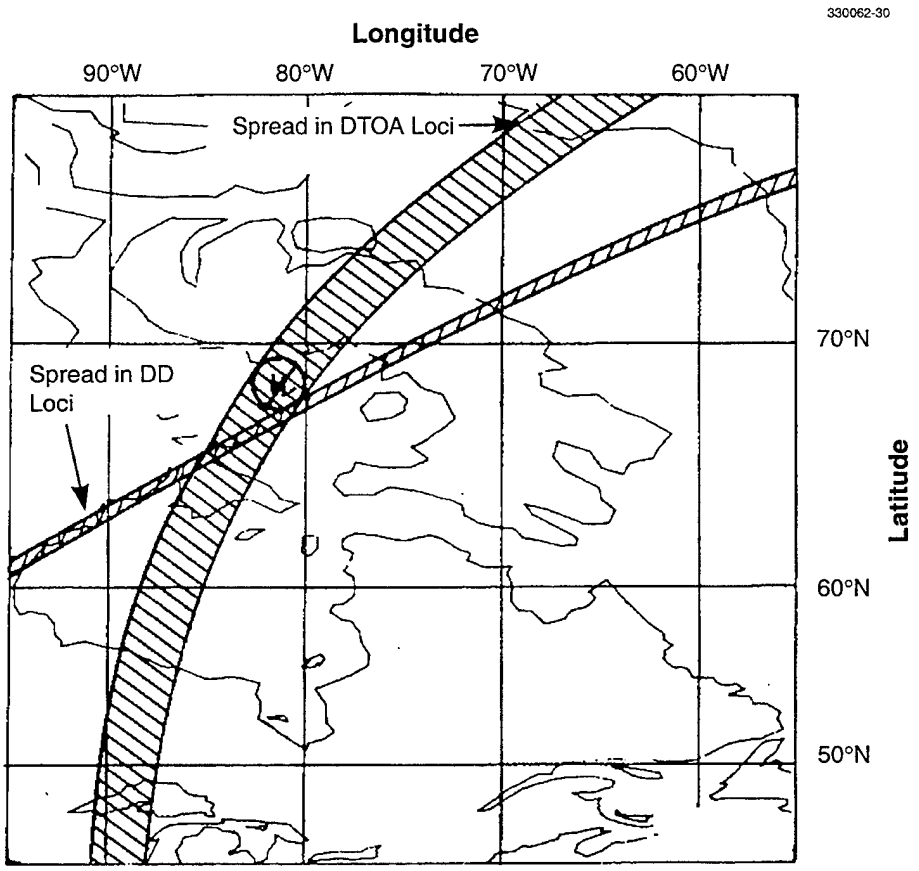

Figure 31. Spread in DTOA/DD loci from four observations of Hall Beach in narrowband mode, 1 July 1981.

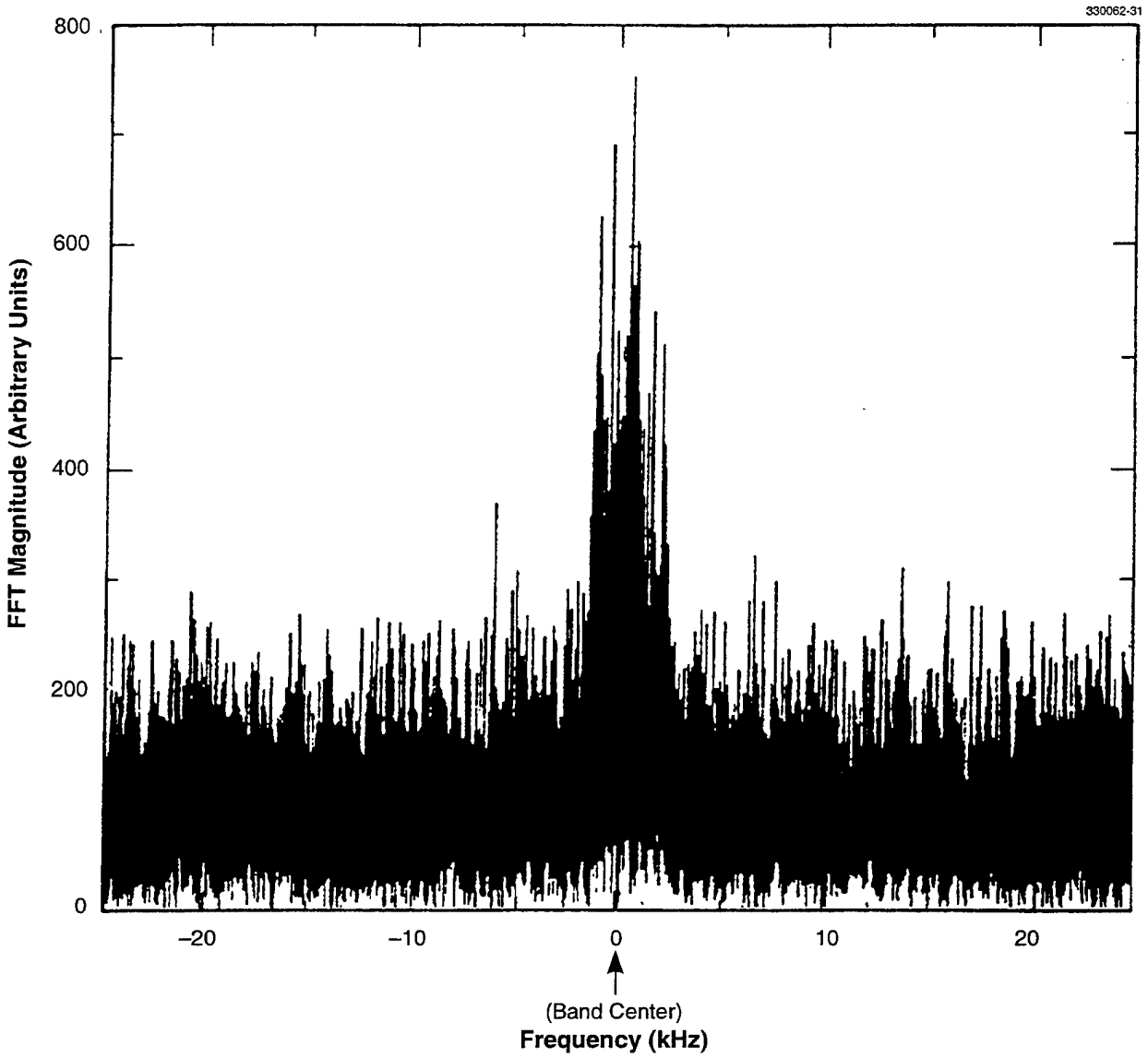

Figure 32. Hall Beach spectrum on 379.5 MHz as received in wideband mode in LES-8, 18 August 1981.

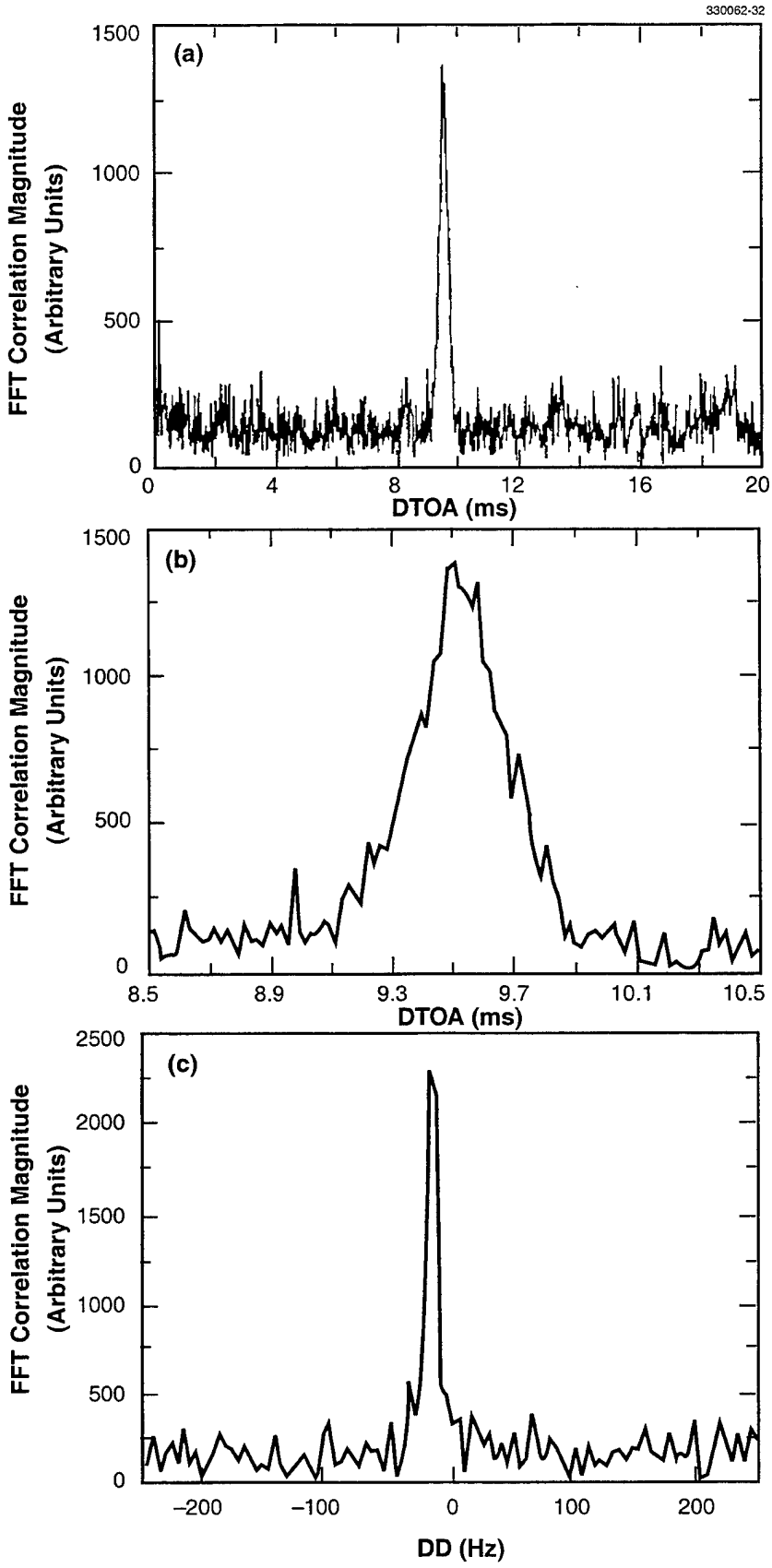

Figure 33. Cross-correlation for (a), (b) DTOA, and (c) DD for Hall Beach, 379.5 MHz in wideband mode.

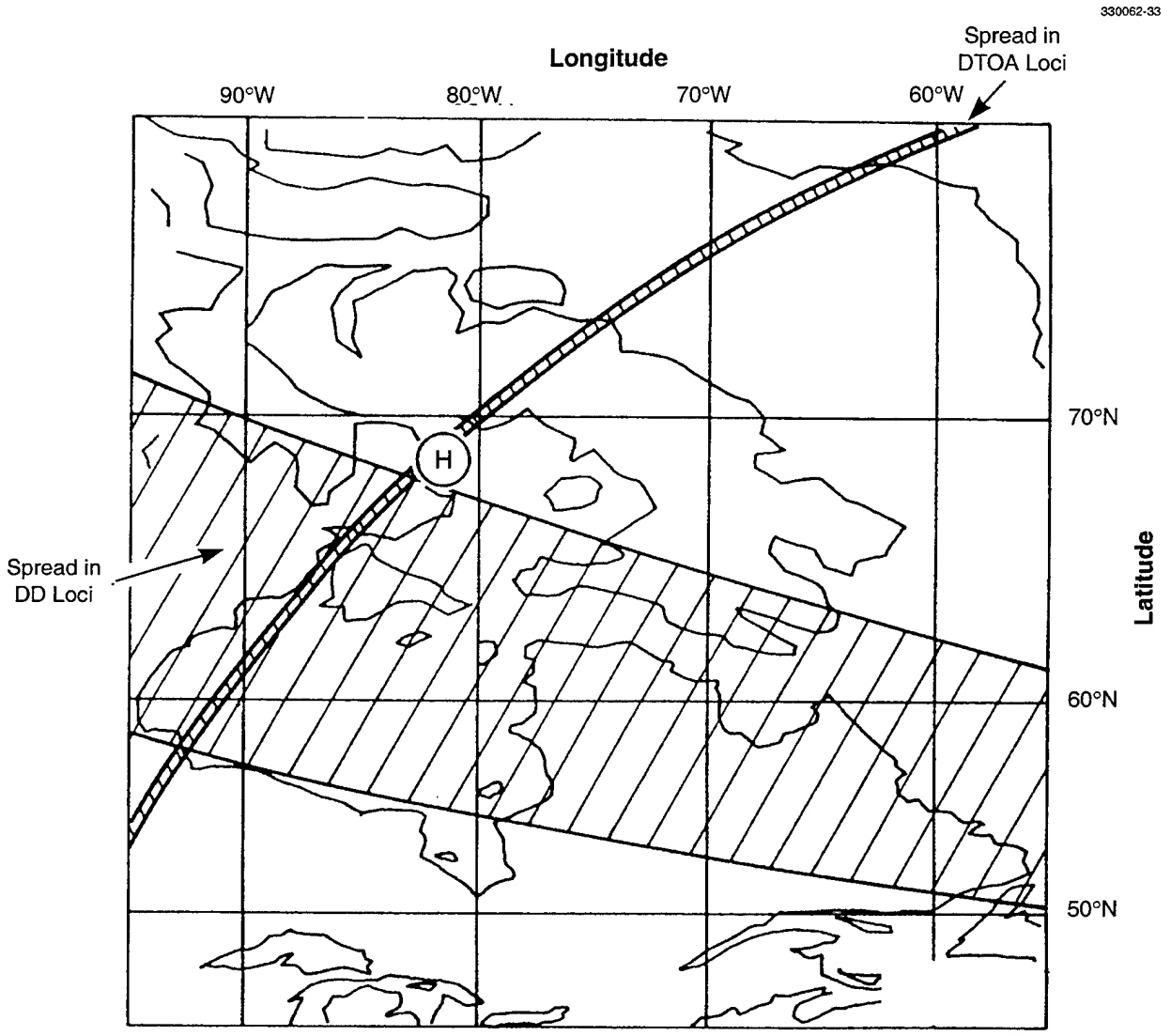

Figure 34. Spread in DTOA/DD loci from six observations of Hall Beach in wideband mode, 18 August 1981.

because of the large observed DD rates-of-change and the fact that for some of the DD estimates, no solutions for loci could be found on the surface of the earth. This experience led to an analytic and experimental investigation of the effects of source velocity on emitter location accuracy. If the source velocity is known, the DD data can be corrected for its effect via equation (4.6). In practice, however, the velocity will not be known and erroneous location estimates will result, even in the absence of other errors. It is straightforward to predict the location errors for a given source velocity using the basic source location equations. However, an opportunity arose to conduct an emitter location test with LES-8/9 and an aircraft with on-board transmitter made available by Lincoln Laboratory's Division 4.

The flight experiment took place on 17 September 1982 and originated from Hanscom AFB in Bedford, Massachusetts. The aircraft, a twin-engine Cessna, was outfitted with a UHF transmitter operating on 303.4 MHz with an EIRP of approximately 10 watts. A short pre-flight ground test verified transmitter operation and signal reception by LES-8/9. Since no signal modulation is required for DD investigation, CW transmission was used throughout the test. No attempt was made to use DTOA data. Test coordination was managed by a separate two-way VHF voice radio link between the aircraft and the data-recording center in the Laboratory.

The flight requirements of constant ground speed, altitude and heading were met by careful choice of the flight plan. The approximately rectangular flight plan shown in Figure 35 was chosen to have a direct line between two VHF Omni Range (VOR) aircraft-aid-to-navigation stations for each flight leg. The ground speed, which varied between 125 and 180 knots, was measured and reported from the aircraft through the use of the VOR stations. Twelve 10 s data sets per flight leg were recorded through the narrowband-reception mode of LES-8/9 in four counter-clockwise circuits of the flight plan. Ground speed relative to the VOR station, and heading from the aircraft gyroscopic compass were reported over the VHF link and recorded for each of the data sets for later use in the data processing.

Average correction for true versus magnetic north and for aircraft crabbing due to wind velocity were applied to all headings. Aircraft ground-speed errors due to flight path deviation from the intended pattern were considered negligible and were not corrected. It was assumed, also, that the aircraft maintained a perfectly level flight path over the period of each data set.

The data received from the two satellites was correlated in the usual way to obtain DD estimates. Position loci were plotted, treating the transmitter as though it were stationary, i.e., no velocity correction was made. The resultant DD loci were, of course, then considerably displaced from the actual aircraft positions. The intent was to observe the location errors that would be induced by the aircraft motion. No DTOA loci were calculated. In addition, the aircraft velocity and heading information were used to compute an aircraft velocity vector $\underline{v}_T$ to substitute in equation (4.6). A predicted DD was then calculated from the equation and was used to generate position loci which were compared to those obtained from the actual DD data.

Table 5-1 is a comparison of observed and predicted DD values for 11 data sets. The DD error, i.e., the difference between observed and predicted DD, can be attributed to inaccuracies in the aircraft heading and velocity data, in the satellite ephemerides, deviations from a level flight path, etc. In general, it was felt that the two sets of data were in good enough agreement not to warrant further investigation of the discrepancies. It appears that the analytic results predict the actual DD fairly well if accurate source-velocity information is available.

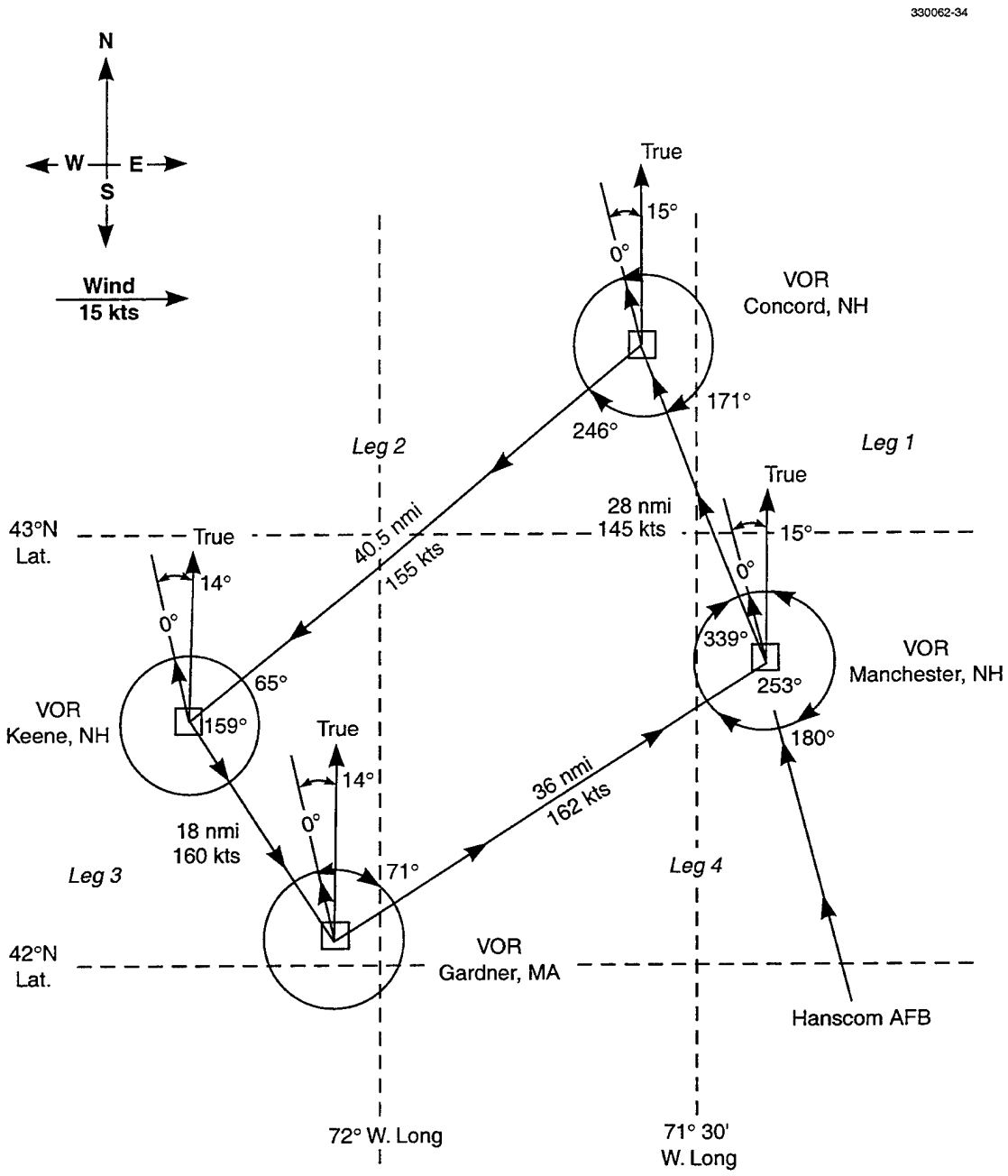

Figure 35. Airborne-emitter experiment flight plan.

TABLE 5-1

Comparison of Observed and Predicted Differential Doppler for Airborne Emitter, 17 September 1982

Data Set		Differential Doppler (Hz)		Difference (Hz)
Flight Leg	Time, UTC	Observed	Predicted	Observed – Predicted
1	1551	–18.115	–18.532	+.417
1	1554	–18.397	–18.424	+.027
2	1425	–14.114	–14.992	+.878
2	1558	–11.149	–11.696	+.547
2	1600	–11.150	–11.643	+.493
3	1531	–3.079	–3.0338	–.0452
3	1615	–3.604	–3.502	–.102
4	1445	–10.297	–10.7707	+.473
4	1450	–10.206	–10.6383	+.432
4	1537	–9.261	–9.5916	+.3306
4	1624	–6.917	–7.2484	+.3314

Figure 36 plots three representative pairs of position loci for observed and predicted DD data, corresponding to three different legs of the flight pattern. Flight leg #1 gave DD values which would not yield loci on the surface of the earth. The large difference between the actual and predicted loci in the figure for leg #2 is attributable to a large geometric error sensitivity. What is clearly evident is that large location errors are caused by a transmitter moving at aircraft speeds. The position errors vary widely with aircraft heading, despite more or less constant aircraft speed.

The experimental and analytic results point to the following conclusions:

(1) The assumption that the transmitter is stationary when in fact it is moving can lead to highly erroneous estimates of location when only DD data is used and aircraft velocity are involved. The magnitude of the errors will, in general, increase with increasing velocity.

(2) The actual errors, however, can also be very sensitive to source heading for a given speed. In one scenario, it was calculated that if the aircraft heading in the flight experiment were changed by one degree and the speed were held fixed, the DD loci would be translated by approximately 300 km.

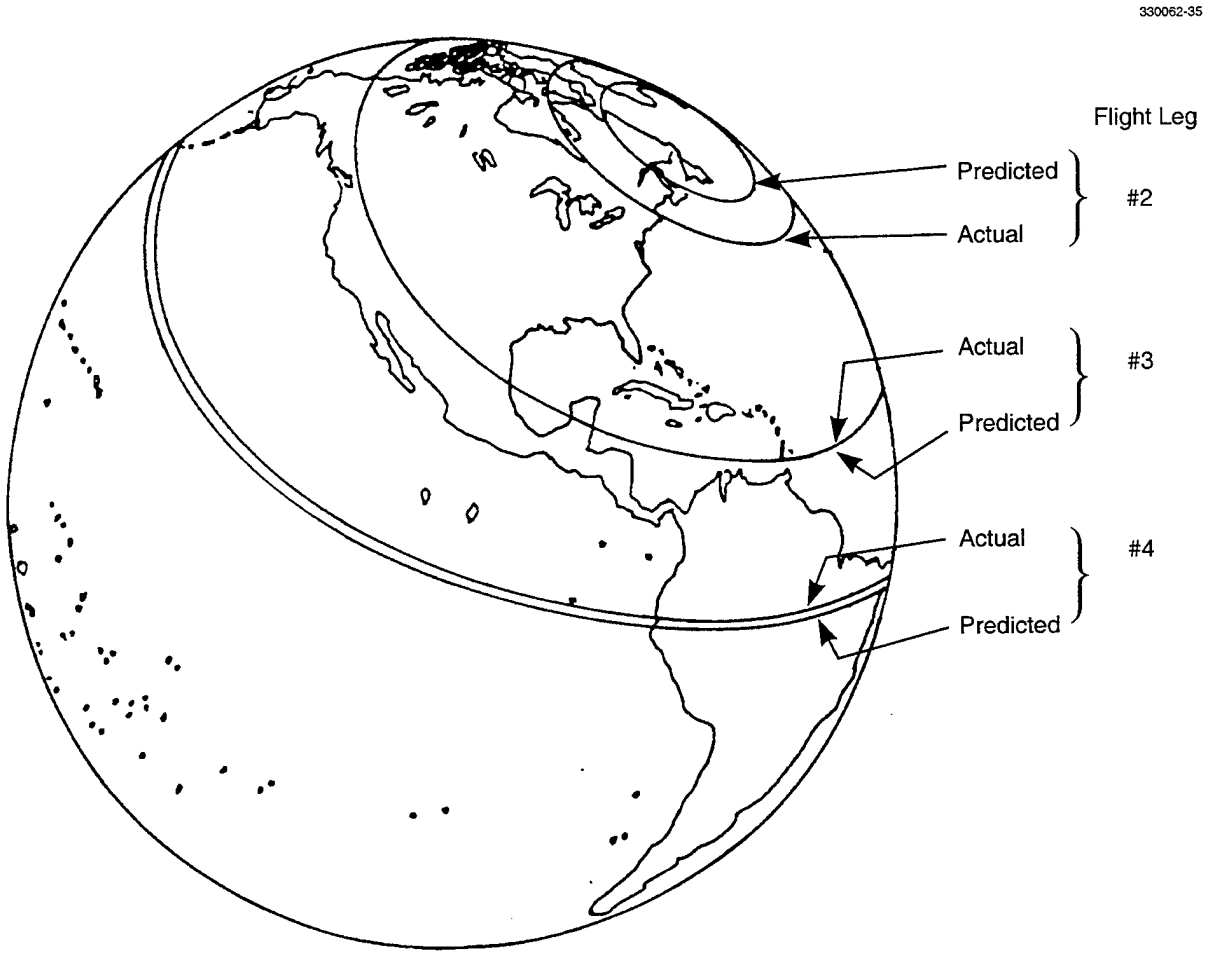

Figure 36. Typical loci for three flight legs of airborne-emitter experiment.

(3) In practice, the existence of transmitter motion will not be known *a priori*. Determining whether or not motion is present may require several hours or more of signal data to be taken. DD values that fall outside the allowable range for fixed sites on the earth or have very large rates of change are indicative of transmitter motion. However, if observed only for a short period, the DD data from a moving source may not exhibit these characteristics, but their absence does not necessarily imply the source is fixed. If sufficient acceleration is present, transmitter movement may be inferred from the smearing which will be induced in the DD correlation profile.

(4) If the transmitter is determined to be moving, the only realistic approach to estimating its location is not use its DD data. As discussed in Section 4, estimating the velocity is not practical. In fact, knowing the velocity and heading even relatively well does not guarantee highly accurate location estimates because of their sensitivity to velocity errors. The only resort is to employ the DTOA technique if possible.

6. CONCLUSION

We conclude by summarizing and assessing the LES-8/9 emitter-location capability using DTOA and DD. Development of this system was made possible by exploiting some of the unique operational characteristics of the satellites. Since LES-8/9 were not originally designed for emitter-location operation, some characteristics such as the satellite orbits, and some of the satellite subsystems are not the "ideal" ones for this application. Nonetheless a useful emitter-location capability at UHF employing DTOA and DD has been developed and demonstrated.

Much of the utility of the DTOA/DD approach stems from the fact that a location estimate can be made on the basis of a relatively short observation of the RFI source. By correlating the received-signal data from the two satellites, both DTOA and DD can be estimated simultaneously from a single observation. The DTOA and DD data each yield different location loci on the surface of the earth, with the intersection of the loci giving the location estimate. With LES-8/9 it was demonstrated that as little as one to ten seconds of received-signal data is sufficient to generate such an estimate. Multiple observations are generally taken, however, to improve overall location estimation accuracy. Although simultaneous use of DTOA and DD is the preferred emitter-location approach, a source can also be located on the basis of only DTOA or only DD, in which case multiple observations over a period of time are required. The present DTOA/DD system has a number of advantages over the terminator-motion and Doppler trace-matching emitter-location techniques which had been employed in the past with LES-8/9.

The location-estimation accuracy of the DTOA/DD method in general is limited ultimately by the accuracy with which the DTOA and DD themselves can be estimated from data which is inevitably noisy. Bounds on how well these parameters can be measured were given. In the case of LES-8/9, other limitations exist. Hard-limiting and sampling of the signals as received in each satellite impose restrictions on DTOA/DD estimation accuracy. Other receiver effects such as long-term oscillator drifts and time-synchronization errors also degrade performance. It was shown that satellite/emitter geometry is an important consideration. Favorable geometries make location-estimation accuracy less sensitive to errors in the DTOA/DD estimates. Analysis indicates location-estimation errors in the range of one to several hundred kilometers can be expected with LES-8/9. In many cases, systematic errors, such as orbit-fitting errors, and not the noise-induced DTOA/DD estimation errors are the limiting factor in location-estimation accuracy. In general, however, because of the many factors involved, this accuracy can be highly scenario-dependent.

Test results using transmissions from Lincoln Laboratory in Lexington and from a USAF transmitter at Hall Beach, Canada, demonstrate the location-estimation accuracies predicted analytically can be realized in practice. The Lincoln Laboratory experiments provide the most optimistic indication of achievable accuracy because of the highly controlled nature of those tests. The Hall Beach test results are more representative of what can be accomplished in a real-world situation since that transmitter was non-cooperating. The airborne-emitter experiment points to the difficulties of locating moving sources with DD, at least when airplane velocities are involved. Knowledge of the source velocity is essential to accurate location-finding, but in reality, this information cannot be expected to be known or estimated from the satellite data.

From the standpoint of accuracy, it is recognized that a number of improvements are desirable or possible. Perhaps the greatest improvement with LES-8/9 would result from larger physical separation of the two satellites so as to reduce the geometric error sensitivity. (However, their common coverage area on the earth would decrease, too.) Since the present satellite stations are decided primarily on the basis of considerations other than emitter-location, there is little prospect for change in this area in the near future. If one were to redesign the satellite receivers with emitter-location as an important function, considerable performance improvement could be obtained by better sampling/quantizing schemes. Careful design of components and subsystems could reduce the various systematic time and frequency errors described in Section 4. More accurate satellite ephemerides could be provided by more frequent and careful orbit-fitting, although in practice, this would impose a considerable burden on the resources used currently for managing LES-8/9 operations. From a user point of view, real-time or near-real-time processing of the data received from the satellites may be desired. Fast signal-processing and loci-determining algorithms could be developed and a dedicated computing system would probably be required for this purpose. Other possibilities include extension of the emitter-location capability to frequencies other than just those covered by LES-8/9. Networks of satellites with multiple receivers could increase coverage area and could also be used to deal with problems where moving sources are involved and where more than two receivers would be beneficial.

The work described in this report represents the limits to which the DTOA/DD emitter-location capability of LES-8/9 is likely to be developed. In reality, further improvements would require considerable additional expenditure of time and resources. However, the existing system provides a unique capability which is generally not available otherwise. Determining the location of an RFI source with the accuracy attainable with LES-8/9 can be of significant utility when one considers the *a priori* location uncertainty is likely to be a large portion of the earth. The experience in employing the DTOA/DD technique with LES-8/9 indicates the feasibility of using satellites for this application and also suggests areas for significant improvement.

APPENDIX A
ORBIT FIT QUALITY

This appendix gives the results of a study of the accuracy of the LES-8/9 position and velocity information provided by the PEP orbit-fitting program. PEP gives orbital predictions which are updated periodically to match ranging data taken on the satellites. The orbital information generated by PEP for the day ranging data obtained is as close to the true values as possible and tends to become less accurate with the passage of time.

To quantify the degeneration in orbital-prediction accuracy, the predictions for a given day—obtained from a new updated fit—are compared with those from a previous fit for that same day. The discrepancies between the two fits give a measure of the degradation in accuracy over the period of time between updates and, therefore, represent an estimate of the worst-case errors incurred by using a fit which is not "fresh."

Figure 37-40 plot the differences in the values of the satellites' X-Y-Z position and velocity coordinates as predicted from new and old orbit fits for a day close to that on which the new fit was generated. The data shown for LES-8 is obtained from a different set of orbit fits than that for LES-9. the dates of the orbit fits being compared are indicated in the figures. The results shown for the two satellites tend to indicate two extremes in orbit-fitting errors and they point out by how much orbit-fit quality can vary. The LES-8 errors are approximately an order of magnitude smaller than those for LES-9 in both position and velocity. Based on these results, the position errors can be said to vary between a few km and a few tens of km in each of the position coordinates. Velocity errors range between a few tenths of a m/s and a few m/s in each coordinate. The magnitudes of the individual errors are observed to vary significantly, in some cases, over the course of a day. It is emphasized again that these are worst-case errors and are not necessarily "typical" errors.

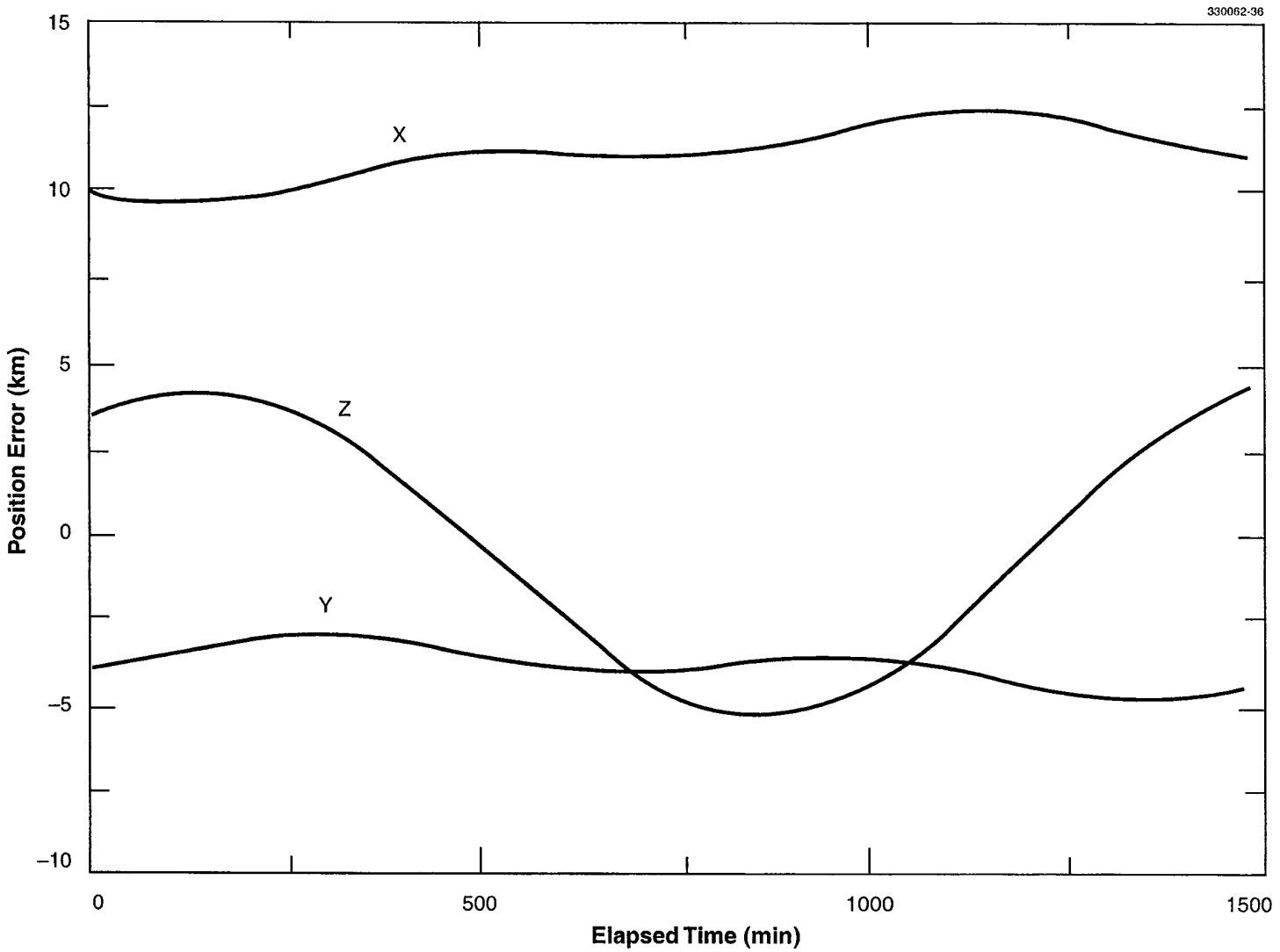

Figure 37. LES-8 calculated position errors for 25 November 1981 from PEP orbit fit 8AB1 (9 September 1981) referenced to fit 8CC1 (24 November 1981).

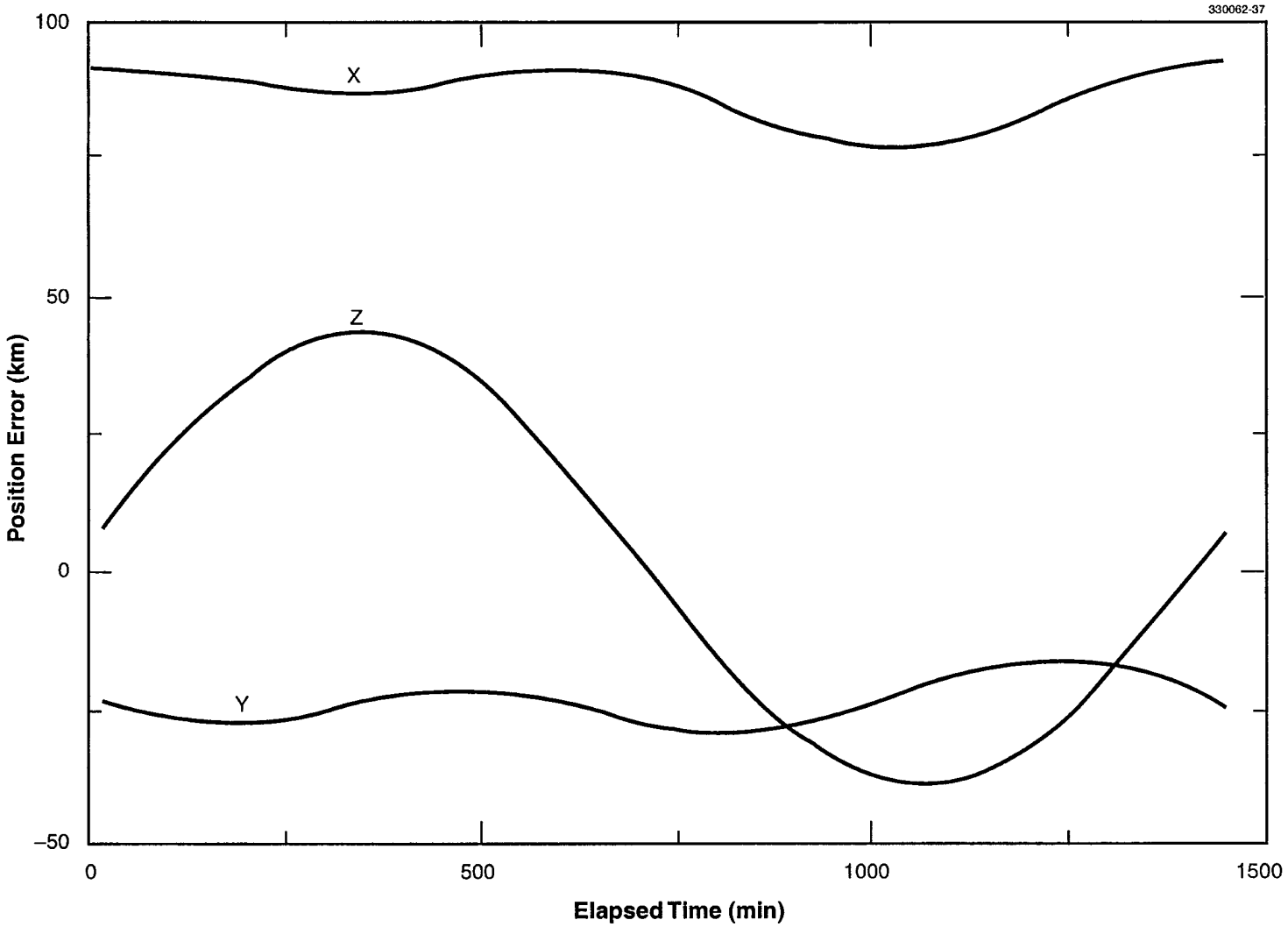

Figure 38. LES-9 calculated position errors for 30 September 1981 from PEP orbit fit 9AA1 (3 August 1981) referenced to fit 9AB1 (28 September 1981).

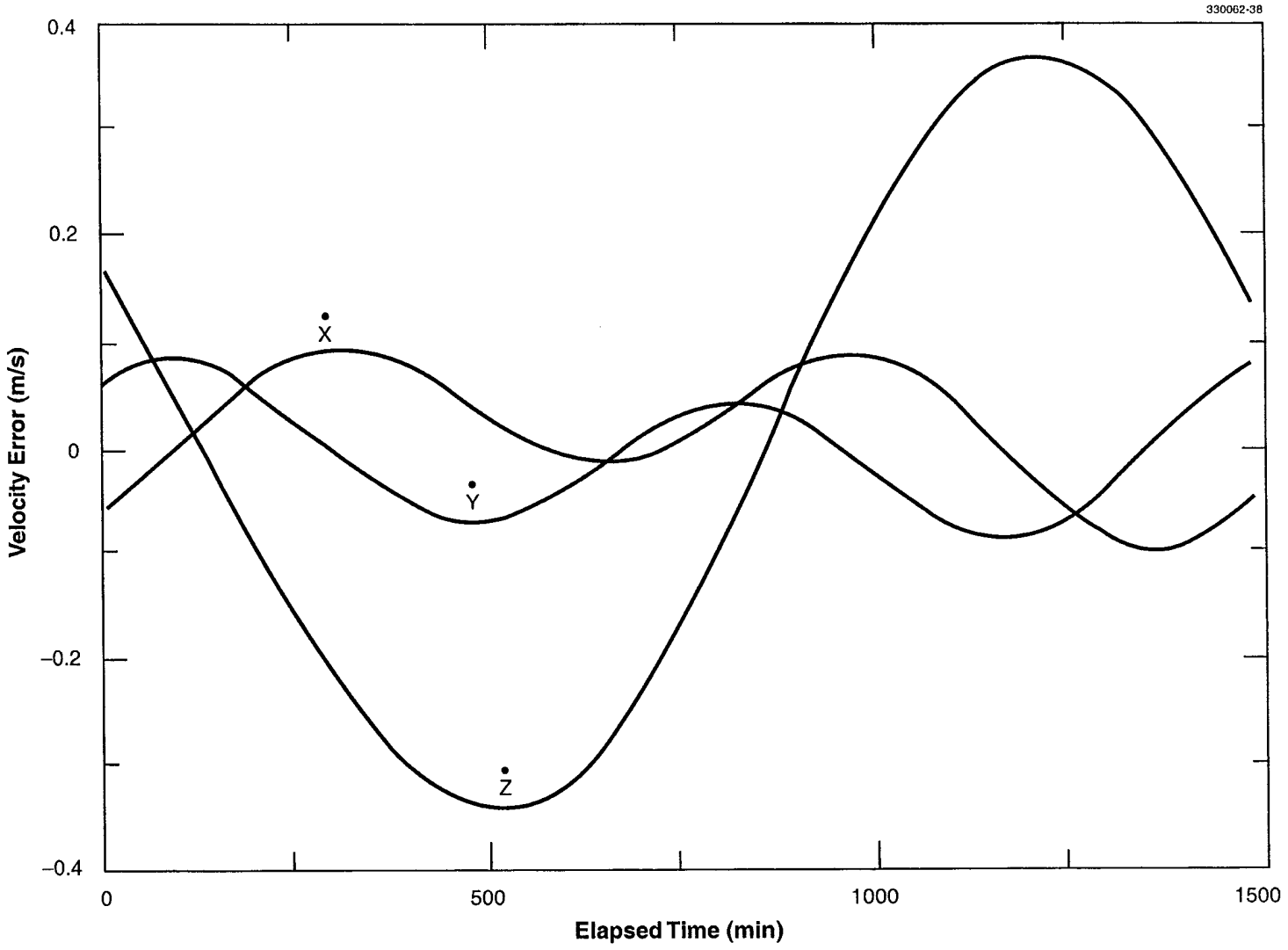

Figure 39. LES-8 calculated velocity errors for 25 November 1981 from PEP orbit fit 8AB1 (9 September 1981) referenced to fit 8CC1 (24 November 1981).

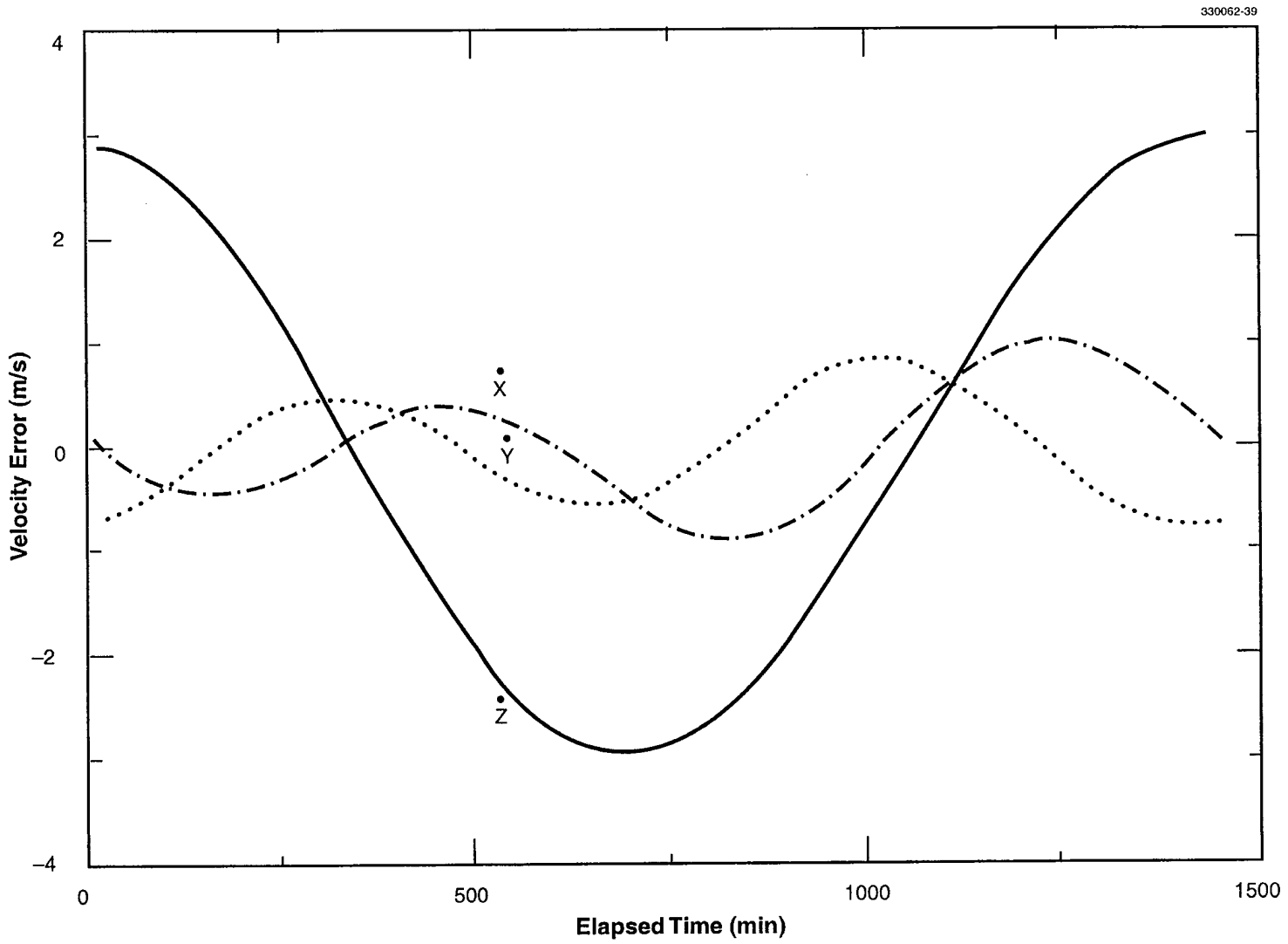

Figure 40. LES-9 calculated velocity errors for 30 September 1981 from PEP orbit fit 9AA1 (3 August 1981) referenced to fit 9AB1 (28 September 1981).

APPENDIX B
SAMPLE CALCULATION FOR DTOA/DD ESTIMATES

The results of a sample calculation to obtain DTOA/DD estimates are given for illustrative purposes here using actual test-signal data transmitted from Lincoln Laboratory with the spectrum shown in Figure 17. The sequence of calculations follows the three steps described in Section 3.3, Three-Step Correlation/ Estimation Procedure: (1) "coarse" correlation, (2) "fine" correlation, and (3) interpolation. The FFT correlations for the first step are shown in Figures 19 and 20. The time and frequency cells corresponding to 8.0 ms and 0 Hz, respectively, are identified as the DTOA and DD values for the peak of the FFT cross-correlation. The search for the DTOA/DD estimates is then narrowed to within one cell (±200 μs and ±0.61 Hz) of these coarse estimates and is continued in the second step.

Table B-1 gives the results of the "fine" correlation operation which uses all available data samples. The cross-correlation is computed for the DTOA values of 7800, 8000, 8200 μs, and at each DTOA point it is computed at 13 DD frequencies equally spaced between –0.61 and 0.61 Hz. (The separation between these frequency points is T^{-1} Hz, where T = 9.836 s is the duration of the observation in this example.) The peak of the discrete cross-correlation is found at DTOA and DD values of 8000 μs and 0.305 Hz, respectively.

TABLE B-1

"FINE" CORRELATION RESULTS

		DTOA (μs)		
		7800	**8000**	**8200**
DD (Hz)	–0.610	1490.15	2951.07	2143.09
	–0.509	2578.03	3753.93	2259.35
	–0.407	1272.15	1363.25	1189.69
	–0.305	1555.70	3406.12	2018.41
	–0.203	2756.94	4729.08	2343.20
	–0.102	1145.58	1875.49	849.56
	0.000	8541.77	12057.20	8251.07
	0.102	8186.23	15430.20	7580.55
	0.203	11671.30	20011.28	10919.93
	0.305	15529.71	26289.22	14550.43
	0.407	6028.27	7927.86	5767.83
	0.509	1519.46	877.10	1420.10
	0.610	3202.43	5209.67	2923.70

Interpolation Estimate (Using 9 Points):
DTOA = 7995.5 μs
DD = 0.2821 Hz

The final estimate is obtained by interpolating between nine points of the discrete cross-correlation. These points correspond to the correlation peak and the eight surrounding points: 0.305 Hz ± one frequency cell, or 0.203, 0.305, and 0.407 Hz and the DTOA values of 7800, 8000, 8200 μs at each DD value. The peak of the best-fitting paraboloid gives 7995.5 μs and 0.282 μs as the DTOA/DD estimates.

REFERENCES

1. M.E. Ash, "Determination of Earth Satellite Orbits," [U], MIT Lincoln Laboratory Technical Note 1972-5, 19 April 1972, DDC AD-742301.
2. Lincoln Experimental Satellites LES-8 and LES-9, Lincoln Manual, LM-98, Vols. 1-10.
3. D.M. Snider, D.B. Coomber, "Satellite-to-Satellite Data Transfer and Control," Seventh AIAA Communications Satellite System Proceedings, 24-27 April 1978, pp. 457-470.
4. S. Stein, "Algorithms for Ambiguity Function Processing," *IEEE Transactions on Acoustics, Speech, and Signal Processing,* Vol. ASSP-29, No. 3, June 1981, pp. 588-599.
5. T. Berger, "Bias and Variance of DTOA Estimates Based on Noisy, Sampled, Clipped Data," 1981 IEEE Symposium on Information Theory, Santa Monica, CA, Feb. 9-12, 1981
6. Lincoln Experimental Satellites LES-8 and LES-9, Communications System, Lincoln Manual, LM-98, Vol. 4, pp. 2-53.
7. P. Chestnut, "Emitter Location Accuracy Using DTOA and Differential Doppler," *IEEE Transactions on Aerospace and Electronic Systems,* Vol. AES-18, No. 2, March 1982, pp. 214-218.
8. D. Torrieri, "Statistical Theory of Passive Location Systems," *IEEE Transactions on Aerospace and Electronic Systems,* Vol. AES-20, No. 2, March 1984, pp. 183-198.
9. R.R. Newton, "The Near-Term Potential of Doppler Location," Applied Physics Laboratory, Johns Hopkins University N79-21041, Available NTIS.

GLOSSARY

AWGN	Additive White Gaussian Noise
BPSK	Binary Phase Shift Keying
DD	Differential Doppler
DTOA	Differential Time of Arrival
ELS	Emitter Location System
ESR	Elastic Shift Register
FFT	Fast Fourier Transform
GPS	Global Positioning System
LES	Lincoln Experimental Satellite
LOP	Line of Position
LORAN	Long Range Navigation
MLSR	Maximal-Length Shift Register
PEP	Planetary Ephemeris Program
PLSS	Precision Location Strike System
RFI	Radio-Frequency Interference
RTG	Radioisotope Thermoelectric Generator
SNR	Signal-to-Noise Ratio
UHF	Ultra High Frequency
USAF	United States Air Force

REPORT DOCUMENTATION PAGE

Form Approved
OMB No. 0704-0188

1. AGENCY USE ONLY (*Leave blank*)	2. REPORT DATE 8/21/85 reissued 31 March 2000	3. REPORT TYPE AND DATES COVERED Technical Report

4. TITLE AND SUBTITLE

Emitter Location with LES-8/9 Using Differential Time-of-Arrival and Differential Doppler Shift

5. FUNDING NUMBERS

C — F19628-85-C-0002

6. AUTHOR(S)

John E. Kaufmann and Warren K. Hutchinson

7. PERFORMING ORGANIZATION NAME(S) AND ADDRESS(ES)

Lincoln Laboratory, MIT
244 Wood Street
Lexington, MA 02420-9108

8. PERFORMING ORGANIZATION REPORT NUMBER

TR-698 (Rev. 1)

9. SPONSORING/MONITORING AGENCY NAME(S) AND ADDRESS(ES)

Air Force Systems Command, USAF
Andrews AFB
Washington, DC 20334

10. SPONSORING/MONITORING AGENCY REPORT NUMBER

ESD-TR-85-213

11. SUPPLEMENTARY NOTES

None

12a. DISTRIBUTION/AVAILABILITY STATEMENT

Approved for public release; distribution is unlimited.

12b. DISTRIBUTION CODE

13. ABSTRACT (*Maximum 200 words*)

Development of an emitter-location capability using differential time-of-arrival (DTOA) and different Doppler shift (DD) with the Lincoln Experimental Satellite 8 and 9 (LES-8/9) is described. Location of UHF sources over a large part of the earth can be estimated from observations as short as a few seconds by the two satellites. The principles of this emitter-location method, DTOA and DD estimation procedures, and limitations on location-estimation accuracy are discussed. Results of tests using transmissions from Lincoln Laboratory, Lexington, Massachusetts, and from a USAF transmitter at Hall Beach, Canada, demonstrate the level of accuracy achievable in practice with LES-8/9.

This report was originally Classified. It is being reissued with corrections of a few minor errors and misprints.

14. SUBJECT TERMS

RFI (Radio Frequency Interference)
Emitter Location
LES-8/9
Direction Finding
UHF Satellite Communication
Frequency Allocations

15. NUMBER OF PAGES

16. PRICE CODE

17. SECURITY CLASSIFICATION OF REPORT	18. SECURITY CLASSIFICATION OF THIS PAGE	19. SECURITY CLASSIFICATION OF ABSTRACT	20. LIMITATION OF ABSTRACT
Unclassified	Unclassified	Unclassified	Same as Report